University of Alberta

Evaluation of the Effects of Canadian Climatic Conditions on Pavement Performance Using the Mechanistic Empirical Pavement Design Guide

by

Jhuma Saha

A thesis submitted to the Faculty of Graduate Studies and Research
in partial fulfillment of the requirements for the degree of Master of Science
in

Transportation Engineering

Department of Civil and Environmental Engineering

Edmonton, Alberta
Fall 2011

Abstract

This thesis attempts to explore the implementation of the Mechanistic Empirical Pavement Design Guide (MEPDG) in Canada, specifically in Alberta. In order to achieve this goal, quality of Canadian climate data files used for the MEPDG and its effects on flexible pavement performance were evaluated. Results showed that temperature and precipitation data used in the MEPDG are close to Environment Canada data. This study demonstrated that asphalt concrete rutting, total rutting and longitudinal cracking were sensitive to Canadian climate. However, alligator cracking, transverse cracking and International Roughness Index (IRI) were found less sensitive to climatic factors.

In addition, this study compared Alberta Transportation Pavement Design (ATPD) method and the MEPDG. Comparison results revealed that pavement performance (IRI) is quite close (< 8% difference) using these two methods. According to the MEPDG, pavement designed by the ATPD method underestimates pavement thickness at poor subgrade and high traffic conditions.

This Thesis is dedicated to my parents and husband

Acknowledgements

I would like to thank my advisor Dr. Alireza Bayat for his support and invaluable guidance during this research. His mentorship and advice were instrumental in the course of this exploration. Many thanks also go to Dr. Hamid Soleymani for sharing his ideas, experience and guidance to complete substantial part of this thesis. His sage advice, insightful criticisms, and patient encouragement aided the writing of this thesis in innumerable ways. Without his hard work, experience, and genuine support, this report would not have been possible. His steadfast support on this thesis was greatly needed and deeply appreciated.

Many thanks go to my husband, Baidya Nath Saha, for being by my side, and for his encouragement and his patience for being a husband, a father, a worker, and a student in the same time. I could not have done this without him, and I am so grateful for his presence in my life. I also express my gratitude to Avighna, my son, who was born during the preparation of this dissertation. When he was smiling for me I was given more hope and more energy to be done with the dissertation, and so thank you my little one.

I would like to thank my friends and colleagues for their friendship and support during the time of my studying.

Furthermore, I would like to thank my mother, my elder sister, and my niece, Adrija for their love and support. I appreciate what my mother did for us. The time that she spent caring for Avighna made it possible for me to work on some of the most difficult portions of this dissertation. Her help and support were invaluable. I feel so lucky to have such a great mom.

Table of Contents

List of Tables

List of Figures

GLOSSARY

TAC	Transportation Association of Canada
AASHTO	American Association of State Highway &Transportation Officials
PSI	Present Serviceability Index
SN	Structural Number
AT	Alberta Transportation
AADT	Annual Average Daily Traffic
AADTT	Annual Average Daily Truck Traffic
ESAL	Equivalent Single Axle Load
SUT	Single Unit Truck
TTC	Tractor Trailer Combination
PCC	Portland Cement Concrete
AC	Asphalt Concrete
IRI	International Roughness Index
MEPDG	Mechanistic Empirical Pavement Design Guide
EICM	Enhanced Integrated Climatic Model
CMS (model)	Climatic Material Structural Model
ID (model)	Infiltration and Drainage Model
CRREL	Cold Regions Research and Engineering Laboratory
NCHRP	National Cooperative Highway Research Program

Chapter 1

1. Introduction

Canada's road infrastructure has an estimated value of $150 billion [1]. This big road infrastructure enables transportation of people and resources, which is a major source of our economic prosperity. The total length of Canada's road and street system is nearly 840,000 kilometers: 63% is earth and gravel and 37% is paved roads [2]. In Canadian context, the deterioration of these roads is mainly caused by climatic factors such as long winter sessions with cold temperature and moisture as well as freeze thaw cycles [2].

Climatic factors affect the behaviour of all pavement layers by changing material properties. Bound materials are sensitive to temperature variations. At low temperatures asphalt concrete tends to contract. As a result, asphalt becomes hard and brittle and builds tensile stress in the materials that result in transverse cracks when the tensile stress exceeds the material strength [2]. At high temperatures asphalt becomes soft and viscous, weakening the pavement structures. As a result, the asphalt layer creates pavement rutting under heavy traffic loads [3]. Temperature and moisture variations affect the behavior of unbound layers. With an increase of moisture content unbound layers reduce their bearing capacity. In winter when subsurface temperatures drop below the freezing point, frost penetrates pavement materials and subgrade soils and freezes the water in the soils that creates ice lenses. Ice lenses cause an increase in the strength and stiffness of the unbound pavement layers and subgrade soil [3]. When the ice lenses thaw, the increased moisture content in the soil weakens structural capacity of the pavement structure [4 and 5].

Freeze - thaw action is the key reason for pavement damage in cold climate regions. Canada has a cold climate with freezing index more than 1000ºC-days in 90% area of Canada [6]. The pavement damage mechanism in cold climates is considerably different from that in warmer climates. The effect of frost makes huge differences in roughness during winter. The spring thaw causes quick damage during a somewhat short time of the year. Thus climatic factors decrease the structural capacity and functional serviceability of the pavement. Many studies in literature have explored the effect of climatic factors on road deterioration. Nix (2001) shows that 20 to 50%

of road damage is caused by vehicles and 50 to 80% is due to weather depending on pavement construction and traffic level [7]. A paper from Transport Quebec (Saint-Laurent et Corbin, 2003) reported that according to several authors 30 to 80% of all annual road damage occurs during the spring thaw period depending on the length of the spring thaw season [8]. Therefore, pavement design practices in cold climatic regions such as Canada need to adequately incorporate the effects of climatic factors responsible for pavement damages.

1.1 Current Pavement Design Practices in Canada

In the United States, the Federal Highway Administration (FHWA) provides funds for pavement construction and rehabilitation or setting pavement design standards. However, there is no single agency like the FHWA in Canada [9]. Pavement design for the primary highway network in Canada is governed by provincial governments with the federal government responsible for National Parks Roadways [9]. Provincial agencies are free to implement whatever design procedure they choose for pavement design and rehabilitation. Most of the provincial transportation agencies (British Columbia, Alberta, Manitoba, Ontario, Quebec, New Brunswick, Nova Scotia Public Works and Government Services Canada (PWGSC)) use the American Association of State Highway Transportation Official (AASHTO)-1993 whereas Saskatchewan and Prince Edward Island use Asphalt Institute method for flexible pavement design method. The AASHTO-1993 is an empirical pavement design method whereas the Asphalt Institute method is a mechanistic pavement design method.

The AASHTO-1993 empirical model was drawn from field performance data measured at the AASHO road test that was conducted in the late 1950's under a specific climatic condition, set of subgrade, and pavement materials with typical traffic loading and characteristics. AASHTO-1993 empirical method served well for the last four decades; however, these were not representative of the current world scenario due to varied climate, traffic loading and volume around the world. Recent studies demonstrated that AASHTO-1993 over- or under -estimates pavement designs (thicknesses) in various situations since climate, traffic and other pavement design inputs have not been adequately considered in these empirically based methods [10]. The inherent limitation in this method is the empirical nature of the decision process, which was derived from a road test conducted almost 50 years ago

in Ottawa, Illinois. Besides, AASHTO-1993 pavement designs procedure has limited environmental inputs: drainage and seasonal variation of subgrade support are included, but these are not sufficient to completely predict the changes in pavement response due to different climates. These limitations and deficiencies of the AASHTO-1993 method motivated the development of a design guide based on the mechanistic principles under the National Cooperative Highway Research Program (NCHRP 2004). Literature reveals that the recently developed Mechanistic-Empirical Pavement Design Guide (MEPDG) incorporates effects of climate, traffic and materials on pavement performances in a comprehensive manner that made MEPDG a more cost effective design procedure than existing empirical-based pavement design methods [11].

1.2 Benefits of MEPDG over Empirical Based Approaches

Currently, many transportation agencies are considering the implementation of mechanistic procedures and analytical methods rather than empirically based design and analysis procedures for the design and evaluation of pavement structures. The mechanistic pavement design procedures are capable of predicting pavement responses (i.e., stress, strain, deflection) under traffic and environmental loads and relating these predicted responses to pavement performance. The benefit of the mechanistic procedure is the ability to calibrate design procedures to local climate conditions and material properties. The current MEPDG, introduced by the recently completed NCHRP project 1-37 A, is under evaluation by many transportation agencies in North America.

The newly released MEPDG has adopted a mechanistic-empirical pavement design procedure, in which pavement distresses are calculated through nationally calibrated distress prediction models based on material properties and local climatic conditions. The calibrated distress prediction models are based on the critical pavement responses mechanistically calculated by a structural model, and coefficients determined through national calibration efforts using the Long-Term Pavement Performance (LTPP) database. The MEPDG requires many input parameters to map the calibrated distress prediction models with traffic, environmental factors, and material properties. All the distresses considered in the MEPDG are affected by environmental factors to some degree [12]. The Enhanced Integrated Climate Model

(EICM) is a powerful climate effects modeling tool, is used to model temperature and moisture within each pavement layer and subgrade in the MEPDG software [13]. The version of the EICM incorporated into the MEPDG is based on improvements to an earlier version of the Integrated Climate Model [14]. EICM offers distinct benefits compared to previous procedures [15].

The EICM requires climate data files which include inputs of hourly air temperature, wind speed, sunshine percentage (used to define cloud cover), precipitation, relative humidity and water table depth in a specified format by the MEPDG software [13]. Temperature profile, changes in ground water table, precipitation/infiltration, freeze-thaw cycles, and other external factors are modeled in the MEPDG procedure in a very comprehensive manner [13]. The MEPDG helps to evaluate pavement performances and it can be upgraded if extra efforts and resources are involved to better characterize materials, improve traffic data quality, and effectively use environmental conditions [10].

To date, only in the United States have there been significant studies depicting the consequences of climate on pavement performances using the MEPDG. One such study was done by Johanneck *et al.* which was a sensitivity study on 610 complete weather stations across the US [3]. This study attempts to evaluate some environmental aspects required for the implementation of MEPDG for designing pavements in Canada and especially in Alberta.

1.3 Objectives

The objective of this study was two-fold. The broad objectives and the specific objectives are as follows:

1. **Evaluation of Canadian climatic files and their effects on pavement performances using the MEPDG**
    - Evaluate the accuracy of temperature and total precipitation data used for the MEPDG application,
    - Evaluate the accuracy of freezing index data computed by the MEPDG
    - Compare maximum frost depth computed by the MEPDG with the Modified Berggren method.

- Study the effects of Canadian climatic factors on pavement performances using the MEPDG,
- Investigate the effect of Canadian climate zones on pavement distresses
- Evaluate the effects of latitude & longitude on pavement performances, and
- Evaluate of the application of Virtual Weather Station (VWS) in the MEPDG.

2. **Comparison between Alberta Transportation Pavement Design (ATPD) method and the MEPDG**
   - Compare the ATPD with the MEPDG method in terms of pavement distress prediction International Roughness Index (IRI), and
   - Evaluate pavement performances using the MEPDG.

1.4 Scope

- MEPDG version 1.1 was used for pavement performance evaluation in this study.
- Since most pavements in Canada are flexible pavements, only flexible pavement sections were considered.
- Two hundred and six weather station files in Canada including 27 weather station files in Alberta were evaluated.
- Four weather factors such as temperature, precipitation, freezing index and frost depth were evaluated in this study.
- The accuracy of Canadian weather station files was evaluated using Environmental Canada data records and Modified Berggren method.
- Pavement distresses in terms of IRI, longitudinal cracking, alligator cracking, transverse cracking, AC rutting and total pavement rutting were considered for discussion in this study.
- Since most of the Canadian provinces follow the AASHTO method for pavement design, in this study the ATPD method, which is based on AASHTO-1993, was compared with MEPDG.

1.5 Organization of This Thesis

This thesis is organized as follows: Chapter 1 presents the introduction, objectives and scope of this work. Chapter 2 presents an overview to the relevant background information as well as specific inputs and outputs of empirical-based pavement design procedure AASHTO and recently developed MEPDG. Chapter 3 describes the procedure of evaluation of Canadian climatic files used for the MEPDG. Chapter 3 also includes an analysis of the effects of Canadian climatic files on pavement performances at three levels: (a) provincial; (b) climatic weather zones and (c) geography (across latitude and longitude). Chapter 4 demonstrates a comparison between the pavement design method adopted by Alberta Transportation agencies and the MEPDG. Chapter 5 includes work summary, conclusions, contributions and recommendation for future studies. This thesis ends with references and appendices.

Chapter 2

2. Literature Review

This study aims to evaluate the effects of climatic factors on pavement performance and to conduct a comparative study between the Alberta Transportation Pavement Design (ATPD) method and the Mechanistic Empirical Pavement Design Guide (MEPDG). The related literature of this study is discussed in this chapter. Mainly a brief overview of two different pavement design methods, American Association of State Highway Transportation Official (AASHTO)-1993 method and MEPDG is discussed. First, an introductory discussion on empirical based pavement design methods and the newly developed MEPDG is provided. Then, AASHTO-1993 pavement design procedure, important input and output parameters, the advantages and limitations of the AASHTO-1993 is briefly discussed. Subsequently, the MEPDG pavement design procedure, environmental factors and climatic models as well as different pavement performance prediction models used in the MEPDG is discussed. Finally, comparison between the AASHTO-1993 and the MEPDG is mentioned.

2.1 Pavement Design and Analysis Methods

There are two different types of tools available in literature for pavement design and performance analysis: the empirical design approach and the mechanistic-empirical (M-E) design approach. Under the action of traffic and environmental loading, an ideal design tool will predict the state of stresses and strains within the pavement structure. Materials that are available for the construction of pavement have a major influence on design [16]. The pavement design tool should be equipped with material models capable of capturing the mechanistic response of the various materials used to construct the road. This type of model is regarded as a mechanistic model. In the early 1960s, knowledge gaps prevailed between mechanics and material science that caused the evolution of the empirical modeling method as an alternative [17].

2.1.1 Empirical Pavement Design Approach

Empirical design approach is the well-known approach for pavement design and its

performance evaluation to date. An empirical approach is one which is based on the results of experiments or experience. Generally, it requires a number of observations to be made in order to ascertain the relationships between input variables and outcomes. As long as the limitations to the approach are recognized, it is not necessary to firmly establish the scientific basis for the relationships between variables and outcomes [18]. Specifically, it is not prudent to use empirically derived relationships to describe phenomena that occur outside the range of the original data used to develop the relationship. In some cases, it is much more expedient to rely on experience than to quantify the exact cause and effect of certain phenomena. The design inputs of empirical pavement design approach include standardized traffic loading, physical properties of pavement materials, and environment conditions. These inputs are required to estimate the pavement performance based on results from previous field experiments and, in some cases, on practical experience [17].

Empirical design methods can range from extremely simple to quite complex. The simplest approaches specify pavement structural designs based on what has worked in the past. For example, local governments often specify that city streets should be designed using a given cross section (e.g., 100 mm (4 inches) of Hot Mix Asphalt (HMA) over 150 mm (6 inches) of crushed stone) because they have found that this cross section has produced adequate pavements in the past. More complex approaches are usually based on empirical equations derived from experimentation. Some of this experimentation can be quite elaborate. For example, the empirical equations used in the American Association of State Highway Transportation Official (AASHTO)-1993 Guide are largely a result of the original AASHO Road Test. There are several empirical design methods available, such as the National Crushed Stone Association [19], the California Method and the most commonly used pavement design method, various versions of the AASHTO design Guides [20, 21, 22, 23]. Among these methods AASHTO is the worldwide most popular method.

2.1.2 Mechanistic-Empirical (M-E) Design Approach

In the mechanistic approach, a mathematical model is used to describe the relationship between the structural response (stresses, strains and deflection) and the physical causes (inputs). However, this mechanistic approach is not capable alone for complete pavement analysis because mechanistic approach are based on

mathematical model which are theoretical . As a result M-E design approaches were developed as an alternative to fulfill the gap between the empirical and mechanistic methods. In the M-E approaches, the performance prediction models use the stresses, strains and deflections to predict pavement distress using the empirical formulas [17]. In other words, in the M-E method, the mechanical model is based on elementary physics and determines pavement response to the wheel loads or environmental condition in terms of stress, strain, and displacement [24]. The empirical part of the design uses the pavement response to predict the life of the pavement on the basis of actual field performance [25].

The Mechanistic Empirical Pavement Design Guide (MEPDG) combines both empirical and mechanistic procedures for pavement design. The MEPDG is explained in more details in Section 2.3.

2.2 Outline of AASHTO Pavement Design Method

The AASHTO pavement design procedure uses empirical equations to relate observed or measurable phenomena (pavement characteristics) with outcomes (pavement performances). The empirical equations were developed from the AASHO road test conducted near Ottawa, Illinois, during the period 1958-62. The original design procedure was modified several times over the last 50 years to improve the procedure and to incorporate new research outcomes. With each revision, new concepts were incorporated into it, resulting in an ongoing upgrade to the overall procedure. For example the reliability concept was introduced with the release of the 1986 guide to deal with uncertainties related to design variables. The guide also introduced the concept of the resilient modulus M_R (elastic response) in place of pavement support. Drainage coefficients were added by replacing the regional factor (R) [16]. The 1993 version of AASHTO improved the design procedure for rehabilitating of existing pavements. The most recent version of the AASHTO pavement design guide is AASHTO-1993. This guide is used by the majority of Canadian provincial road authorities [26].

2.2.1 AASHTO Design Procedure

The main features of the ASSHTO-1993 pavement structural design procedure are captured in Figure 2.1. The basic equation associated with the guide for flexible

pavement design is shown below as Equation 2.1. This basic equation of the AASHTO-1993 design guide permits engineers to determine a structural number (thickness index) necessary to carry a selected traffic load.

$$\log W_{18} = Z_R S_0 + 9.36\left[\log_{10}(SN+1)\right] - 0.2 + \frac{\log_{10}\left[\Delta PSI / 2.7\right]}{0.40 + 1094/(SN+1)^{5.19}}$$
$$+ 2.32 \log_{10} M_R - 8.07 \qquad (2.1)$$

where,

W_{18} = predicted number of 80 kN (18,000 lb.) equivalent standard axle load (ESAL)

Z_R = standard normal deviate

S_0 = combined standard error of the traffic prediction and performance prediction

SN= structural number (an index that is indicative of the total pavement thickness required)

$= a_1D_1 + a_2D_2m_2 + a_3D_3m_3 + \ldots$

a_i = i^{th} layer coefficient

D_i = i^{th} layer thickness (inches)

m_i = i^{th} layer drainage coefficient

ΔPSI = difference between the initial design serviceability index, p_0, and the design terminal serviceability index p_t

M_R = subgrade resilient modulus (in psi)

Figure 2.1: Flow Chart for the AASHTO-1993 Structural Design Procedure [17]

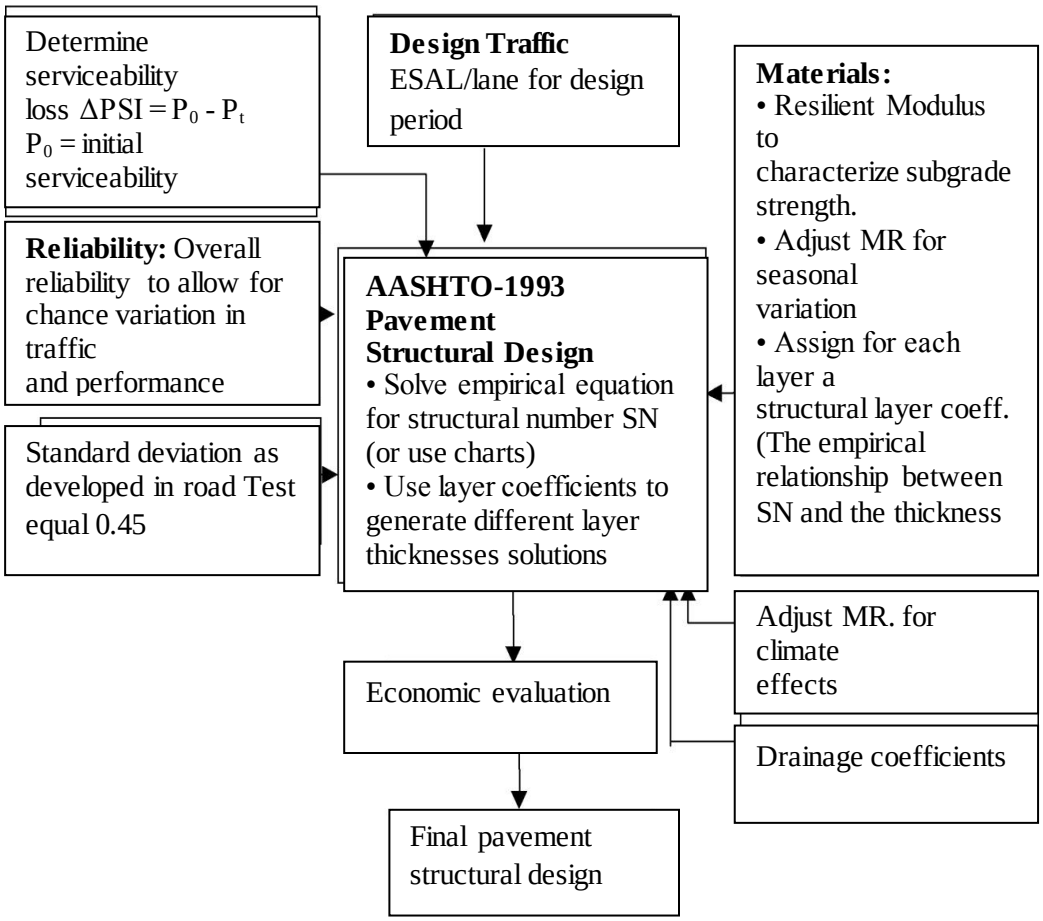

2.2.2 Traffic

The basic traffic unit used in AASHTO-1993 is the 18-kip single standard axle. Different axle types are converted to Equivalent Single Axle Loads (ESALs) using the Load Equivalency Factors (LEF). LEF is defined as the number of repetitions of the 18-kip single standard axle that causes the same damage as a single application of a particular configuration. The AASHTO method does not account for the concept of the relative damage because it is based on empirical results of the ASSHTO Road Test. Traffic consideration in the AASHTO method has not incorporated the concept of multiple axle configurations such as tire types and pressures. The AASHTO-93 design practice does not account for vehicle speed. Slower speeds and stop conditions for a longer period of time result in greater rutting damage. Today traffic volumes, vehicle characteristics, type of truck loadings, classifications and distribution have changed significantly. These factors have not been reflected in AASHTO-1993.

2.2.3 Reliability

"The reliability of the pavement design-performance process is the probability that a pavement section designed using the process will perform satisfactorily over the traffic and environmental conditions for the design period" [23]. Reliability was introduced in the AASHTO Guide to provide some degree of assurance (R) to the designer to use in the design process so that various design alternatives will last for which they were designed. Reliability is intended to account mostly for chance deviations in traffic prediction and performance prediction. Reliability of design performance is measured through the multiplication of reliability factor F_R with design period traffic prediction (W_{18}) to produce design applications for the design equation. The reliability factor is a function of the overall standard deviation (S_0) that accounts for both chance variation in the traffic prediction and normal variation in pavement performance prediction for a given W_{18} [17]. The AASHTO Guide recommends reliability for various functional classifications of roads, from 50 to 99.9%, whether urban or rural [26].

2.2.4 Materials Characterization

The basis for materials characterization in the AASHTO Design Guide is the resilient modulus of subgrade. This lets the pavement designer quantify the relative damage a pavement is subjected to during each season of the year [27].

2.2.4.1 Roadbed Soil Characterization

For roadbed materials, laboratory resilient modulus tests using AASHTO Test Method T274 should be performed on representative samples under stress and moisture conditions simulating those of the moisture and temperature seasons. This is considered as the first attempt at implementing a mechanistic property in pavement design. The original AASHTO resilient modulus (M_R) test procedure has been modified (SHRP – P-46) to the current procedure entitled "AASHTO T294-92" [16]. The resilient modulus is a means of characterizing the elastic property of soil that recognizes definite nonlinear characteristics. The empirical model in the AASHTO Guide is sensitive towards variations in the M_R parameter. When direct test facilities of M_R are not available, the resilient modulus can be estimated from other tests such as California Bearing Ratio (CBR), R-value and soil index test results using

correlation relationships recommended by the Guide. The value of the resilient modulus is stress-strain dependent, that is, the value changes as stress and strain conditions change. The AASHTO guide outlines two procedures to be followed for determining the seasonal variation of the modulus based either on the laboratory relationship between the resilient modulus and moisture content, or from back-calculated moduli for different seasons. The Guide comprises a procedure for determining the effective roadbed soil resilient modulus based on an estimate of relative damage (u_f) that corresponds to the seasonally adjusted subgrade modulus for each month of the year [16].

2.2.4.2 Pavement Layer Material Characterization

AASHTO-93 has not incorporated pavement material characteristics directly in the structural design but the factors of pavement material properties hich is called layer coefficients. The layer coefficients of different unbound materials are related to the resilient modulus. Those layer coefficients can be determined using AASHTO T274 test methods. On the other hand the bound material or asphalt concrete can be characterized using results of the repeated load indirect tensile test (ASTM D 4123). Structural coefficients can also be estimated from available charts of various base-strength parameters and resilient modulus test values in the AASHTO Guide. The effectiveness of the ability of various drainage methods to remove moisture from the pavement is not described with detailed criteria, but is recognized through the use of modified layer coefficients [28]. The layer coefficient, which is a measure of the relative ability of the material to function as a structural component of the pavement, expresses the empirical relationship between the structural number (SN) and thickness [26]. The factor for modifying the layer coefficient is referred to as a drainage factor for i^{th} layer (m_i)value and has been integrated into the structural number (SN) equation along with the layer coefficient (a_i) and thickness (Di) [28]; thus

$$SN = a_1 D_1 + a_2 D_2 m_2 + ... + a_i D_i m_i \qquad (2.2)$$

Where:

SN = Structural number of the pavement structure

a_i = Layer coefficient i

D_i = Thickness of layer i

m_i = Drainage factor for layer i

The layer coefficients could be influenced by many factors such as the thickness of the layer and the underlying support and position within the pavement structure. The AASHTO guide mentioned that the resilient modulus values found by laboratory tests were significantly different from field results. In most of the cases, the layer coefficients values are determined from prior experience. Also layer coefficients values can be determined from long-term pavement response data.

2.2.5 Serviceability

Pavement performance is characterized by the criteria of the structural performance and the functional performance. The structural performance relates to the physical conditions of the pavement, such as the occurrence of cracking or any other conditions that might affect the load-carrying capacity of the road. On the other hand, the functional performance describes how comfortable the ride is for the user and is measured using the serviceability-performance concept [17].

The Present Serviceability Index (PSI) is a numerical index computed from objective measurements of certain types of pavement surface characteristics. The PSI indicates the pavement's ability to serve traffic at any time in its life history. This index method was developed by the AASHO Road Test Present Serviceability Rating (PSR) on a scale of 0 to 5. From 0 to 1 PSI was termed very poor, and 4 to 5 was very good. The PSI was developed to correlate various parameters about the distress of pavement such as slope of variances, cracking, rutting and patching.

In the AASHTO-1993 system, the loss of serviceability is the difference between the initial serviceability and terminal serviceability. It is the only performance indicator. In the AASHTO system the roughness scale for ride quality ranges from 5 to 0. For pavement design it is necessary to select both an initial and terminal serviceability index. An initial serviceability index of 4.2 is suggested to reflect a newly constructed pavement. A terminal serviceability index of 2.5 is suggested to be used in the design of major highway agency such as Alberta Transportation [28]. The design serviceability loss, ΔPSI, is the difference between the newly constructed pavement serviceability and that accepted before rehabilitation.

2.2.6 Advantages of the AASHTO-1993 Design Method

AASHTO-1993 has been the most popular pavement design method around the world for more than 50 years. There are several advantages of AASHTO-1993 design method exists in compare to other empirical methods such as United States Army Corps of Engineers (USACE), National Crushed Stone Association (NCSA), and Portland Cement Association (PCA) and so on. AASHTO-1993 pavement design method is very simple in nature. Due to its simplicity, the AASHTO-1993 design method is very easy to implement. Users can design pavements within a very short time using different design charts available in the guide or by plugging a design equation into Microsoft Excel or an equivalent tool.

2.2.7 Limitation of the AASHTO-1993 Design Method

The AASHTO design guide was developed based on the specific conditions of the AASHO Road Test. This guide is not realistic to use empirically derived relationships to explain phenomena that occur outside the range of the original data used to develop the empirical relationships. The limitations of the AASHTO-1993 Guide are: (a) Design errors may occur if pavement is designed with materials and roadbed soils other than those used in the AASHO road test ; (b) Less accurate results may occur if pavement is used in different environments than that of AASHO road test; (c) this guide does not consider incremental effects of loadings; (d) this guide may produce inaccurate results if traffic distributions differ from those used in the AASHO road test ; (e) AASHTO-1993 pavement design procedures do not adequately represent climatic effects on pavement performances. AASHTO-1993 has only two input parameters related to the environment: drainage and the seasonal variation of sub-grade support. Though these two parameters are important, however, they alone are not adequate. (f) One major deficiency of the empirical approach is that it is insufficient in evaluating the performance of the pavements. There is no provision to predict other modes of failure, such as fatigue, rutting and thermal cracking. In fact, these types of failures in many cases dictate the scheduling of maintenance and planning of rehabilitation [3]. (g) The empirical nature of the AASHTO design approach does not account for the mechanistic response of asphalt concrete. The mix design procedure relies on physical properties, which cannot relate to the pavement structural response [17]. Empirical nature of AASHTO, results above shortcomings

that have been addressed by Mechanistic Empirical (M-E) pavement design method.

2.3 Overview of the MEPDG

The Mechanistic Empirical Pavement Design Guide (MEPDG) was recently introduced in the United States [3]. This guide was developed by the National Cooperative Highway Research Program (NCHRP 1-37 A) under sponsorship by the American Association of State Highway and Transportation Officials (AASHTO). MEPDG aims at providing the highway community with a modern practice tool for designing new as well as rehabilitated pavement structures, based on mechanistic-empirical principles. The MEPDG and other associated software are suitable for analyzing and predicting the performance of different types of flexible and rigid pavements.

The MEPDG analyzes input data for traffic, climate, materials and proposed structure using mechanistic-empirical numerical models. The models estimate damage accumulation over the service life of the pavement. The Guide is primarily concerned with the concept of pavement performance which accounts for structural and functional performance [29]. The benefit of the mechanistic procedure is the ability to calibrate design procedures to local climate conditions and material properties.

The current version of MEPDG, developed by NCHRP project 1-37 A, is currently under evaluation by several transportation agencies. The goal of these evaluations is to adapt and calibrate the MEPDG software for local conditions. A significant facet of this process is to evaluate the performance prediction models and sensitivity of the predicted distresses to various input parameters for local conditions and, if necessary, re-calibration of the performance prediction models is required.

2.3.1 MEPDG Analysis Procedure

Pavement design through MEPDG is an iterative procedure based on analysis of the MEPDG software results for trial designs proposed by the designer. A trial design is investigated for sufficiency against input performance criteria. The output of the MEPDG software is a prophecy of distresses and smoothness against a set of reliability values. If the predictions do not meet the expected performance criteria at the given reliability, the trial design is amended and the evaluation is repeated. The designer can control incremental adjustments to the pavement structure and the

specification of each performance criterion used in the pavement design procedure. Figure 2.2 shows a process for designing flexible pavements.

Figure 2.2: Overall Design Process for Flexible Pavements in MEPDG [13]

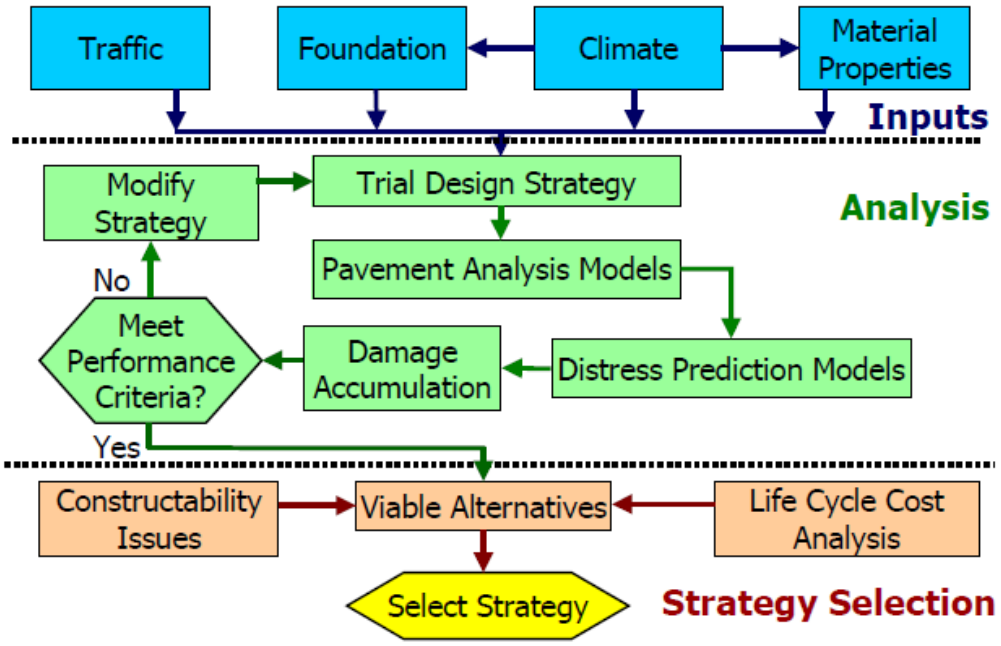

The MEPDG design approach brought a radical change from previous empirical pavement design methods. Unlike generating a structure with specific layer thicknesses like AASHTO, the MEPDG requires an initial assumption of the layered pavement structure and generates a prediction of the pavement's performance. The initial layer thicknesses can be calculated from experience or by using old design methods. The MEPDG helps to evaluate pavement damage incrementally, which incorporates the hourly effect of climate as well as material properties throughout pavement design life. Three design levels were integrated in the model for users to select according to their needs. The MEPDG software requires extensive information on traffic, climate, and material properties as input to create the initial layered structure. Different design levels and information regarding traffic, climate and material input are described in the following sections.

2.3.2 Design Input Level Hierarchy

Three input levels were incorporated in the MEPDG. Three levels of input depend on

the importance of the project, availability of input information to the designer, and the sensitivity of the pavement performance to a given input. These three levels of design inputs are discussed as follows.

Level 1

This level of input requires the most precision input values. It requires site and/or material-specific inputs which can be obtained through direct testing or measurements such as site-specific axle-load data collection and laboratory testing of dynamic modulus for Hot Mix Asphalt (HMA). This level involves more time and resources.

Level 2

This is an intermediate level in terms of prediction and accuracy. If resources or laboratory testing equipment are not available, the designer can use data from limited testing, an agency data base, or correlations. For example, the dynamic modulus could be estimated based on existing test results from binders, aggregate gradation and mix properties.

Level 3

This level produces the lowest accuracy. In this level the designer selects the input from national or regional default values, such as characterizing the HMA using its physical properties (gradation) and type of binder used.

2.3.3 Environmental Factors Affecting Pavement Performances

There are two main environmental factors, moisture and temperature, which can change the pavement layer and subgrade material's properties for a pavement structure and, consequently its strength, durability and load-carrying capacity [13]. During the cold winter months, the asphalt-bound materials modulus value can increase by 20 times its value of the hot summer months. Asphalt stripping happens drastically with excessive moisture. Similarly, at freezing temperatures, the resilient modulus of unbound materials becomes very high in comparison to the thawing months. Also the moisture content breaks up the cementation between soil particles and affects the state of stress of unbound materials. If the moisture content increases, then the modulus of the unbound materials decreases.

In short, environmental factors play a significant role in pavement performance [30]. All the distresses considered in the MEPDG are affected by environmental factors to some degree [12]. The Enhanced Integrated Climate Model (EICM) is a powerful climate effects modeling tool, used to model temperature and moisture within each pavement layer and sub grade in the MEPDG software [13]. The version of the EICM incorporated into the MEPDG is based on improvements to an earlier version of the Integrated Climate Model (ICM) [14]. EICM offers distinct benefits compared to previous procedures [15].

2.3.3.1 Enhanced Integrated Climatic Model

EICM was initially developed as the Integrated Climatic Model (ICM) designed for the FHWA in 1989 at Texas A & M University. Larsen and Dempsey revised the original model in 1997, and consequently released the ICM version 2.0 [14]. The EICM was amended for use in the MEPDG and undertook several key modifications under the NCHRP 1-37A study. Version 2.1 is currently referred to as EICM.

EICM is a one-dimensional coupled heat and moisture flow program that implies changes in pavement and sub grade characteristics and behavior along with environmental conditions over the service period of the pavement [31]. It simulates the upper boundary conditions of a pavement-soil system by producing patterns of solar radiation, precipitation, wind speed, cloud cover, and air temperature [32]. The EICM consists of three main components including the Climate-Materials Structural model (CMS Model) developed at the University of Illinois [3], a frost-heave and settlement model (CRREL model) developed at the United States Army Cold Regions Research and Engineering Laboratory, and an Infiltration-Drainage model (ID model) developed at the Texas Transportation Institute at Texas A & M University [33].

EICM has been incorporated in the MEPDG to simulate the climatic effects in the behaviour and characteristics of pavement and sub-grade materials over the design period. The following are the required inputs of EICM [24]:

- Model analysis parameters: the exact date and duration of the analysis period
- Climatic data inputs: hourly air temperature, wind speed, percent of sunshine (used to define cloud cover), precipitation, relative humidity, and water table depth.

- Material properties: thermal conductivity, heat capacity, and total unit weight.
- Pavement structure: select layers type, thickness, and number of elements.
- Base course moisture models: Thornthwaite Moisture Index (TMI) or ID Model.

One of the main outputs of the EICM is a set of adjustment factors for layers of unbound materials. The adjustment factors are responsible for the effects of environmental parameters and conditions such as moisture-content changes, freezing, thawing, and recovery from thawing. These factors are used to calculate the composite environmental adjustment factor (F_{env}), which further is used by the MEPDG to adjust the unbound materials resilient modulus as a function of location and time [24].

Other important outputs of the EICM include the predictions of in situ temperature and moisture profiles. In the MEPDG, the predicted temperature profile through the asphalt layer is used in both fatigue and permanent deformation prediction models, whereas the predicted moisture profile is used in the permanent deformation model for the unbound materials [24]. Also, the EICM computes and predicts the following data throughout the pavement profile: resilient modulus adjustment factors, pore water pressure, water content, frost and thaw depth, frost heave, and drainage performance throughout the complete pavement and subgrade profile for the entire design life of the pavement structure [15].

The function of the model is to document the user-supplied resilient modulus M_R of all unbound layer materials under primary conditions, usually at near-optimum moisture content and maximum dry density. After that the model estimates the probable changes in moisture content and the effect on the user-entered resilient modulus. The model also assesses the effect of freezing on the layer M_R and the effect of thawing and recovery from the frozen M_R condition. The model supplies varying M_R values in the calculation of critical pavement response parameters and damage at different points within the pavement system. For the asphalt-bound layer, the model estimates the changes in temperature to permit the calculation of the dynamic modulus and thermal cracking. This EICM model is applicable to both asphalt concrete (AC) and PCC pavements [13].

2.3.3.2 Way of using climatic parameters by the MEPDG

The MEPDG software uses the climatic input data including hourly air temperature, wind speed, sunshine percentage (used to define cloud cover), precipitation, relative humidity and water table depth in a specified format [13]. Air temperature, wind speed, and percent sunshine are used to estimate the heat transfer between the road and the atmosphere, as shown in Figure 2.3.

Figure 2.3: Heat Transfer between Pavement and Air on a Sunny Day [34]

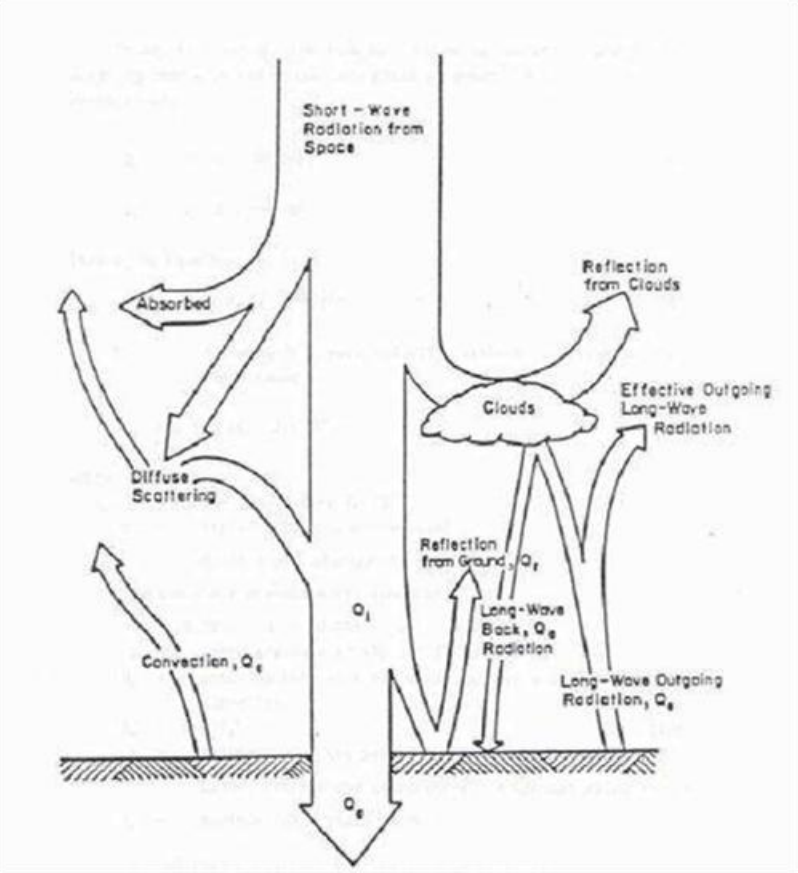

Temperatures throughout the pavement structure are dominated by atmospheric conditions at the surface. While measuring air temperatures is relatively simple, there is not a direct correspondence between the air temperatures and pavement surface temperatures. To estimate the pavement temperature, the energy balance at the surface being used in the CMS model is described in Figure 2.3 and the equation below (2.3). The Design Guide predicts pavement temperature for every hour based on the following equation:

$$Q_i - Q_r + Q_a - Q_e \pm Q_c \pm Q_h \pm Q_g = 0 \quad (2.3)$$

Where,

Q_i = Incoming short wave radiation

Q_r = Reflected short wave radiation

Q_a = Incoming long wave radiation

Q_e = Outgoing long wave radiation

Q_c = Convective heat transfer

Q_h = Effects of transpiration, condensation, evaporation, and sublimation

Q_g = Energy absorbed by the ground

Wind speed affects the convective heat transfer between the pavement and air. Convective heat transfer happens when the air temperature and pavement surface temperature are not the same. Heat transportation always occurs from a warm to a cold place, and results in either a gain or loss of heat to or from the pavement [3]. Higher wind speed increases the rate of convection. In a heat balance equation, the percent of sunshine is used in the calculation at the pavement surface, and can be estimated as a numerical illustration of cloud cover. Incoming shortwave radiation is mostly accountable for daytime radiation heating and is dependent on the angle of the sun and the amount of cloud cover. The angle of the sun is related to the latitude, date, and time of day. To determine the infiltration of moisture in pavements precipitation data is used by the EICM. If the average daily temperature in a month is less than 0°C, in that month all precipitation is assumed to be snow. To model the moisture gradient of both JPCP and CRCP, relative humidity values are used. The EICM needs this information on an hourly basis throughout the entire life cycle of the pavement to make temperature and moisture predictions at all depths. Because the mechanical properties of materials and distress development are impacted by temperature and moisture, the EICM software provides a discrete benefit over previous procedures [35]. To satisfy the requirements for hourly data on the previously mentioned parameters, the EICM uses climatic data obtained from the climate data base available for the station.

The Design Guide is a noteworthy revolution in the way pavement design is carried

out. The climate part in the Design Guide software requires the designer to specify a climate file for the project location stored in the database. The user has an opportunity to generate a weather file by interpolating climatic data from selected nearby weather stations

2.3.4 Traffic

The traffic information is a key element for the structural design of pavement. The traffic description proposed in the MEPDG is more specific than the conventional ESALs technique adopted in AASHTO. In the MEPDG load, spectra for single, tandem, tridem and quad axles are introduced. Traffic data, including truck count by class, by direction and lane, are required for traffic characterization. For each vehicle class, axle-load spectra distributions are developed from axle-weight data. Traffic volumes by vehicle class are forecasted for the design analysis period. The total number of axle applications for each axle type and load group is determined over the design period in the traffic section. To determine the pavement responses and distress prediction the number of applications for each axle type and load increment is used. The pavement response module also needs data related to the axle configuration, such as average axle width, dual tire spacing, tire pressure and axle spacing. Traffic wander impacts the number of load applications over a point. This parameter affects the prediction of fatigue and permanent deformation.

The MEPDG has kept a provision for the special axle configuration which is a vital feature of this guide. This feature helps the user to evaluate pavement performance due to any kind of non-conventional vehicle systems. Vehicle operational speed is one of the important inputs for the flexible pavement design. It directly influences the stiffness response of the asphalt concrete layers. The magnitude and duration of stress pulses produced by the moving traffic is subject to the vehicle speed, type and geometry of pavement structure, and the location of the element under consideration. The dynamic modulus of the asphalt concrete layer is calculated with the use of frequencies corresponding to various vehicle speeds.

2.3.5 Pavement Materials Characterization

Mechanistic pavement design procedures are complex and involve the interaction of the pavement structure model that estimates the state of stresses and strains with the

imposed traffic loads and environmental conditions. Material characterization techniques were investigated to produce mechanistic properties suitable for the new trend in modeling for the ME design approach. MEPDG requires a large set of material properties. The material inputs needed for the design process may be classified in one of the three major groups: pavement response model material inputs, material-related pavement distress criteria, and climatic model material inputs [24] The pavement response models use material properties such as elastic modulus (E) and Poisson's ratio (μ) to compute the state of stress/strain and deflection at critical locations within the pavement structure subjected to traffic loading and temperature variations. These structural responses are used by the distress models along with complementary material properties to predict pavement performance. Climatic-related properties are used to determine temperature and moisture variation inside the pavement structure. Material characterization models interact with the environmental models. This interaction helps to determine the temperature and moisture profile throughout the pavement structure. In the material characterization model, material inputs include engineering properties such as the plasticity index and porosity, and thermal properties such as heat capacity and absorptivity. The state of the different materials forming the road layers and, consequently, the response of the structure, changes with variation in temperature and moisture conditions. An effective analytical model including material characteristics accounts for all of these factors in analysis, leading to a performance-based road design in the MEPDG. Different material characterizations are illustrated in the following subsections [13].

2.3.5.1 Hot Mix Asphalt Concrete (HMA) Materials Characterization

The key input parameter for flexible pavement design is the HMA dynamic modulus (E). At level 1 input, the MEPDG requires the HMA dynamic modulus to estimate from laboratory testing following guidelines presented in AASHTO TP 62 or ASTM D3497. The asphalt binder complex shear modulus and phase angle testing (AASHTO T315) are also necessary for level 1. For levels 2 and 3, Witczak's dynamic modulus prediction model, which requires HMA gradation, air voids, volumetric binder content, and asphalt binder type as inputs, is used to estimate E and develop the Master Curve. Additional testing is necessary to characterize HMA for predicting thermal cracking. The additional testing includes tensile strength

(AASHTO T322), creep compliance (AASHTO T322), and thermal conductivity and heat capacity (ASTM E 1952 and ASTM D2766) [24].

2.3.5.2 Portland Cement Concrete (PCC) Materials Characterization

The material characterization input parameters required for the MEPDG to design and analyze the rigid pavement include: the elastic constants (elastic modulus, Poisson's ratio) of the PCC to compute the developed stresses and strains in the concrete slab. The modulus of rapture of flexural strength (MR) is required to estimate the fatigue life of the concrete. The coefficient of thermal expansion (CTE) is necessary to calculate the joint opining and curling-induced stresses in the slab. The composite modulus of subgrade reaction (k-value) is used to calculate the surface deflections and joint faulting [24].

2.3.5.3 Chemically Stabilized Materials Characterization

The chemically stabilized materials covered in the MEPDG include lean concrete, cement stabilized, cement treated open-graded drainage layer, soil cement, lime, cement, and fly ash treated materials. The elastic modulus of the layer is the primary input parameter for chemically stabilized materials. For lean concrete and cement treated materials in new pavements, the elastic modulus is determined using ASTEM C 469. For lime stabilized materials, AASHTO T 307 protocols apply [24].

2.3.5.4 Unbounded Base, Sub-base, and Subgrade Materials

The main input parameters required by the MEPDG for unbound materials include the resilient modulus at optimum moisture content, Optimum Moisture Content (OMC) and Maximum Dry Density (MDD), specific gravity, saturated hydraulic conductivity, and Soil Water Characteristic Curves (SWCC) parameters.

The resilient modulus input can be obtained as a function of stress state at level 1 for HMA pavements. However, this approach is not recommended at this time in the MEPDG. At levels 2 and 3, they can be estimated with other, more easily obtained soil properties. For example, at level 2, the unbound layer M_r can be estimated through correlations with several other commonly tested soil properties such as the California Bearing Ratio (CBR), R-value, and AASHTO layer coefficients (a_i). At level 3, the resilient modulus of unbound materials is selected based on the unbound material classification (AASHTO or USC) either from agency-specific testing or by

adopting the MEPDG defaults. The MEPDG provides a general range of typical modulus values (based on LTPP averages) for each unbound material classification at their optimum moisture content and maximum dry density [24].

2.3.6 Flexible Pavement Response Models

The flexible pavement response model determines the structural response of the pavement system due to external loads such as traffic loads and environmental influences. Environmental load is applied on the pavement structure directly (e.g., strains due to thermal expansion and/or contraction) or indirectly through alterations in the material properties such as changes in stiffness due to temperature and/or moisture effects.

The pavement response model produces the stresses, strains, and displacements within the pavement layers. In MEPDG the critical response variables are used as inputs to the pavement distress models which are as follows:

- Tensile horizontal strain at the bottom/top of the HMA layer to predict fatigue cracking;
- Compressive vertical stresses/strains within the HMA layer for prediction of HMA rutting;
- Compressive vertical stresses/strains within the base/sub base layers for prediction of rutting of unbound layers; and
- Compressive vertical stresses/strains at the top of the subgrade for prediction of subgrade rutting.

Critical response variables need to be evaluated at the critical location within the pavement layer where their values are maximum. The critical locations are decided by inspection for a single wheel loading. For example, for a single wheel load, the tensile horizontal strain reaches its maximum value under the center of the wheel at the bottom of the HMA layer. For multiple wheels and/or axles, the position of the critical location depends on the wheel load configuration and the pavement structure. The critical location within the pavement structure of the pavement response parameters will not be same for all vehicle types in mixed traffic conditions (single plus multiple wheel/axle vehicle types). The pavement response model explores the

critical location for each response parameter in these cases.

Two flexible pavement analysis methods have been implemented in the MEPDG which are discussed below:

2.3.6.1 Multilayer Linear Elastic Analysis Method

There are different considerations related to this method ,such as each layer is homogeneous, has finite thickness except for the subgrade, is isotropic, leads to full friction developing between layers at each interface, and has no surface shearing forces. Two material properties such as elastic modulus and Poisson's ratio of each layer are crucial to determine pavement stress and strain in this method [17].

2.3.6.2 Finite Element Method

A nonlinear finite element procedure is used to consider the unbound material nonlinearity instead of determining the pavement stresses, strains, and displacements.

2.3.7 Design Reliability

The design of flexible pavements deals with many factors that lead to a considerable amount of uncertainties. These factors include traffic levels, material properties and construction quality, model prediction errors, and calibration measurement errors. These uncertainties can be dealt with in pavement design through both deterministic and probabilistic framework. Each design factor has a fixed value based on the factor of safety assigned by the designer in the deterministic method. In addition, each design factor is assigned a mean and a variance in the probabilistic method.

Reliability (*R*) is described as the probability (*P*) that each of the fundamental distress types and smoothness levels will be less than a selected critical level throughout the design period. *R* = *P* [Distress over Design Period < Critical Distress Level]. Design reliability is defined for smoothness (IRI) as follows: *R* = *P* [IRI over Design Period < Critical IRI Level]. Design reliability for key distress such as fatigue cracking is defined as follows: *R* = *P* [Fatigue Cracking over Design Period < 20 percent lane area]. Note that this definition is different from the AASHTO Design Guide in that it considers each distress and the IRI directly in the definition. AASHTO defines reliability in terms of the number of predicted equivalent single axle loads to terminal serviceability (*N*) being less than the number of equivalent single axle loads actually

applied (n) to the pavement. $R = P$ [$N < n$]. AASHTO produced results indicating that thicker pavements always increased design reliability. However, this is not always true for the key performance measures adopted in the MEPDG. In the approach taken in MEPDG, several design features other than thickness (e.g., HMAC mixture design, dowels for jointed plain concrete pavements, and sub-grade improvement for all pavement types) can be considered to improve the reliability estimate of the design [17].

Recommended levels of reliability for predicted distresses by the MEPDG are based on the functional class of the roadway as shown in Table 2.1.

Table 2.1: Illustrative Levels of Reliability for New and Rehabilitation Design [13]

Functional Classification	Recommended Level of Reliability for Pavement Distresses	
	Urban	Rural
Interstate/Freeway	85 – 97	80 – 95
Principal Arterials	80 – 95	75 – 90
Collectors	75 – 85	70 – 80
Local	50 – 75	50 – 75

2.3.8 The MEPDG Distress Prediction

In the MEPDG the critical stress and/or strain values computed by the pavement response model discussed in the above section are transformed to incremental distresses, either in absolute terms, such as in rut depth calculation, or in terms of a damage index in fatigue cracking. The calibrated distress prediction models transform the cumulative damage to physical cracking and at the end of each analysis the output is tabulated and plotted for each distress type by the MEPDG software.

The different structural distresses considered in flexible pavement design and analyses are as follows:

- Bottom-up fatigue cracking (alligator);
- Surface-down fatigue cracking (longitudinal);
- Fatigue in chemically stabilized layers (in semi-rigid pavements);
- Thermal cracking; and
- Permanent deformation (rutting).

The MEPDG achieves the feasible pavement designs in an iterative manner. The steps of the design process include [13]:

1. Decide pavement performance criteria such as rutting level, cracking, and smoothness at the end of the design life and the desired level of reliability for each.
2. Perform a trial design based on the other pavement design guide or prior experience.
3. Forecast performance over the design life.
4. Estimate the predicted performance against the design limits.
5. If the design criteria are not satisfied, revise design and repeat steps 3 and 4 until the design does satisfy the performance requirements.

2.3.9 Performance Prediction Models

Pavement structure accumulates damage due to traffic and environmental load with time. Performance predictions of a road are expressed in terms of pavement distresses and ride quality. The major distresses predicted by the MEPDG for flexible pavements are as follows:

- Permanent deformation (rutting).
- Fatigue cracking (bottom-up and top-down).
- Thermal cracking.

In addition, pavement smoothness (IRI) is predicted based on these primary distresses and other factors. The MEPDG design procedure empirically correlates IRI with other distresses for all types of pavement.

The methodology in the MEPDG uses an incremental damage approach in pavement design and analysis. Distress or damage is estimated and accumulated for each analysis interval. The basic unit for estimating the damage is assumed as an analysis interval of one month. However, the analysis time interval reduces to bimonthly during freeze and thaw periods due to the quick change in the modulus under these conditions. The change in temperature and moisture conditions directly affects the material response and hence the performance. The pavement performance prediction models are elaborated in the following sections.

2.3.9.1 Permanent Deformation

One of the most significant load-induced distresses occurring in flexible pavement structure is permanent deformation. Permanent deformation includes rutting in the wheel path, which grows gradually with accumulation of load repetitions. Rutting normally appears as longitudinal depressions in the wheel paths accompanied by small upheavals to the sides. The intensity of rutting is highly dependent upon the pavement structure (layer thickness and quality), traffic matrix and quantity as well as the environment at the design site [13]. Regardless of the material type considered, there are generally three distinct stages for the permanent deformation behavior of pavement materials under a given set of material, load and environmental conditions which can be described as follows [13]:

• Primary Stage: high initial level of rutting, with a decreasing rate of plastic deformations, predominantly associated with volumetric change.

• Secondary Stage: small rate of rutting exhibiting a constant rate of change of rutting that is also associated with volumetric changes; however, shear deformations increase at increasing rate.

• Tertiary Stage: high level of rutting predominantly associated with plastic (shear) deformations under no volume change conditions.

The MEPDG employs the incremental damage approach to calculate the damage or rutting in each layer in the pavement structure. The MEPDG models only the initial and secondary permanent deformation stages shown in Figure 2.4. The primary stage is modeled using an extrapolation of the secondary stage trend. The tertiary stage is not considered in the model [17]. Once the material type of each sub-layer is identified, an appropriate model is used by the system to calculate the accumulated plastic strains at the mid-depth of each sub-layer in each sub-season. The total permanent deformation is then calculated as the sum of permanent deformation in each sub-layer [24].

Figure 2.4: Pavement Deformation Behaviour of Pavement Materials [17]

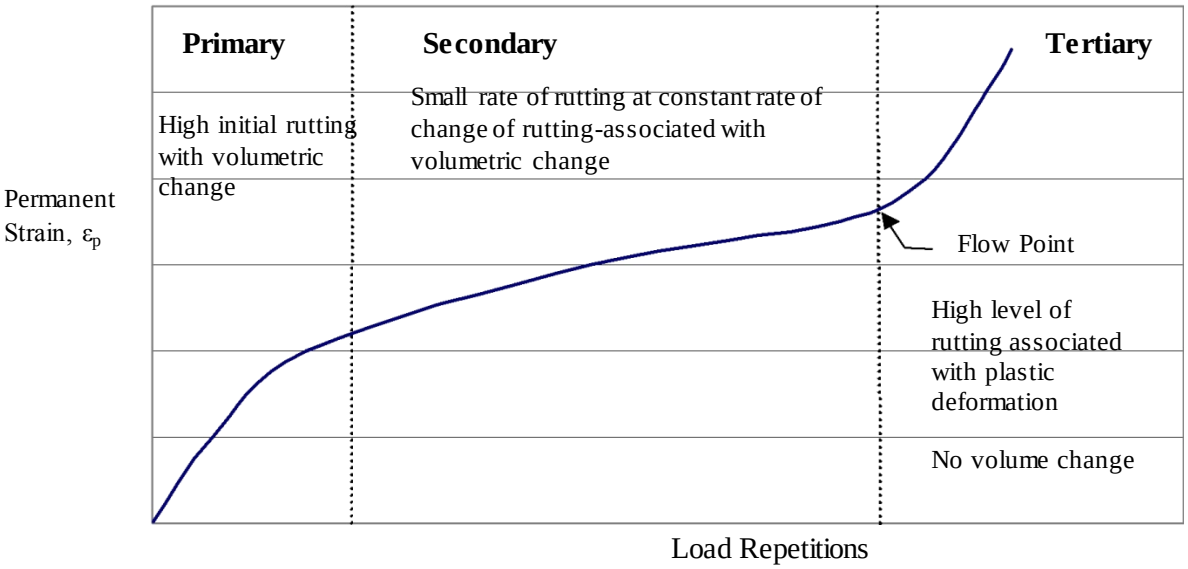

For a layered pavement, cross-section vertical strain at any given depth is computed by the structural response model using the elastic properties of the material which is given by the equation,

$$\varepsilon_{rz} = \frac{1}{E} * \left(\sigma_z - \mu\sigma_x - \mu\sigma_y\right) \tag{2.4}$$

where, ε_{rz} is the resilient strain, σ_x, σ_y and σ_z are the stresses developed along x, y and z axis respectively, μ is the Poisson ratio and E is the elastic modulus of the material.

Laboratory test results determine the plastic strain, which has the following form:

$$\varepsilon_p / \varepsilon_r = a_1 T^{a2} N^{a3} \tag{2.5}$$

Where:

ε_p = accumulated plastic strain at *N* repetitions of load (in/in)

ε_r = resilient strain of the asphalt material as a function of mix properties, temperature and time rate of loading (in/in)

N = number of load repetitions

T = temperature (deg F)

a_i = non-linear regression coefficients

The total permanent deformation is the summation of incremental rutting for different conditions over the design period. Details of the method for calculating the permanent deformation of each layer are given in Part 3-Chapter 3 of the MEPDG documentation [13].

2.3.9.2 Fatigue Cracking

Tensile and shear stresses are developed in the asphalt layer due to repeated traffic loads. Fatigue cracking starts at locations of critical strain and stress. Critical strain occurs at the locations where the subjected load is maximum. Critical strain depends on the stiffness of the asphalt layer. Two types of fatigue cracking occur in the asphalt layer. The first type is known as fatigue cracking that commences due to bending action, which develops flexural stresses at the bottom of the asphalt layer. The second type of fatigue cracking, which propagates from the surface to the bottom, is assumed to be due to critical tensile and or shear stresses which occur at the surface due to high contact pressures at the tire edges-pavement interface. When the asphalt layers are very thin and old, second type fatigue cracking is more likely to happen.

Both types of fatigue cracking are estimated based on Miner's law which is as follows.

$$D = \sum_{i=1}^{T} \frac{n_i}{N_i} \tag{2.6}$$

where,

D = pavement damage

T = total number of periods

n_i = actual traffic for period i

N_i = traffic allowed under conditions prevailing in i

The model used to represent fatigue cracking is given below:

$$N_f = Ck_1(1/\xi_t)^{k_2}(1/E)^{k_3} \tag{2.7}$$

where,

N_f = number of repetitions to fatigue cracking

ε_t = tensile strain at the critical location

E = stiffness of the material

k_1, k_2, k_3 = laboratory regression coefficients

C = laboratory-to-field adjustment factor

2.3.9.3 Thermal Cracking Model

The thermal fracture of the pavement is modeled in the MEPDG based on the visco-elastic properties of the asphalt mixture. The Thermal Cracking Model (TCMODEL), is an enhanced version of the Strategic Highway Research Program (SHRP) model. The procedure measures the creep compliance at one or three temperatures depending on the level of analysis with the help of the HMA mix representation in an indirect tensile mode. The master creep compliance curve is then expressed by a power model as follows:

$$D(\xi) = D_0 + D_1\xi_m \tag{2.8}$$

where

D (ξ) = creep compliance at reduced time ξ

D_0, D_1 = Prony series parameters

m = power slope parameter

Then the relation between compliance D(t) and the relaxation modulus E_r of the asphalt mix is established using viscoelastic transformation theory. The relaxation modulus is expressed by a generalized Maxwell model using a Prony series relationship:

$$E(\xi) = \sum_{i=1}^{N+1} E_i e^{\frac{-\xi}{\lambda i}} \tag{2.9}$$

where:

E(ξ) = relaxation modulus at reduced time ξ

E_i, λi = Prony series parameters for master relaxation modulus curve (spring constants or moduli and relaxation times for the Maxwell elements)

The thermal stresses in the pavement can be computed using equation (2.10) once the relaxation modulus is known from equation (2.9)

$$\sigma(\xi) = \int_0^{\xi} E(\xi - \xi') \frac{d\xi}{d\xi'} d\xi' \qquad (2.10)$$

where,

$\sigma(\xi)$ = stress at reduced time ξ

$E(\xi\text{-}\xi')$ = relaxation modulus at reduced time $\xi\text{-}\xi'$

ε = strain at reduced time $\xi = (\alpha\,(T(\xi') - T_0))$

α = linear coefficient of thermal contraction

$T(\xi')$ = pavement temperature at reduced time ξ'

T_0 = pavement temperature when $\sigma = 0$

ξ' = variable of integration.

The Paris law of crack propagation predicts the amount of crack propagation made by a given thermal cooling cycle which is shown in equation (2.11)

$$\Delta C = A\Delta K^n \qquad (2.11)$$

where:

ΔC = change in the crack depth due to a cooling cycle

ΔK = change in the stress intensity factor due to a cooling cycle

A, n = fracture parameters for the asphalt mixture

The stress intensity K is estimated based on an analytical finite element method analysis shown in equation (2.12).

$$K = \sigma(0.45 + 1.99C_0^{0.56}) \qquad (2.12)$$

where:

K = stress intensity factor

σ = far-field stress from pavement response model at depth of crack tip

C_o = current crack length, feet

The value of the parameter (n) in Equation (2.11) is given by Equation (2.13)

$$n = 0.8(1 + 1/m) \quad (2.13)$$

where the value of m given in equation (2.13) is determined from the master creep compliance curve power function in equation (2.8). The fracture parameter (A) given in equation (2.11) is given by equation (2.14)

$$A = 10^{(\beta*(4.389 - 2.52\log(E*\sigma_m*n)))} \quad (2.14)$$

where

E = mixture stiffness, psi

σ_m = undamaged mixture tensile strength, psi

β = calibration parameter

The length of the thermal cracks is estimated based on the relationship between the probability distribution of the log of the crack depth to the HMA layer thickness ratio and the percent of cracking. The thermal crack depth is found by the following equation:

$$C_f = \beta * N(\log C / h_{ac} / \sigma) \quad (2.15)$$

where:

C_f = observed amount of thermal cracking

β_1 = regression coefficient determined through field calibration

N (z) = standard normal distribution evaluated at (z)

σ = standard deviation of the logarithm of crack depth of in the pavement
C = crack depth

h_{ac} = thickness of asphalt layer

The thermal cracking model assumes a maximum crack length of 400 ft in every 500 ft, which is equivalent to a crack across a lane width of 12 feet spaced at 15 feet along the pavement length. The model can only predict 50% of this maximum amount. The model assumes failure occurs when the average crack depth reaches the thickness of the asphalt layer.

2.3.9.4 Smoothness Models (IRI)

All pavement distresses discussed in section 2.3.9.1 to 2.3.9.3 are responsible for the

loss of pavement smoothness. Smoothness of a road surface is usually measured by its roughness. The smoothness is defined as the variation of surface elevation that causes vibrations in navigating vehicles. The MEPDG accepted the international roughness index (IRI) as a measure for smoothness. In addition to the other pavement structural distresses, a terminal IRI is specified at a defined level of design reliability as the performance criteria for smoothness. The smoothness model accumulates changes due to the increase in individual distress, site conditions and maintenance activities to the initial smoothness (IRI) over the design period. These distresses include rutting, bottom-up/top-down fatigue cracking, and thermal cracking for flexible pavements. The IRI model uses the distresses predicted using the models included in the MEPDG, initial IRI, and site factors to predict smoothness over time. The site factors include sub-grade and climatic factors responsible for the roughness caused by shrinking or swelling soils and frost-heave conditions. IRI is estimated incrementally over the entire design period.

The MEPDG distress prediction models, such as fatigue cracking, permanent deformation and thermal cracking are empirically correlated to smoothness. The smoothness model considers other distresses as well, such as potholes, longitudinal cracking outside the wheel path, and block cracking if there is potential of occurrence. The user needs to set an initial IRI value, typically between 50 to 100 in/mile, to estimate the terminal IRI value using the MEPDG smoothness (IRI) prediction model. Long Term Pavement Performance (LTPP) data were used to embed the following equations to predict IRI for new HMA pavement in the MEPDG.

$$IRI = IRI_0 + 0.0150(SF) + 0.400(FC_{total}) + 0.008(TC) + 40.0(RD) \qquad (2.16)$$

where,

SF = Site Factor

FC_{total} = Area of fatigue cracking (combined alligator, longitudinal, and reflection cracking in the wheel path), percent of total lane area. All load-related cracks are combined on an area basis – length of cracks is multiplied by 1 foot to convert length into an area basis

TC = Length of transverse cracking (including the reflection of transverse racks in existing HMA pavements), ft/mi.

RD = Average rut depth (in)

The site factor (SF) is calculated in accordance with the following equation.

$$SF = FROSTH + SWELLP * AGE^{1.5} \quad (2.17)$$

where:

FROSTH = LN([PRECIP+1]*FINES*[FI+1])

SWELLP = LN([PRECIP+1]*CLAY*[PI+1])

FINES = FSAND + SILT

AGE = pavement age, years

PI = sub-grade soil plasticity index

PRECIP = mean annual precipitation, in.

FI = mean annual freezing index, deg. F Days

FSAND = amount of fine sand particles in sub-grade (percent of particles between 0.074 and 0.42 mm)

SILT = amount of silt particles in sub-grade (percent of particles between 0.074 and 0.002 mm)

CLAY = amount of clay-size particles in sub-grade (percent of particles less than 0.002 mm)

2.3.10 Comparison between the AASHTO-1993 and the MEPDG

The MEPDG demonstrated significant improvements over the AASHTO 93 guide for pavement design and analysis which is explained below.

- The MEPDG addresses a wide range of pavement structures including new construction and rehabilitation of existing pavements. Pavement design and analysis are also now possible for composite structures, which address the importance of overlay AC pavement with PCC or the opposite.
- The MEPDG significantly improved the treatment of traffic-related variables. AASHTO-1993 depends on an equivalent standard axles load (ESAL), which is unable to incorporate explicitly the impact of the various characteristics of vehicles using the roadway network. The MEPDG extends characterization of road vehicles to consider tire pressure, axle load and distribution.
- The MEPDG incorporates the effect of the climate on the material response by

adjusting the values of the AC dynamic modulus and unbound resilient modulus according to seasonal changes in moisture and temperature.

- The MEPDG model has introduced a mechanistic material characterization that helps to evaluate the performance of newly developed materials such as engineered binders, unconventional gradations, and recycled materials, whereas, the limitations of AASHTO-1993 included dependence on information collected for a single native soil and road construction material within unique environmental and traffic conditions on which the AASHO Road test was performed in the 1960s.
- MEPDG enables to analyze foundation material (native soil) and existing pavement adequately that facilitate the model to evaluate a number of design options before implementation.

2.4 Summary

The AASHTO -1993 Guide is used by most of the road agencies throughout the world. The design process yields a set of layer combinations that satisfy the structural number. There are various deficiencies in the design process that were identified and described in the previous section. Progress made in engineering mechanics, analytical modeling and material characterization techniques inspired the road community to use the mechanistic design approach, such as the MEPDG, where the shortcomings of the AASHTO method could be overcome. Competencies of the proposed MEPDG are anticipated to inspire road agencies to switch to the new guide [16]. Improvements in the proposed MEPDG are expected to lead to more road agencies switching to the new guide. However, the sensitivity of different inputs and outputs of the MEPDG needs to be evaluated before implementation. Chapter 3 of this study aims for a sensitivity analysis of climatic parameters through evaluation of Canadian pavement performances. Also different pavement distress models of the MEPDG are examined in this study. Chapter 4 is focused on the comparison between the AASHTO-based Alberta Transportation Pavement Design method and the MEPDG. Chapter 4 also includes evaluations of the effects of traffic, subgrade strength and climatic factors on Alberta pavements.

Chapter 3

3. Evaluation of Canadian Climatic Files and Its Effects on Pavement Performances using the MEPDG

[Saha J. and Bayat A. Evaluation of the Canadian Climate Information and Its Effect on Pavement Performance through MEPDG Prediction, proceeding of Transportation Research Board annual conference, Washington DC, 2011.]

3.1 Introduction

Environmental factors such as precipitation, temperature, freeze-thaw cycles and depth to water table have significant influence on pavement performances [13]. The Mechanistic Empirical Pavement Design Guide (MEPDG) has incorporated the climatic effects through the Enhanced Integrated Climatic Model (EICM). Climatic information of 851 weather stations across the US was included as part of the MEPDG [3]. To advance the implementation of the MEPDG in Canada, the Transportation Association of Canada (TAC) has recently developed a climate database with a specific format to use in the MEPDG software.

Empirical pavement design procedure, such as the American Association of State Highway and Transportation Officials (AASHTO) – 1993, is the most popular pavement design procedure implemented by most transportation agencies around the world. However, it has only limited input climate parameters including drainage. Although this parameter is important, it is not adequate for pavement design and performance prediction. It is generally accepted that climate impacts pavement performance; however, it is difficult to quantify this impact from AASHTO – 1993 and other previous pavement design procedures. Unlike the AASHTO [23] method which has been described in detail in literature reviews, the MEPDG pavement performance prediction model exclusively incorporates the effects of environmental factors on pavement performances.

The objective of this study was to evaluate the Canadian climate files for the MEPDG and to investigate the influence of climate data on pavement performance. Available Canadian weather station files were categorized into several categories based on the

annual freezing index and mean annual precipitation to monitor the effects of climatic factors on pavement performance.

Existing Canadian climate files were evaluated and then incorporated to evaluate pavement performances using the MEPDG software version 1.1. In this study, a typical pavement cross-section was chosen and analyses were performed on this pavement for all 206 Canadian weather station files that are available for MEPDG application. Johanneck and Khazanovich performed a similar study for all weather stations across the US [3]. Pavement performances for different Canadian climate zones in terms of the International Roughness Index (IRI), Asphalt Concrete (AC) rutting, and total permanent pavement deformations and longitudinal cracking were studied and discussed.

3.2 Literature Review Related to the Evaluation of Climatic Effects on Pavement Performances using the MEPDG

Different literatures on pavement design and analysis methods including the AASHTO and MEPDG were reviewed in Chapter 2. In some literature, authors have conducted different studies to investigate the effects of climatic factors on pavement performances. Those literatures were also reviewed and some of them are provided in this section because they are related to the topic of this chapter.

Johanneck *et al.* [3] evaluated the US climatic database used for the MEPDG application and the effects of US climate on pavement performance predictions. To evaluate the quality of the climate data they first predicted pavement performances using actual climatic data of one station. Then they predicted pavement performances of the same station creating virtual weather station data, which incorporates data from nearby stations. Pavement performances found by using the actual and virtual weather data were compared. It was assumed in this analysis that the pavement performances predicted by using the actual and virtual weather station should produce similar results. However, these analyses produced significantly different results due to low-quality data of the nearby station or the test station. Johanneck *et al.* also conducted a comprehensive sensitivity analysis of different climate parameters on pavement performance prediction through the MEPDG using a climatic database consisting of 610 US weather station files available for the MEPDG

application. Analysis was performed at the national, regional and local levels and it was illustrated that the environment has a significant effect on predicted pavement performance. Johanneck *et al.* demonstrated that AC rutting and total permanent pavement deformation have a significant effect on pavement performance. However, they recommended that the IRI model used in the MEPDG needs to be calibrated because it is less sensitive towards climatic factors. They also illustrated some inconsistencies attributed to the low quality of the climatic data and emphasized developing a climatic database including large amounts of high-quality data that can eliminate year-to-year variations as well as yield more reliable prediction.

Breakah *et al.* [37] investigated the importance of using accurate climatic data to predict pavement performances using the MEPDG. Pavement performances predicted by using climatic files available with the MEPDG design guide and ones developed based on historic information for counties in the state of Iowa through the Iowa Environmental Mesonet were compared in the Breakah study. The climatic files that were interpolated from the data available within the design guide predicted higher rutting in both total and asphalt concrete layer, lower thermal cracking and lower IRI compared to the files developed in the Breakah study. Breakah *et al.* also found that there is a strong correlation between environmental factors (especially temperature and rainfall) and pavement distresses such as rutting in the AC layer, total pavement rutting, transverse cracking, and IRI and concluded that effects of climate on these pavement distresses are statistically significant. The outcomes of the study include: (a) temperature has a strong effect on thermal cracking and rutting in the AC layer; (b) moisture strongly affects unbound layers; (c) fatigue cracking results show evidence of the effects of temperature and moisture but the absolute values of the distresses were very low; and (d) effects of temperature and moisture were not prominent on longitudinal cracking in their study for the selected counties of the state of Iowa. They recommended considering more pavement sections to predict the fatigue and longitudinal cracking using the MEPDG. Breakah *et al.* recommended the following guidelines for designing pavements in the future using the MEPDG:

(a) Complete climatic data should be used for predicting pavement performances using the MEPDG. Climate data file requires information about hourly precipitation, air temperature, wind speed, percentage of sunshine, relative humidity, etc. for a minimum of 24 months for the MEPDG computational purposes [3].

(b) Climatic data files can be developed by each state's department of transportation and need to be continuously updated.

(c) Climatic data files that cover the project duration should be generated from the existing data files and these files should be used to simulate pavement performance during the given project life.

Tighe *et al.* [38] conducted a series of MEPDG analyses to assess the impact of pavement structure, material characteristics, traffic loads and climate on incremental and terminal pavement deterioration and performance on low volume roads at six site locations in British Columbia, Alberta, Manitoba, Ontario, Quebec and Newfoundland in Canada. The results of this study were dependent on many assumptions, especially those regarding the selection of sites and manipulation of climatic scenarios. Sites were selected from the Long Term Pavement Performance (LTPP) program for that study. As an outcome of the Tighe *et al.* study, it was revealed that climate has a significant effect on rutting (asphalt, base and sub-base layers), longitudinal and alligator cracking. However, transverse cracking was not as sensitive to the climate of their selected project site. This study also demonstrated the effects of climate change on selected pavement sections in southern Canada. The study showed that the current pavement design practices using temporal data do not fully achieve their design lives. Analysis of their deterioration-relevant climate indicators at the selected sites shows that over the next 50 years, low temperature cracking will become less problematic. Structures will freeze later and thaw earlier with correspondingly shorter freeze seasonal lengths. This will lead to higher extreme in-service pavement temperatures that will increase the possibility of pavement rutting. Additional maintenance and rehabilitation costs may be required to compensate for additional distresses related to climate change.

Smith *et al.* [1] conducted temperature and precipitation sensitivity analysis on pavement performance similar to the study conducted by Tighe *et al.* [38]. The study was conducted in Alberta and Ontario using the MEPDG and showed that: (a) IRI increases as temperature and precipitation increase; (b) As IRI increases, the other pavement performance indicators also increase; (c) Longitudinal cracking increases with more precipitation; (d) Alligator cracking increases as temperature and precipitation increase; and (e) Transverse cracking is not greatly affected by changes in temperature and precipitation except as seen in Ontario where transverse cracking

decreased when the temperature increased by 5ºC. Smith *et al.* also studied the effects of climate change on pavement performance. They mentioned that the estimated increment of average temperature in Canada is between 2ºC and 5ºC and the estimated increase in average precipitation is 0% to 10% over the next 45 years. This study shows the consequences of change of temperature and precipitation on pavement performances. This study quantifies the impact of climate change in the Canadian environment through the MEPDG using Canadian data from the Long-Term Pavement Performance program. This study showed that an increase in temperature has a negative impact on pavement performance in the Canadian environment. If the temperature increases 1ºC it would minimally affect maintenance, reconstruction, and rehabilitation (MR&R) activities. The initial study shows that Canadian transportation agencies would likely not change MR&R activities until a 2ºC or higher increase in temperature. Based on the analyses conducted at the selected sites in Alberta and Ontario it was observed that the MEPDG was not sensitive enough to precipitation or transverse cracking.

3.3 Availability of Canadian Climate Data for the MEPDG

To facilitate the implementation of the MEPDG in Canada, climate files are required based on specific climate factors and format for all Canadian provinces. Transportation Association of Canada (TAC) hired a consultant company to develop Canadian weather station files for the implementation of the MEPDG in Canada.

The Canadian climate data base applicable for the MEPDG includes a total of 232 weather station files. All 232 weather files were reviewed. It was found that out of 232 weather stations, one station in the Yukon does not have any data. Also, one weather station in Newfoundland and Labrador and eight weather stations in the Yukon have been reported twice. Therefore, there are 222 weather station files are available for the MEPDG spread out in different provinces of Canada. Of these 222 weather stations, 16 stations in different provinces have incomplete climate information or less than the 24 months worth of data recommended by the MEPDG software for computational purposes [14]. Therefore, only 206 weather stations in Canada were found to have complete climate data which can be used by the MEPDG. It is noted that a complete climate data file requires information about hourly precipitation, air temperature, wind speed, percentage of sunshine, relative humidity,

etc. for a minimum of 24 months for the MEPDG computational purposes [3]. Literature indicates that out of 851 available weather station files in the US, 610 had complete data files for the MEPDG [3]. The climatic information details (station name, location, latitude, longitude, mean annual air temperature, mean annual precipitation, start and end date of climate data record, number of available months of climate data and the classified climate zone) of 206 Canadian weather stations are presented in the Appendix A.1.1.

Table 3.1 presents the distribution of total and complete weather station files that are applicable for the MEPDG for each province in Canada. It also provides the mean, minimum, and maximum number of months available for the accessible weather stations in each Canadian province and territories for the MEPDG application. One sample of the climate data input file is provided in Appendix A.1.2. The input file contains weather-related information including year, month, day, hour, air temperature, total precipitation, wind speed, percent of sunshine and relative humidity.

Table 3.1: Distribution of Canadian Weather Station Files for the MEPDG

Canadian Province	Area	Number of weather station files		Density	Number of monthly data available in a weather file		
	(sq km)	Total number of files	Complete files*	Number of Station / 1000 sq.km	Max.	Min.	Mean
Alberta (AB)	661,848	27	27	4.1	240	34	201
British Columbia (BC)	944,735	29	28	3.1	240	29	209
Manitoba (MB)	649,950	14	10	2.2	240	20	208
New Brunswick (NB)	72,908	7	6	9.6	240	22	181
Newfoundland & Labrador (NL)	405,720	24	20	5.9	240	40	186
Northwest Territory (NT)	1,346,106	11	11	0.8	240	58	183
Nova Scotia (NS)	55,284	12	12	21.7	240	73	172
Nunavut (NU)	1,935,200	14	13	0.7	240	43	163
Ontario (ON)	1,076,395	34	34	3.2	240	34	209
Prince Edward Island (PEI)	5,684	2	2	35.2	240	240	240
Quebec (QC)	1,542,056	24	20	1.6	240	33	211
Saskatchewan (SK)	591,670	16	15	2.7	240	145	233
Yukon (YT)	482,443	8	8	1.7	240	141	194
Total	**9,769,999**	**222**	**206**		**240**	**20**	**200**

Note: Max.= Maximum, Min.= Minimum

***** Complete weather file refers to at least 24 months of data in a weather file for the MEPDG application.

From Table 3.1 it is observed that existing Canadian climate data files contain various quantities of climate data ranging from 20 to 240 months. In this study, it was found that there are 31 weather station files that have climate data for less than 10 years and 13 stations that have climate data for less than 5 years. For the stations

having less than 20 years of climate data, the MEPDG software reuses the existing annual climate data [3]. For instance, if a pavement is designed for 20 years with only 10 years of available climate data, then 10 years of data is used twice. The area of each province is tabulated in Table 3.1 to observe the density of available weather stations that are available for the MEPDG application. The density column shows that Nova Scotia and Prince Edward Island have the highest density of available weather stations. However, in the Northwest Territories and Nunavut, the station density is very low; there is less than one station in 1000 square km area. In Alberta, on average, four weather stations are available per 1000 square km for the MEPDG application.

3.4 Evaluation of Canadian Climate Data Files for the MEPDG

There are several sources such as Environment Canada web site, a tool called World Index, the Canadian Encyclopedia, and a Tech Solutions 605.0 document made by DOW where climatic parameters of some Canadian weather stations are available. Out of these sources, Environment Canada has largest historical data record of Canadian weather stations. Environment Canada keeps climate data records on a yearly, monthly, daily and hourly basis. In this study, the Canadian climate database prepared and formatted for the MEPDG was evaluated. To evaluate the existing climate database, one weather station was chosen randomly from each province. To evaluate the accuracy of climatic parameters available in Canadian weather files, the following tasks were performed in this study:

- Climatic parameters such as temperature and total precipitation data used for the MEPDG analysis were compared with the Environment Canada historical data record for each randomly chosen weather station from each province of Canada for the same time period (details are presented in section 3.4.1).
- The freezing index computed by the MEPDG Software version 1.100 for each selected weather station was compared with the freezing index documented from other sources (also further elaborated in section 3.4.2).
- The MEPDG-computed maximum yearly frost depth of a selected weather station was compared with the frost depth computed by the Modified Berggren method (this methodology is explained in section 3.4.3).

The other MEPDG-required climatic parameters such as wind speed, percent of sunshine and relative humidity were not evaluated because that is beyond the scope of this study.

3.4.1 Evaluation of Temperature and Total Precipitation Data used for the MEPDG Application

The accuracy of temperature and total precipitation data of Canadian weather files used in the MEPDG were evaluated in this study. Appendix A.1.3 shows details of the climate (temperature and total precipitation) data used in the MEPDG analysis and also climate data recorded by Environment Canada for the same time period for one randomly chosen weather station from each province. The table showing differences in the climate data records are also presented in Appendix A.1.3. To evaluate climate (temperature and total precipitation) data used for the MEPDG, temperature and total precipitation data used in the MEPDG were compared with the publicly available historical climate data recorded by Environment Canada for the same year, month and day for 13 randomly chosen weather stations (one station from each province) in Canada. These comparative results are illustrated in Table 3.2 and 3.3. They are graphically presented in Figures 3.1 and 3.2 respectively.

Table 3.2: Comparison of Temperature Data Recorded by Environment Canada and by TAC Used for the MEPDG Application

Weather Station	Number of available months in data file	Difference in temperature (°C) between MEPDG climate data and Environment Canada Historical data			
		25^{th} Percentile	50^{th} Percentile	75^{th} Percentile	90^{th} Percentile
Calgary Int. Airport_AB	227	0.09	0.20	0.32	0.46
Kamloops Airport_BC	227	0.11	0.20	0.32	0.45
Gimli Airport_MB	215	0.06	0.10	0.26	0.42
Saint John Airport_NB	227	0.14	0.30	0.43	0.59
Argentia Airport_NF&L	191	0.09	0.20	0.31	0.41
Halifax_NS	107	0.20	0.40	0.56	0.72
Inuvik Airport_NT	227	0.14	0.30	0.43	0.63
Baker Lake Airport_NU	191	0.06	0.20	0.28	0.40
Hamilton Airport_ON	35	0.06	0.10	0.22	0.36
CharlotteTown Airport_PEI	227	0.09	0.20	0.34	0.52

Weather Station	Number of available months in data file	Difference in temperature (°C) between MEPDG climate data and Environment Canada Historical data			
		25th Percentile	50th Percentile	75th Percentile	90th Percentile
Bagotville Airport_QC	227	0.08	0.20	0.34	0.45
Broadview Airport_SK	131	0.15	0.30	0.53	0.82
Aishihik Airport_YU	155	0.17	0.30	0.48	0.70

Table 3.2 demonstrates that the 25th, 50th, 75th and 90th percentiles of the difference in temperature (ºC) data between the MEPDG and Environment Canada historical data record are less than 0.2 ºC, 0.4 ºC 0.5 ºC and 0.8 ºC respectively for all 13 randomly selected weather stations in Canada. This indicates that data collected by TAC for MEPDG is consistent with the Environment Canada data.

The distribution of these absolute differences in temperature (ºC) data recorded by TAC and Environment Canada is shown graphically by the box plot that is illustrated in Figure 3.1.

Figure 3.1: Absolute Difference in Temperature (ºC) between the Environment Canada Recorded and the MEPDG Used Data

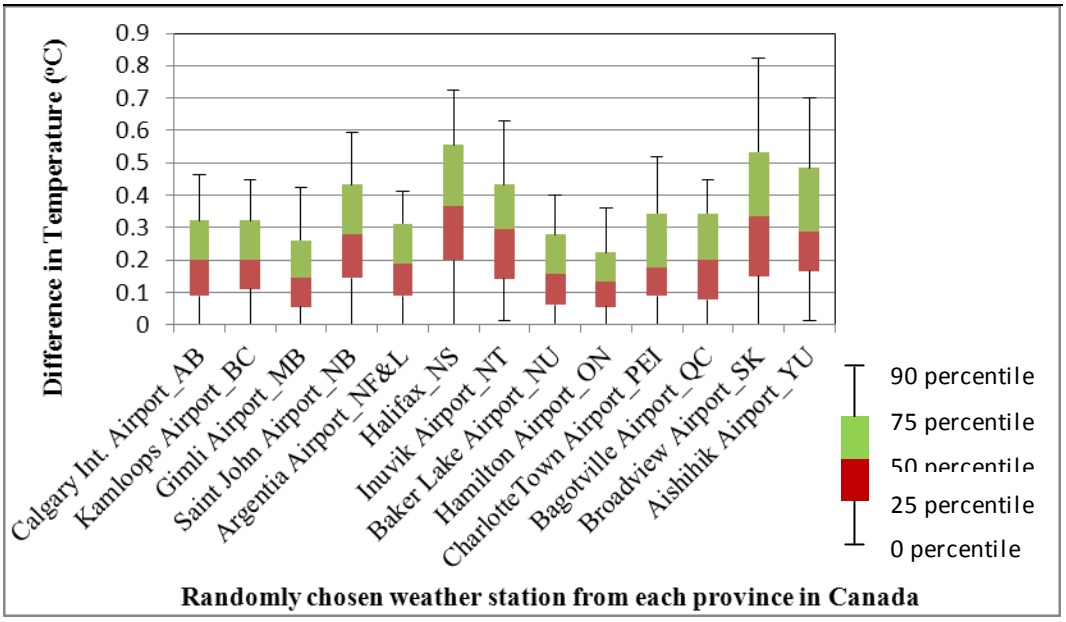

Figure 3.1 shows the 25th, 50th, 75th and 90th percentiles of the differences of the temperature data recorded by two different sources as mentioned above. The maximum difference of 0.82 ºC occurs at the 90th percentile at Broadview Airport in Saskatchewan. This demonstrates that the temperature data between the two sources (TAC and MEPDG) are consistent.

Table 3.3 shows the absolute differences in precipitation (mm) data recorded by TAC and Environment Canada, which are shown graphically in the box plot illustrated in Figure 3.2.

Table 3.3: Comparison of Total Precipitation Data Recorded by Environment Canada and by TAC Collected for the MEPDG Application

Weather Station	Number of available months in data file	Difference in precipitation (mm) between MEPDG climate data and Environment Canada Historical data			
		25th Percentile	50th Percentile	75th Percentile	90th Percentile
Calgary Int. Airport_AB	227	0.07	0.11	0.13	0.46
Kamloops Airport_BC	227	0.08	0.09	0.13	0.42
Gimli Airport_MB	215	0.06	0.09	0.12	0.42
Saint John Airport_NB	227	0.11	0.13	0.23	5.61
Argentia Airport_NF&L	191	0.03	0.02	0.09	0.30
Halifax_NS	107	0.02	0.01	0.01	2.46
Inuvik Airport_NT	227	0.12	0.09	0.17	0.61
Baker Lake Airport_NU	191	0.01	0.01	0.01	0.11
Hamilton Airport_ON	35	0.08	0.11	0.15	0.45
CharlotteTown Airport_PEI	227	0.11	0.14	0.17	0.82
Bagotville Airport_QC	227	0.13	0.09	0.18	0.62
Broadview Airport_SK	131	0.01	0.01	0.01	0.04
Aishihik Airport_YU	155	0.01	0.02	0.01	0.05

Table 3.3 and Figure 3.2 show the 25th, 50th, 75th and 90th percentiles of difference in precipitation (mm) data recorded by TAC for the MEPDG application, and by Environment Canada. These results show that the 75th percentile of the difference of the precipitation data recorded by two different sources is less than 0.5 mm for all 13

randomly selected weather stations in Canada respectively. This indicates that data collected by TAC for the MEPDG demonstrate consistency with Environment Canada data in terms of precipitation. However, the maximum 90th percentile difference (5.61 mm) of precipitation was observed at Saint John Airport.

Figure 3.2: Absolute Difference in Precipitation (mm) between the Environment Canada Recorded and the MEPDG Used Data

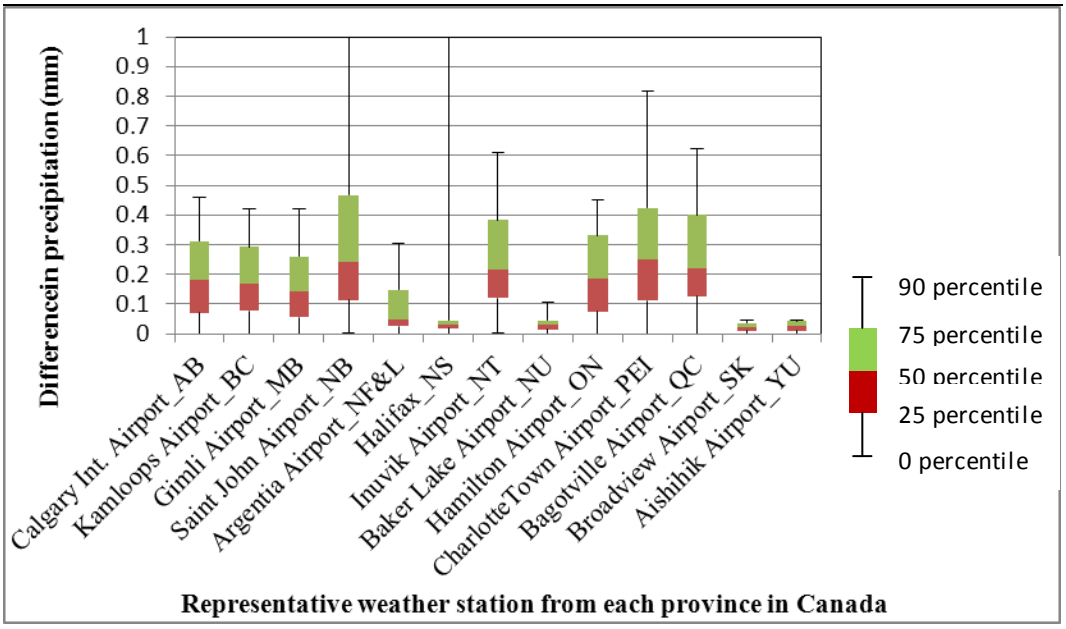

Figure 3.2 shows the 25th percentile, 50th percentile, 75th percentile and 90th percentile of the differences of the precipitation data recorded by two different sources (MEPDG and Environment Canada). The 90th percentile precipitation difference between the two sources exceeds 1.0 mm at the Saint John Airport in New Brunswick and in Halifax, Nova Scotia. These 90th percentile values are not shown in Figure 3.2 because they do not fit the scale of the figure.

3.4.2 Evaluation of Freezing Index Data computed by the MEPDG

The Freezing Index (FI) is the number of degree-days between the highest and lowest points on the cumulative degree-days time curve for one freezing season. It is used as a measure of the combined duration and magnitude of below-freezing temperatures occurring during any given freezing season. The total annual freezing index has been widely used to predict permafrost distribution, maximum depth of ground-frost penetration, etc. [39, 40]. At freezing temperatures, water in soil freezes and the

resilient modulus rises to values 20 to 120 times higher than the value of the modulus before freezing; the process may be accompanied by the formation of ice lenses that create zones of greatly reduced strength in the pavement when thawing occurs [29]. Consequently pavement damage occurs. The Freezing Index influences the IRI values. The IRI model uses the freezing index to calculate the site factor for flexible pavement [29]. Therefore, it is necessary to verify the accuracy of the MEPDG computed freezing index.

To measure the accuracy of freezing indexes resulting from the MEPDG output, those freezing indexes computed by the MEPDG were compared with the freezing index in other sources available for the Canadian weather stations. One of the reference sources was the Tech Solutions 605.0 document published by DOW Chemical Canada ULC which is available online [41]. The DOW document has been prepared for calculating building insulation that needs to estimate and control frost depth by comparing the freezing index. In this document, freezing indices from various weather stations across Canada have been reported based on weather data records from 1931 to 1960 prepared by the division of building research office, National Research Council, Atmospheric Environment Service, and Environment Canada.

Table 3.4 presents the differences in freezing index values between two sources, the MEPDG and Tech Solution 605, for 13 randomly selected weather stations, one from each province.

Table 3.4: Comparison of Freezing Index Values from the MEPDG Output, and Tech Solution 605 Document

Weather Station	Freezing Index (ºC-days)		Absolute Difference of Freezing Index (ºC-days) between MEPDG & Tech Solution 605
	Prediction from the MEPDG outputs	Tech solution 605	
Calgary Int. Airport-AB	983	995	12
Kamloops Airport-BC	333	335	2
Gimli Airport-MB	1954	1898	56
Saint John Airport-NB	803	632	171
Argentia Airport-NF&L	289	264	25
Halifax-NS	377	309	68
Inuvik Airport-NT	4109	4680	**571**
Baker Lake Airport-NU	5299	Not available	-
Hamilton Airport-ON	617	368	249
CharlotteTown Airport-PEI	741	667	74
Bagotville Airport-QC	1514	1593	79
Broadview Airport-SK	1809	1802	7
Aishihik Airport-YU	3005	2799	206

Note: The bold font displays the maximum absolute differences of freezing indexes between MEPDG and the Tech Solution document.

The maximum absolute differences of freezing index values between MEPDG & Tech Solution 605 was 571°C-days in Inuvik Airport, Northwest Territories (NT) as shown in Table 3.4. This high difference (nearly 10%) of freezing index could be the result of the high difference between the temperature data used in the MEPDG, Tech solution 605 and World Index. Except for a few other stations (such as Hamilton Airport-ON, Saint John Airport-NB and Aishihik Airport-YU), the freezing index values computed by the MEPDG and two other sources are less than 100ºC-days for other Canadian weather stations available for the MEPDG application.

3.4.3 Verifying Maximum Frost Depth Computed by the MEPDG with the Modified Berggren Method

To evaluate the accuracy of Canadian climate data files available for the MEPDG application, frost depths predicted by the MEPDG were reviewed. The MEPDG

software output provides frost depth for each month of the pavement design life. To justify the frost depth computation by the MEPDG, maximum frost depth values of one randomly selected year for each representative station were compared with the frost depth values calculated using the Modified Berggren method [42]. One randomly selected year out of a 20-year design life of pavement was selected to calculate the maximum frost depth for one randomly selected weather station from each province. To compute frost depth by the Modified Berggren method, necessary temperature data was used from Environment Canada historical data. The surface freezing index (*nF*) used in the modified Berggren method to compute the frost depth was calculated using the European method. According to the European method, the freezing index is the sum of the mean daily temperature ($^{\circ}F$) minus the freezing temperature ($32^{\circ}F$) for the freezing days of a year. A day is called a freezing day if the mean temperature of the day is below the freezing temperature ($32^{\circ}F$). Mathematically, freezing index (*nF*) is defined as,

$$nF = -\sum(\overline{T} - 32^{0}F) \tag{2.17}$$

Where, $\overline{T}$ = mean daily temperature $= 0.5(T_1 + T_2)$

T_1= Maximum daily air temperature,

T_2= Minimum daily air temperature

One sample calculation of frost depth values from the Modified Berggren method is shown in Appendix A.1.4. The inherent assumption of the modified Berggren formula is that the soil is a semi-infinite mass with uniform properties and existing initially at a uniform temperature (T_i) and the surface temperature is suddenly changed from T_i to T_s (below freezing). The frost depth computation method using the Modified Berggren equation is described as below.

The Modified Berggren equation for homogeneous soil is [42]:

$$X = \lambda(48k\frac{nF}{L})^{\frac{1}{2}} \tag{3.1}$$

Where:

X = depth of frost (ft)

k = thermal conductivity (Btu/(ft hr ºF))

λ = correction factor, (Ref: Figure A.1.1 in Appendix 1)

nF = surface-freezing index (ºF-days)

L = latent heat (Btu/ft^3)

In this analysis a multilayer solution to the Modified Berggren equation was used for computing frost depth of layered pavement structure by determining that portion of the surface freezing index required to penetrate each layer [43]. Depth of freeze (or thaw) is calculated by adding the thicknesses of all the frozen layers. The partial freezing (or thawing) index required to penetrate the top layer is given by:

$$F_1 = \frac{L_1 d_1}{24\lambda_1^2}\left(\frac{R_1}{2}\right) \tag{3.2}$$

Where,

d_1 = thickness of first layer (ft)

$R_1 = d_1/k_1$ = thermal resistance of first layer.

k_1, L_1 and λ_1 are the thermal conductivity, latent heat and correction factor of the first layer.

The partial freezing (or thawing) index required to penetrate the second layer is given by,

$$F_2 = \frac{L_2 d_2}{24\lambda_2^2}\left(R_1 + \frac{R_2}{2}\right) \tag{3.3}$$

Similarly, the partial freezing (or thawing) index required to penetrate the nth layer is given by,

$$F_n = \frac{L_n d_n}{24\lambda_n^2}\left(\sum R + \frac{R_n}{2}\right) \tag{3.4}$$

Where $\sum R$ is the total thermal resistance above the nth layer and equals

$$\sum R = R_1 + R_2 + \cdots\cdots\cdots + R_{n-1} \tag{3.5}$$

The summation of partial freezing indexes, F_1, F_2, …, F_n is equal to the surface-freezing index (ºF-days), *nF, i.e.,*

$$nF = F_1 + F_2 + F_3 + \cdots\cdots\cdots + F_n \tag{3.6}$$

Surface-freezing index (ºF-days), *nF* was computed by European method. F_1, F_2, …, F_n was computed and added until right hand side of equation (3.6) was not equal to the left hand side of equation (3.6). Few iteration is required to match both hand side of the equation (3.6).

When surface-freezing index, *nF* becomes equal to the summation of the *n* number of partial freezing indexes, F_1, F_2, …, F_n. Then the summation of the thickness of *n* number of layers, $d_1, d_2, \ldots, d_n$ gives the frost depth, *FD, i.e.,*

$$FD = d_1 + d_2 + d_3 + \cdots\cdots\cdots + d_n \tag{3.7}$$

Now, for computing partial freezing index for *n*-th layer, the values of d_n, k and λ are needed to be known ahead. λ is a function of μ and α where α is a function of V_0 (Initial temperature differential), V_s (Average surface temperature differential) and μ (Fusion Parameter) is a function of V_s, C , L. As an example, the frost depth beneath a multilayer pavement structure (top layer: Asphalt Concrete (AC), middle layer: Granular Base Layer (GBC) and bottom layer: clay Subgrade) can be determined with the following conditions:

- Mean annual temperature, MAT =43.3 (^{0} F)
- Surface freezing index, *nF* (^{0}F-days) = 1138.1
- Number of freezing days (t) = 84

The list of required parameters to calculate frost depth for above conditions are tabulated in Table 3.5

Table 3.5: List of Required Parameter to Calculate Frost Depth in Different Layers by Modified Berggren Method

Values of the parameters	Top Layer (Asphalt Concrete)	Middle Layer (Granular Base Layer (GBC))	Bottom Layer (Subgrade)
Thickness of the pavement layers, d_i (ft)	0.8	1.1	Infinite (depth of soil layer)
Thermal Conductivity, k (Btu/(ft hr ºF))	0.9	1.0	1.2
Latent Heat, L (Btu/ft^3)	0	403.2	403.2
Volumetric Heat Capacity, C (Btu/^{0}F ft^3)	28	25.2	25.2
Average surface temperature differential, $V_s = nF/t$ (^{0}F)	13.5	13.5	13.5
Initial temperature differential, V_0 = MAT-32 (^{0}F)	11.3	11.3	11.3
Partial frost depth, d_i (ft)	0.8	1.1	6.0*
Average Volumetric Heat Capacity, $\bar{C} = \frac{\sum Cd}{\sum d}$ (Btu/^{0}F ft^3)	28.0	26.3	25.5
Average Volumetric Latent heat, $\bar{L} = \frac{\sum Ld}{\sum d}$ (Btu/ft^3)	-	239.7	364.7
Fusion Parameter, $\mu = V_s \frac{\bar{C}}{\bar{L}}$	-	1.5	0.9
Thermal ratio, $\alpha = V_0 / V_s$	0.8	0.8	0.8
Correction factor, λ (From graph A.3.1 shown in Appendix)	-	0.5	0.7
Partial Freezing Indexes (Computed using equation 3.4)	-	100.7	1037.2
Cumulative partial freezing indexes (Computed using equation 3.5)	-	100.7	1137.9*

*Partial frost depth of the subgrade layer is computed iteratively so that cumulative partial freezing indexes become equal to the surface freezing index, 1138.1(^{0}F-days).

The maximum frost depth for this example, *FD* (computed using equation 3.6) = sum of the partial frost depth, d_i computed above = 0.8+1.1+6.0 = 7.9 ft. = 2.41 m.

The maximum frost depths computed by the MEPDG and Modified Berggren method are provided in Table 3.6. The absolute differences between frost depths computed by these two methods are also shown in Table 3.6

Table 3.6: Comparison between the Frost Depths Computed by MEPDG Predicted and the modified Berggren method

Weather Station	Frost depth (m)		
	Modified Berggren method computed	MEPDG predicted	Absolute Difference
Calgary Int. Airport_AB	2.4	2.1	0.3
Kamloops Airport_BC	1.2	1.1	0.1
Gimli Airport_MB	4.5	4.1	0.4
Saint John Airport_NB	2.7	2.2	0.5
Argentia Airport_NF&L	1.1	1.1	0.0
Halifax_NS	1.2	1.1	0.1
Inuvik Airport_NT	5.3	9.0	3.7
Baker Lake Airport_NU	5.0	8.9	3.9
Hamilton Airport_ON	2.1	1.6	0.5
CharlotteTown Airport_PEI	2.5	1.9	0.6
Bagotville Airport_QC	4.0	3.4	0.6
Broadview Airport_SK	4.3	4.0	0.3
Aishihik Airport_YU	5.0	8.9	3.9

Results obtained from Table 3.6 show that the difference between the frost depths computed by the modified Berggren and MEPDG method is less than or equal to 0.6 m except in three stations including the Inuvik Airport in the Northwest Territories, Baker Lake in Nunavut and Aishihik Airport in the Yukon, respectively. These stations are situated in permafrost regions. Permafrost will typically form in any climate where the mean annual air temperature is less than the freezing point of water [44]. The MEPDG-computed maximum frost depths were exceptionally high in these three stations and the absolute difference of frost depth was more than 3.7 m between MEPDG and the Modified Berggren method. These differences in frost

depth could be the result of differences in the freezing index which is more than 200ºC-days between the MEPDG and other two methods as found in Table 3.4.

Figure 3.3 shows a bar diagram that illustrates the visual comparison of the maximum frost depths computed by the Modified Berggren and the MEPDG methods.

Figure 3.3: Frost Depth Comparison between the Modified Berggren and the MEPDG Method

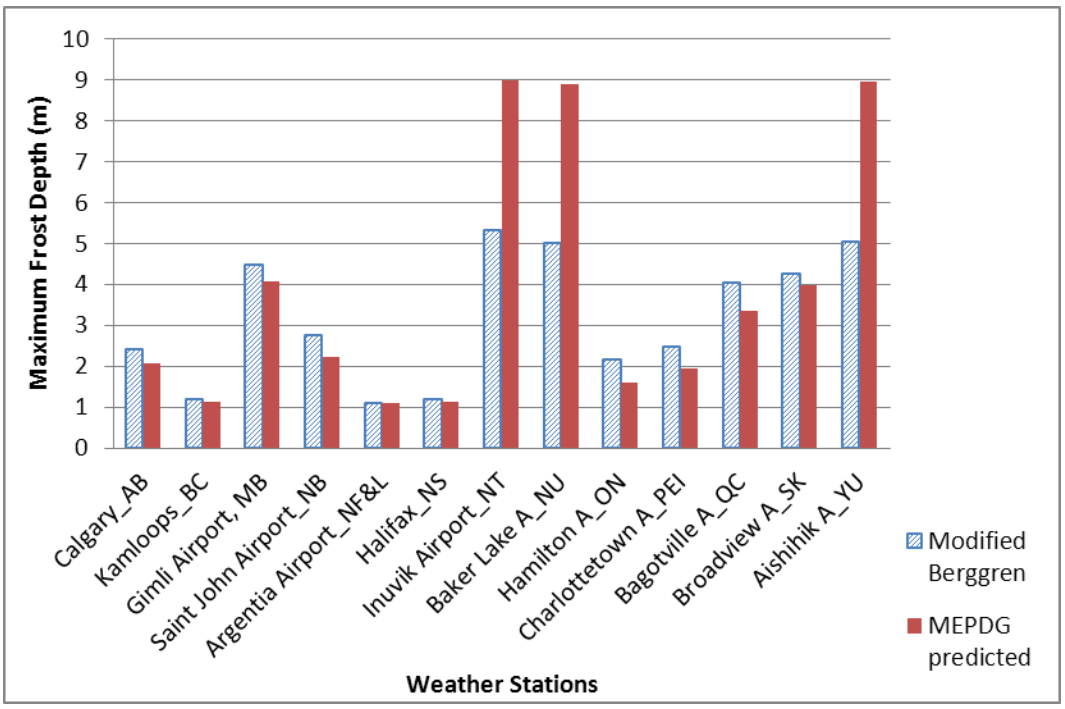

Figure 3.3 illustrates that maximum annual frost depths computed by the MEPDG and modified Berggren methods are consistent since the absolute difference of the frost depth computed by these two methods is equal or less than 0.6 meter for randomly selected weather stations from 13 provinces. However, in the permafrost zone the difference in frost depth computed by the above-mentioned two methods is more than 3.5 meter.

3.5 Evaluating the Effects of Canadian Climatic Factors on Pavement Performances using the MEPDG

The main objective of this study was to evaluate the effects of Canadian climatic factors on pavement performances using the MEPDG. A similar study was conducted

earlier in the US [3]. Different pavement design parameters used in the MEPDG for this study are illustrated in Table 3.7.

Table 3.7: Different Input Parameters for Pavement Performance Prediction

Asphalt Concrete (AC) flexible pavement parameters	Values
Design Period (Years)	20
Traffic (AADTT)	3200
Growth rate of traffic	compound 5%
Number of lanes in design direction	1
Percent of truck in design direction (%)	50
Depth of water table (m)	1.5
AC layer thickness	230 mm (9 inch)
Granular base thickness	330 mm (13 inch)
Asphalt binder	PG 58-28
Sub-grade type	A-6
Sub-grade modulus (MPa)	100
Granular base type	A-1-a
Base modulus (MPa)	275.8
Reliability of all performance criteria	85%

Pavement design input parameters used in the MEPDG for this study as shown in Table 3.7 are chosen from the US study [3]. This study was conducted in a manner similar to that of US study [3] to evaluate the effects of climate on pavement performances using the MEPDG. All other input parameters related to materials and traffic were the MEPDG software default values. One sample of all input parameters used in the analysis is provided in Appendix A.1.5 Calgary Int. Airport weather station. The input level is considered as level 3 for all analysis. Using MEPDG software version 1.1, 206 analyses were performed.

The traffic, binder type and subgrade vary in different locations in Canada. However, with the exception of climatic parameters, when evaluating the effects of the climate on pavement performance, the same inputs were considered for all weather stations available for the MEPDG application across Canada.

3.6 Predicted Pavement Distresses Using the MEPDG

Based on the inputs parameters presented in Table 3.7, the following pavement distresses were investigated for all 206 Canadian weather station files: alligator cracking, longitudinal cracking, transverse cracking, International Roughness Index (IRI), total permanent pavement deformation (total rutting), and Asphalt Concrete (AC) layer rutting. The values of all outputs of pavement performances for all Canadian files are tabulated in Appendix A.1.6 and output summary of all the distresses from all Canadian weather files with their allowable design limits are provided in Table 3.8.

Table 3.8: Output Summary of Pavement Distresses in Different Weather Stations Available for the MEPDG Application Across Canada

Pavement Distresses	Minimum	Mean	Maximum	MEPDG allowable limit
IRI (m/km)	1.45	1.9	2.25	2.29
Longitudinal cracking (m/km)	0.1	44.8	2006.7	378.6
Alligator Cracking (%)	0.7	2.1	3.4	25.0
Transverse Cracking (m/km)	0.2	22.3	399.8	189.3
Asphalt Concrete layer permanent deformation (mm)	0.0	6.1	15.0	6.0
Permanent deformation (Total pavement) (mm)	6.0	14.8	24.0	19.05

Table 3.8 illustrates the minimum, mean, maximum and the MEPDG-specified limiting values of all distresses (IRI, longitudinal cracking, transverse cracking, alligator cracking, AC rutting and total pavement permanent deformation). Transverse cracking values are the same (0.2 m/km) for 196 out of 206 weather station files as provided in Appendix 1.6. Although the climate is different for different weather station files, transverse cracking values are not changing as expected with climate. Therefore transverse cracking is not showing realistic results and hence it needs calibration for local conditions to capture the effects of climate. The value of alligator cracking varies from 0.7 to 3.4% which is much lower than its allowable limiting value (25%). It shows a small range of variation due to different environmental factors. However, this range (0.7 to 3.4%) of alligator cracking values shows consistency with the values suggested by the MEPDG manual for a pavement

having AC layer thickness of 230 mm and sub-grade modulus of 100 MPa [45]. Alligator cracking mainly depends on AC layer thickness, repeated traffic loading and sub-grade strength whereas it is sensitive to environment. The insensitivity of alligator and transverse cracking values indicates that the associated models need calibration for local Canadian climate conditions. The similar findings also were demonstrated in the US study conducted by Johanneck and Khazanovich [3].

On the other hand, the MEPDG predicts expected values for the other four distresses (IRI, AC layer deformation, total permanent pavement deformation and longitudinal cracking) as shown in both Table 3.8 and Appendix A.1.6. The maximum and minimum values of IRI, AC layer deformation, total permanent pavement deformation and longitudinal cracking lie within the expected range. Consequently, only these four distresses were considered in the following sections. The effects of climate on these four distresses (IRI, AC layer deformation, total permanent pavement deformation and longitudinal cracking) were analyzed at three levels:

(a) across different Canadian provinces that are discussed in section 3.7;

(b) across different climate zones that are elaborated in section 3.8 and

(c) geography (across latitude and longitude) which is explained in section 3.9.

3.7 Prediction of Pavement Distresses across Different Canadian Provinces

3.7.1 IRI

The initial IRI value in all analyses was assumed as 0.99 m/km. Figure 3.4 illustrates the distribution of IRI for all 206 Canadian weather stations for the MEPDG application. The results of IRI values were found after applying 50% reliability.

Figure 3.4 Frequency Distribution of IRI

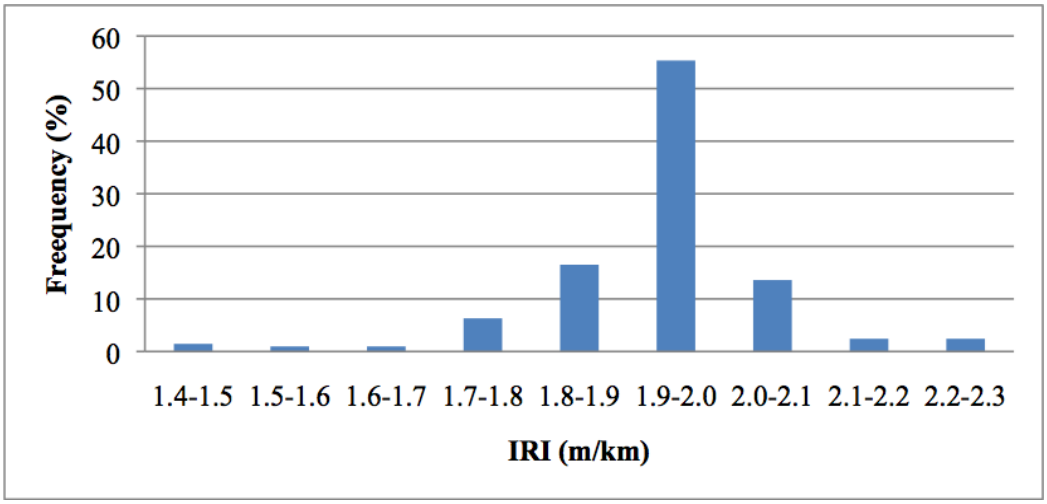

Figure 3.4 illustrates that IRI varies between 1.45 to 2.25 m/km at the end of its 20-year design life for all weather stations in Canada. However, the value of IRI lies between 1.8 to 2.1 m/km in more than 85% of available weather stations. The small range of variation shows that the IRI value for this type of pavement considered in this study was not very sensitive to different factors of climate. This supports similar findings reported for US climate files by Johanneck and Khazanovich [3].

Tables 3.9 illustrates the maximum, minimum, and mean IRI service lives (years) for all the MEPDG-applicable Canadian weather stations that were 20.0, 10.0 and 16.5 years respectively considering terminal IRI value as 2.29 m/km. However the maximum service life might be more than 20 years, since the pavement is designed for a 20-year period and the results shows maximum life as 20 years. A similar design criterion was considered in the US study by Johanneck and Khazanovich [3]. The pavement design and analysis period was considered as 20 years for all stations.

Table 3.9: IRI Service life of Pavement in Different Canadian Provinces

Provinces of Canada	IRI Service life /analysis period (Year)		
	Minimum	Mean	Maximum*
Alberta (AB)	15.3	16.6	17.3
British Columbia (BC)	13.3	16.8	20.0
Manitoba (MB)	15.4	16.1	17.0
New Brunswick (NB)	15.5	16.1	16.7
Newfoundland & Labrador (NL)	16.9	18.1	19.3
Nova Scotia (NS)	15.8	17.0	18.4
Northwest Territories (NT)	15.8	17.8	20.0
Nunavut (NU)	20.0	20.0	20.0
Ontario (ON)	14.7	15.7	18.1
Prince Edward Island (PEI)	16.6	16.7	16.8
Quebec (QC)	10.1	14.9	18.1
Saskatchewan (SK)	10.2	15.9	16.8
Yukon (YU)	9.7	13.3	18.8

Note: *When maximum service life is 20 years, it indicates the maximum analysis period. Therefore the service life could be more than 20 years.

The minimum IRI service life (9.7 year) was found in the Yukon (YU). The IRI service life was 20 years for all 13 stations in Nunavut (NU). In Nunavut no pavement fails in IRI throughout its design life. The reason behind this outcome could be the mean annual air temperature, which is less than -10°C for all stations in Nunavut, and because most of this part of the territory is frozen. The recorded temperature and precipitation details are provided in Appendix A.1.1. In British Columbia (BC) minimum, mean and maximum IRI service lives were 13.3, 16.8, and 20 years or more respectively. This wide variation in service life occurs because in BC weather varies distinctly in different part of the province. Prince Edward Island (PEI) has only two weather stations which have an IRI service life of 16.6 and 16.7 year respectively. In Alberta (AB), Manitoba (MB) and New Brunswick (NB), the difference in maximum and minimum service lives was 2.0, 1.6 and 1.2 years respectively.

Figure 3.5 shows minimum, mean, and maximum IRI service life for all stations in each province across Canada.

Figure 3.5: Distribution of IRI Service Life across Different Provinces of Canada

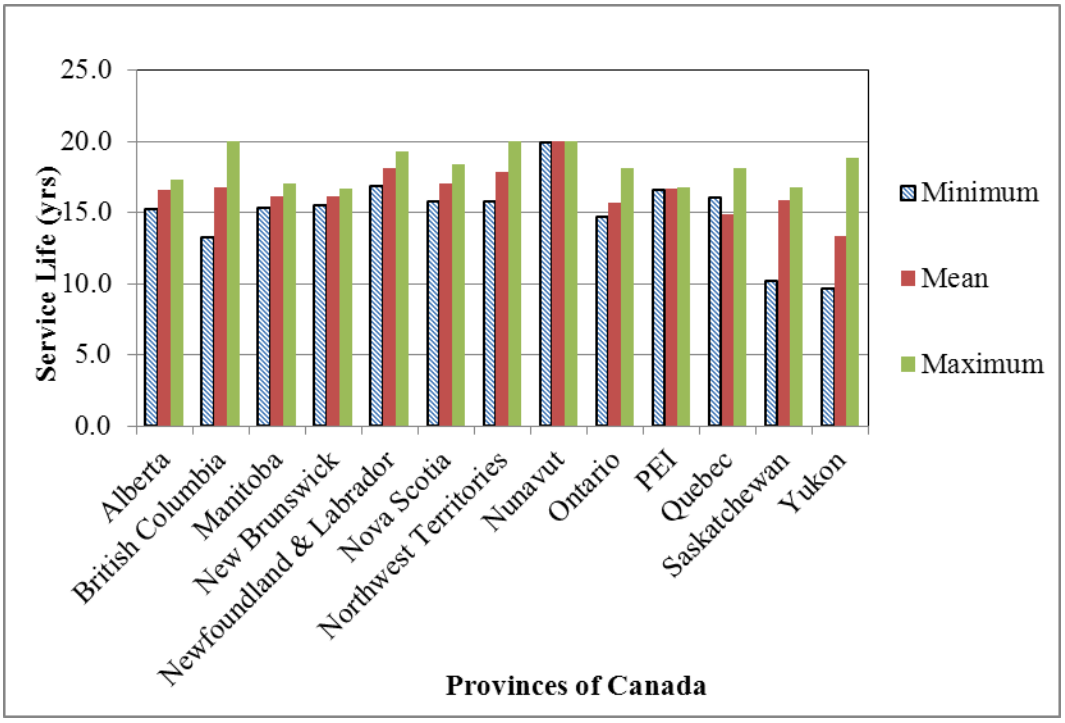

It is observed from Figure 3.5 that the difference between minimum and maximum IRI service life is higher in Quebec (QC), Saskatchewan (SK), BC, and YU than in the other provinces.

3.7.2 AC Rutting

Figure 3.6 illustrates the frequency of AC rutting for all the MEPDG applicable weather stations files in Canada. The values of AC rutting were captured at a reliability level of 50%. Figure 3.6 shows that predicted AC rutting from the MEPDG varied from 0.8 to 15.5 mm. Unlike IRI, this variation indicates that AC rutting is more sensitive to environmental parameters such as temperature, precipitation etc.

Figure 3.6: Frequency Distribution of AC Rutting

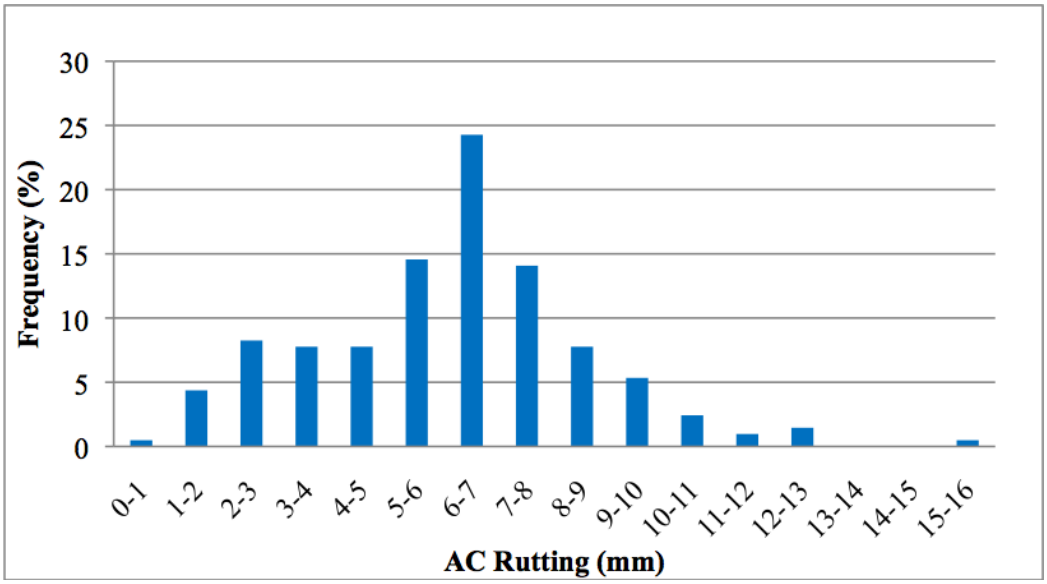

Table 3.10 shows minimum, mean and maximum AC rutting service life in different provinces.

Table 3.10: Predicted AC Rutting Service Life of Pavement in Different Canadian Provinces

Provinces of Canada	AC rutting service life/analysis period (Year)		
	Minimum	Mean	Maximum*
Alberta	6.8	12.7	17.8
British Columbia	2.8	11.6	20.0
Manitoba	8.7	11.8	20.0
New Brunswick	9.7	13.4	16.8
Newfoundland & Labrador	20.0	20.0	20.0
Nova Scotia	10.5	15.8	20.0
Northwest Territories	8.8	16.8	20.0
Nunavut	20.0	20.0	20.0
Ontario	5.8	10.6	20.0
PEI	13.8	14.8	15.8
Quebec	4.8	13.4	20.0
Saskatchewan	7.7	11.1	13.8
Yukon	7.9	15.0	20.0

Note: *When maximum service life is 20 years, it indicates the maximum analysis period. Therefore the service life could be more than 20 years.

Table 3.10 shows that the difference between minimum and maximum AC rutting service life was between 0 to 2 years for NU, Newfoundland and Labrador (NL) and PEI because the maximum mean annual air temperature of all the stations of these three provinces is less than 6ºC as shown in the Appendix. The difference between minimum and maximum AC rutting service life for other provinces was between 6.1 to 17.2 years. This happens because different climates prevail in different part of the provinces. In some provinces maximum service life is seen as 20 years, which is the design period.

Considering an AC rutting limit of 6.0 mm as pavement failure criteria by the MEPDG, the AC rutting service life has been plotted in Figure 3.7.

Figure 3.7: Distribution of AC Rutting Service Life across Different Provinces of Canada

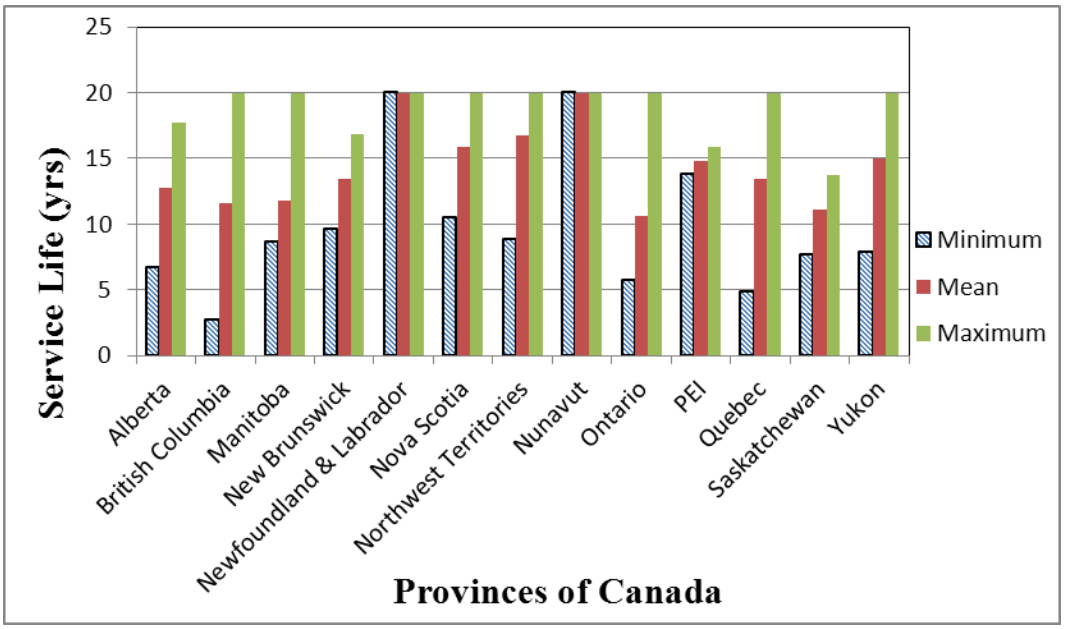

Figure 3.7 shows the minimum, mean and maximum service life of AC rutting for all of Canada's provinces and territories. This figure also depicts that the minimum, mean and maximum service life for AC rutting is 20 years for all stations in NU, where the mean annual air temperature is less than -10°C. Although the NT has similar climatic conditions to NU, the minimum AC rutting service life is not similar to the AC rutting in NU. The reason might be the difference in minimum annual temperatures between the two territories. In the NT, the minimum annual temperature is -2.3ºC whereas in NU it is -9.5ºC as shown in Appendix 1.1. On the other hand, the

difference between minimum and maximum AC rutting service life is almost 17 years for the weather stations in BC since different climate zones prevail across BC. Further details about these climate zones are mentioned in section 3.8.

3.7.3 Total Permanent Pavement Deformation (TPPD)

Figure 3.8 illustrates the frequency of total permanent pavement deformation for all MEPDG-applicable weather station files in Canada. The values of AC rutting were noted at a reliability level of 50%.

Figure 3.8: Frequency Distribution of Total Permanent Pavement Deformation

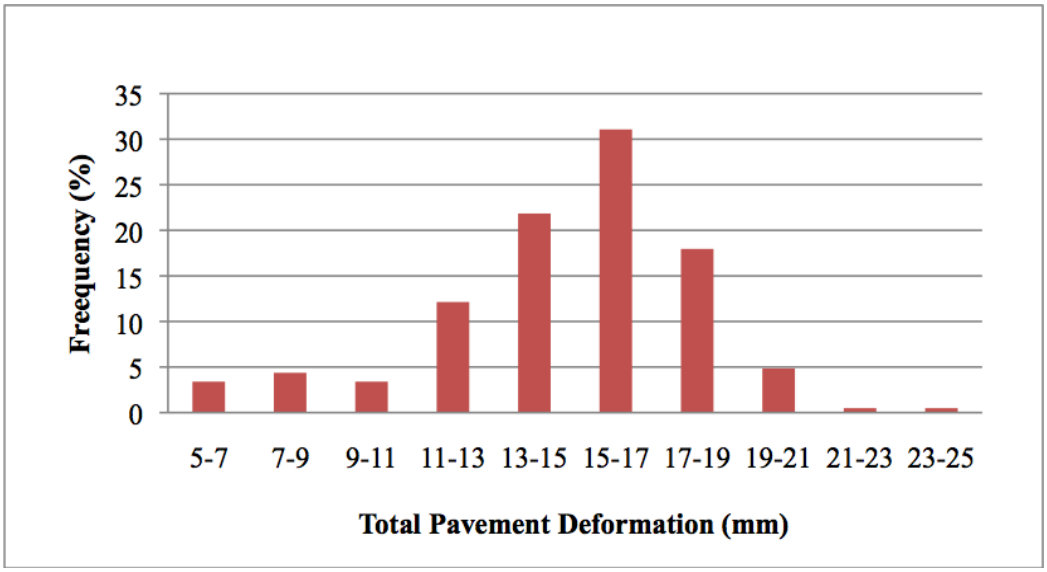

Figure 3.8 shows that total permanent pavement deformation varies from 6 to 24 mm. However, 70% of stations have total pavement deformation between 13 to 19 mm. This variation occurs due to different climates in different parts of Canada. Similar to AC rutting, Total Permanent Pavement Deformation (TPPD) was found to be affected by climate change.

Table 3.11 shows minimum, mean and maximum TPPD service life obtained from the MEPDG taking into consideration the TPPD terminal value as 19 mm for all weather stations in Canadian provinces and territories.

Table 3.11: Predicted Total Permanent Pavement Deformation Service life of Pavement in Different Canadian Provinces

Provinces of Canada	TPPD service life/analysis period (Year)		
	Minimum	Mean	Maximum*
Alberta	13.8	19.5	20.0
British Columbia	6.8	16.8	20.0
Manitoba	15.7	18.5	20.0
New Brunswick	16.8	19.5	20.0
Newfoundland & Labrador	20.0	20.0	20.0
Nova Scotia	18.8	19.9	20.0
Northwest Territories	16.8	19.7	20.0
Nunavut	20.0	20.0	20.0
Ontario	12.8	17.3	20.0
PEI	20.0	20.0	20.0
Quebec	12.8	18.0	20.0
Saskatchewan	15.8	18.8	20.0
Yukon	15.8	19.1	20.0

Note: *When maximum service life is 20 years, it indicates the maximum analysis period. Therefore the service life could be more than 20 years.

From table 3.11 it is seen that the service life of TPPD of all weather station files in Newfoundland & Labrador, Nunavut and PEI was 20 years, which is the design life for the selected pavement. All the stations in these three provinces lie in high freeze zones. Different climate zones are discussed in detail in section 3.8. Since the amount of total permanent pavement deformation decreases as the temperature decreases, the service life of pavement increases for TPPD. The minimum and maximum TPPD service life in BC was 6.8 and 20 years respectively. This significant difference in TPPD service life occurs because different parts of BC are in different climate zones as shown in Appendix A.1.1.

Considering a total permanent pavement deformation limit of 19.0 mm as pavement failure criteria by the MEPDG, the total permanent pavement deformation service life for different provinces of Canada has been plotted in Figure 3.9.

Figure 3.9: Distribution of Total Permanent Pavement Deformation Service Life Across Different Provinces of Canada

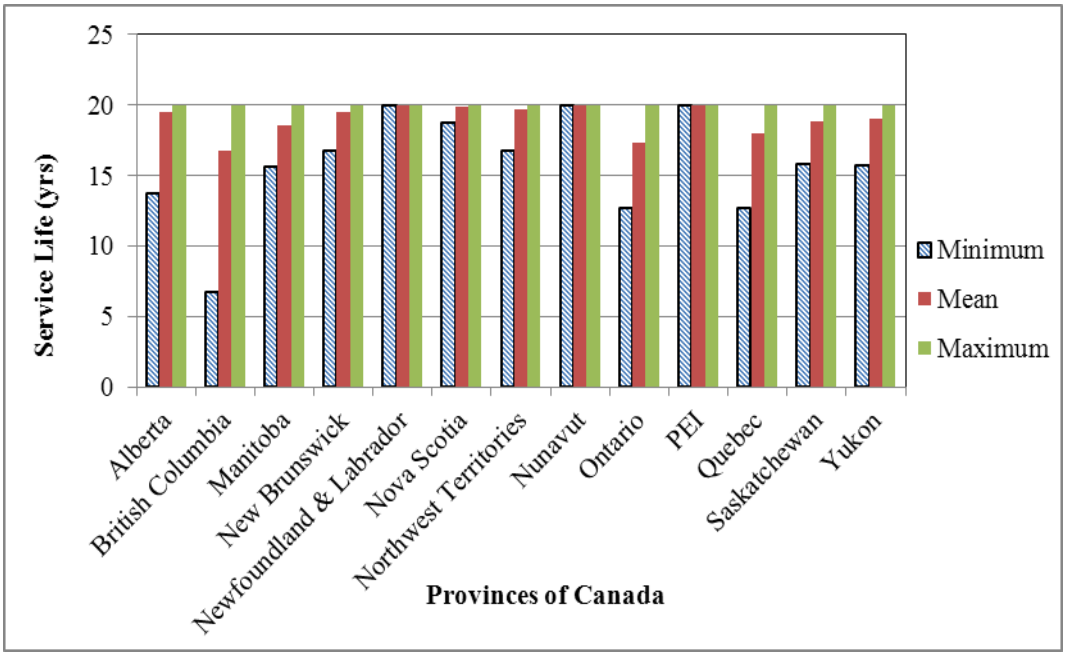

Figure 3.9 shows the minimum, mean and maximum service life of total permanent pavement rutting for all provinces and territories in Canada. This figure also shows that the minimum service life for total permanent pavement deformation is 20 years for the stations in NU, NL and PEI where all the stations of these three provinces lie in the high freeze zone. On the other hand, the difference between minimum and maximum total permanent pavement deformation service life for BC is 13.2 years since different climate zones prevail across BC. Further details about these climate zones are mentioned in section 3.8.

3.7.4 Longitudinal Cracking

Figure 3.10 illustrates the frequency of longitudinal cracking for all MEPDG applicable weather stations files in Canada. The values of AC rutting values were observed at a 50% reliability level.

Figure 3.10: Frequency Distribution of Longitudinal Cracking

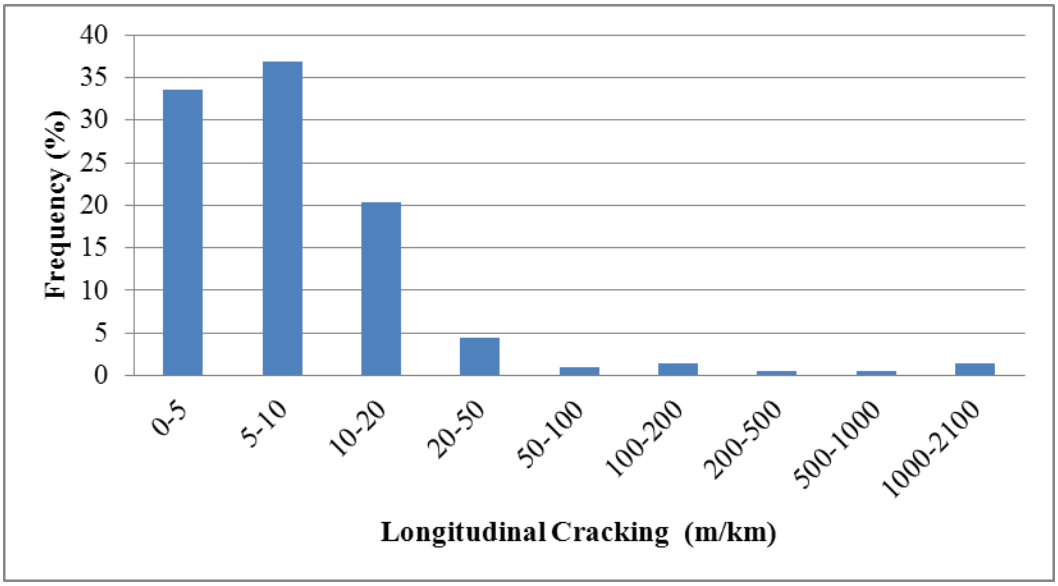

Figure 3.10 shows that the MEPDG-predicted longitudinal cracking values range from zero to 53 m/km for 198 of the 206 weather station files. These values show consistency with the values suggested by the MEPDG manual for a pavement having an AC layer thickness of 230 mm and a sub-grade modulus of 100 MPa [45]. In a few stations in the NT and NU, pavement failed in longitudinal cracking where longitudinal cracking values are exceptionally high like 2006 m/km as provided in Appendix A.1.6. Those stations are located in a permafrost zone where the freezing indexes are extremely high. Due to a high freezing index the sub-grade becomes very stiff which tends to cause a larger tensile strain at the surface layer and results in high longitudinal surface cracking [45]. High longitudinal surface cracking may also occur because of saturation during thawing.

Table 3.12 shows the minimum, mean and maximum longitudinal cracking service life for different provinces in Canada. Table 3.12 illustrates that in the NT and NU the minimum longitudinal cracking service life was less than one year in some stations such as Mould Bay airport in the NT, Cambridge Bay airport, Rea Point airport and Resolute airport in NU. Such a small service life occurs due to excessively high longitudinal cracking value in those stations. The reason for this high longitudinal cracking is that these weather stations are located in the permafrost zones. In other provinces, longitudinal cracking service lives were 20 years for all stations. Therefore, longitudinal cracking is found to be affected by air temperature.

Table 3.12: Predicted Longitudinal Service Life of Pavement in Different Canadian Provinces

Provinces of Canada	Longitudinal Cracking Service Life/analysis period (Year)		
	Minimum	Average	Maximum*
Alberta	20.0	20.0	20.0
British Columbia	20.0	20.0	20.0
Manitoba	20.0	20.0	20.0
New Brunswick	20.0	20.0	20.0
Newfoundland & Labrador	20.0	20.0	20.0
Nova Scotia	20.0	20.0	20.0
Northwest Territories	0.5	17.6	20.0
Nunavut	0.7	13.8	20.0
Ontario	20.0	20.0	20.0
PEI	20.0	20.0	20.0
Quebec	20.0	20.0	20.0
Saskatchewan	20.0	20.0	20.0
Yukon	20.0	20.0	20.0

Note: *When maximum service life is 20 years, it indicates the maximum analysis period. Therefore the service life could be more than 20 years.

Figure 3.11 shows the service life of longitudinal cracking for 206 weather station files that are available for the MEPDG application in Canada considering longitudinal cracking limits of 378.6 m/km. Figure 3.11 shows the minimum, mean and maximum service life of longitudinal cracking for all of the provinces and territories in Canada. This figure also shows that the minimum service life of longitudinal cracking is less than a year for some stations in the NT and NU where these stations are located in the permafrost zone. For other provinces, the minimum longitudinal cracking service life is 20 years which is also the design life for the selected pavement. As mentioned earlier, due to a high freezing index in the permafrost zone, the sub-grade becomes very stiff which tends to cause a larger tensile strain at the surface layer and results in high longitudinal surface cracking [45].

Figure 3.11: Distribution of Longitudinal Cracking Service Life Across Different Provinces of Canada

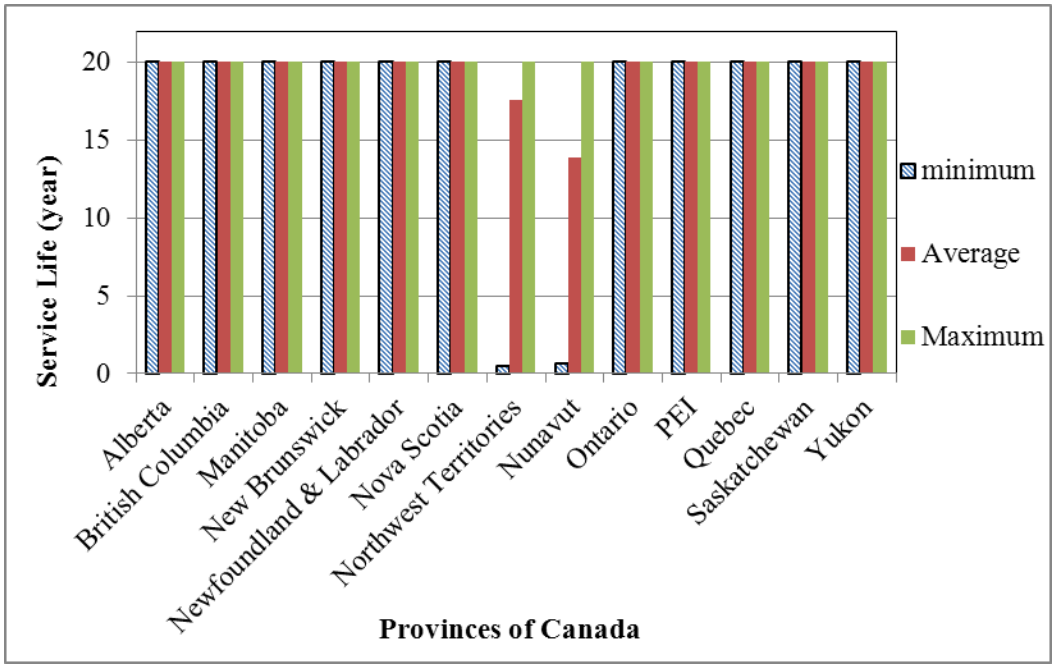

3.8 Prediction of Pavement Distresses in Different Climate Zones Using the MEPDG

In the previous section, predicted pavement distresses from the MEPDG were discussed for all Canadian provinces and territories. However, the differences in pavement distresses found in different provinces could also be attributed to variations in climate zones throughout the country. In this section, pavement distresses in terms of IRI, AC rutting, total permanent pavement deformation and longitudinal cracking are discussed for different Canadian climate zones.

In order to better understand the climatic distribution of climatic files, the 206 weather stations in Canada were categorized into four different climate zones based on the annual freezing index and mean annual precipitation. These four zones are as follows: no to low freeze – dry; no to low freeze – wet; high freeze – dry; and high freeze – wet. The threshold values of the freezing index and precipitation were considered as 400°C and 50 cm precipitation respectively. These threshold values were considered according to Long Term Pavement Performance (LTPP)-defined criteria [46].

Figure 3.12: Locations of Different Climate Zones based on Freezing Index and Precipitation Across Canada on Google Earth

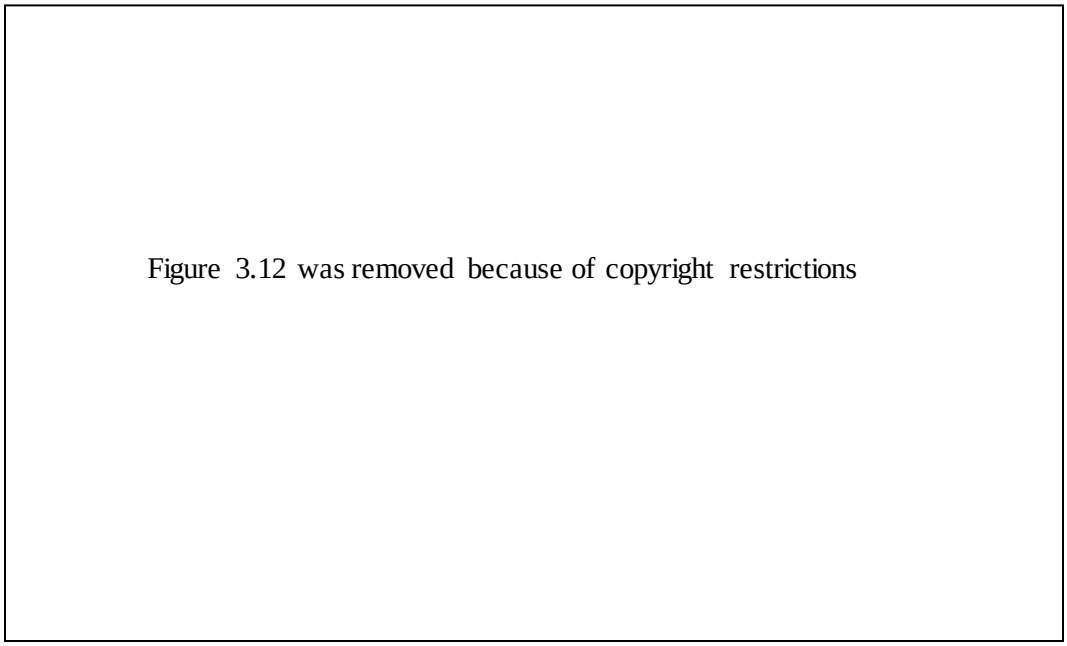

The number of stations located in each of the four climate zones is shown in Table 3.13.

Table 3.13: Classifications of Weather Zones

Zone Index	Different climate zones	Number of stations
1	No to low freeze – dry	4
2	High freeze – dry	83
3	No to low freeze – wet	18
4	High freeze – wet	101
Total		206

Table 3.13 illustrates that out of 206 Canadian weather stations that are applicable for the MEPDG, 184 stations were located in high freeze - wet and high freeze - dry climate zones because annual air temperature of most of the available Canadian weather stations is low. The MEPDG-computed annual freezing index varies from 17°C- days to 5524°C - days with an average of 1641°C-days throughout Canada as provided in Appendix A.1.1. The mean annual precipitation varies from zero to 308 cm with an average of 72 cm. Freezing indexes increase from south to north and

heavy precipitation is observed mainly on the east coast and in a few portion of the west coast of Canada. The effects of different climate zones on pavement performances are discussed below.

3.8.1 IRI

The distribution of IRI predicted by the MEPDG for all 206 weather stations is categorized by different climate zones and is shown by box plot in Figure 3.13.

Figure 3.13: Distribution of IRI for Different Climate Zones

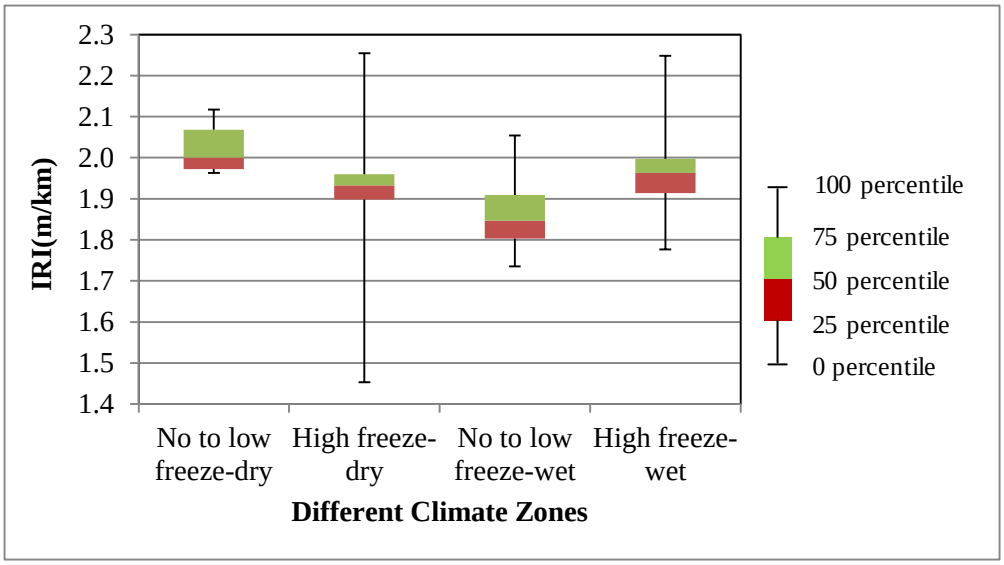

The box plot in Figure 3.13 illustrates that the mid spread (differences between 25th and 75th percentile) for any climate zone is less than 0.1 m/km. It specifies that the IRI values of most of the weather stations in any climate zone are close to each other (< 0.1 m/km). The maximum difference in the average IRI of different climate zones is less than 0.2 m/km. These low values indicate that the IRI was not sensitive to different climate zones.

3.8.2 AC Rutting

The effects of different climate zones on AC rutting are shown by boxplot in Figure 3.14.

Figure 3.14: Distribution of AC Rutting for Different Climate Zones

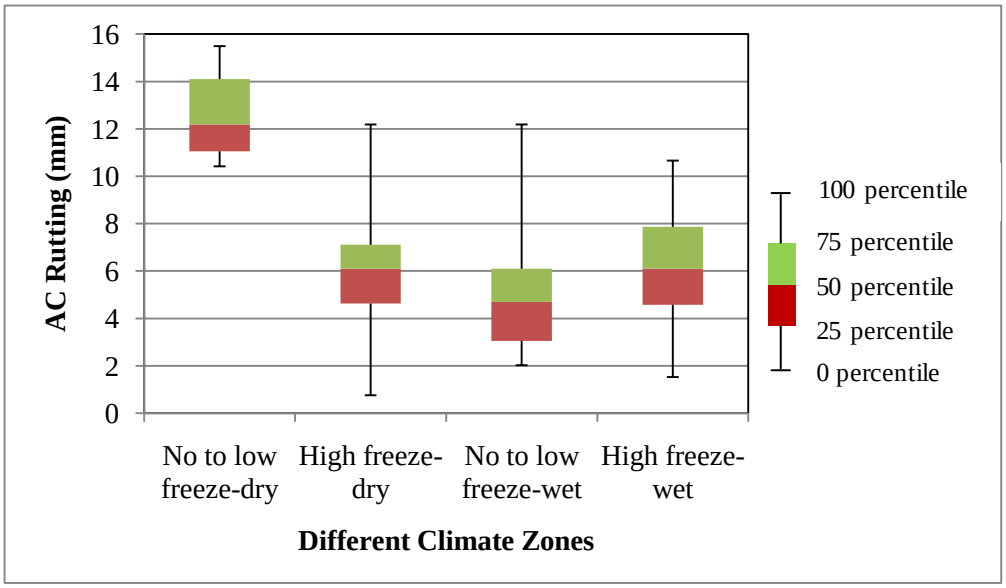

Figure 3.14 illustrates the distribution of AC layer deformation for four climatic zones by boxplot. The height of the box represents the middle fifty (differences between 25th and 75th percentile) for any climate zone. This figure shows that the maximum height of the box is 3 mm and this maximum height is observed at a high freeze-wet zone. It indicates that AC layer deformation values do not vary much among weather stations within a single climate zone (< 3 mm). However, AC layer deformation values greatly among different climate zones (a maximum difference of 7 mm was found between no-to-low freeze-dry and no-to-low freeze-wet). This result shows that different climate zones have an effect on AC layer deformation.

3.8.3 Total Permanent Pavement Deformation (TPPD)

The change in behavior of TPPD for different climate zones is illustrated by boxplot in Figure 3.15.

Figure 3.15: Distribution of Total Permanent Pavement Deformation for Different Climate Zones

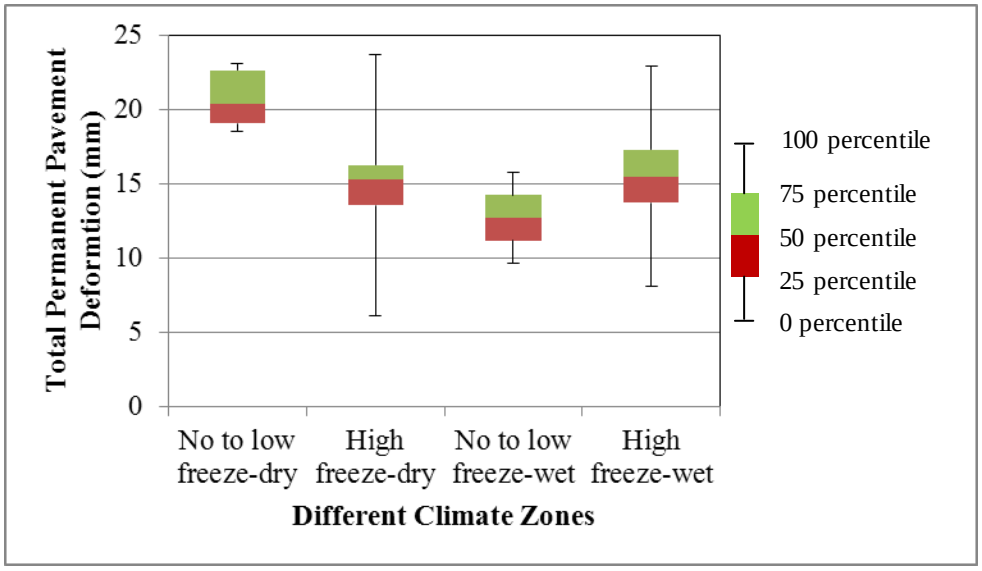

Both inter- and intra- climatic zonal effects on total permanent pavement deformation are captured by box plot in Figure 3.15. Inter-climatic zonal effects are visualized by the height of the box. The height of the box represents the interquartile range (differences between 25^{th} and 75^{th} percentile) for a particular climate zone. Figure 3.15 shows that the maximum interquartile range of TPPD is 3 mm for the no-to-low freeze-dry zone. This result shows that the inter-climatic zonal effect on TPPD is not very significant. However, the intra-climatic zonal effect on TPPD is visualized by the difference among the median of the different climate zones. Figure 3.15 shows that the maximum difference between the median of two different climate zones is found to be ~8 mm (between no-to-low freeze-dry and no-to- low freeze-wet). This result indicates that intra-climatic zonal effects on TPPD are much more prominent than the inter-climatic zonal effects on TPPD.

3.8.4 Longitudinal Cracking

The box plot of longitudinal cracking for different climate zones is shown in Figure 3.16. This plot shows the effects of climatic parameters (temperature and precipitation) on longitudinal cracking. Very few (8 out of 206) weather stations show very high longitudinal cracking (>113 m/km) whereas other values lie between 0-53 m/km. For better visualization, very high longitudinal cracking values were not plotted in Figure 3.16.

Figure 3.16: Distribution of Longitudinal Cracking for Different Climate Zones

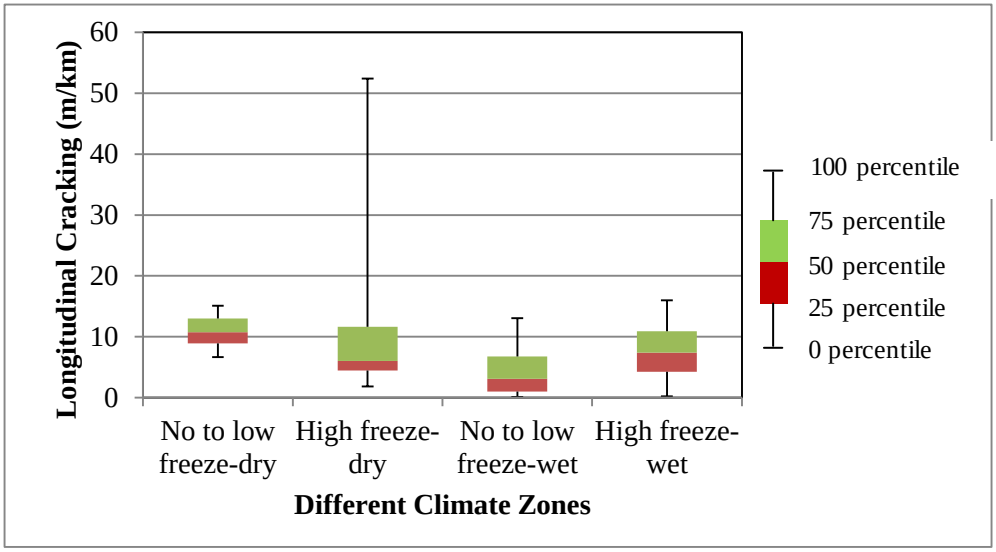

The box plot shown in Figure 3.16 illustrates that the difference in the values of longitudinal cracking of weather stations in a particular climate zone lies within 7 m/km. This difference in the values of longitudinal cracking within a particular zone is reflected in the height of the boxes as shown in the above box plot. It indicates that longitudinal cracking values at most of the weather stations in a particular climate zone are close to each other. On the other hand, the median of the values of longitudinal cracking at different climate zones are different (maximum difference was found 10 m/km between no-to-low freeze-dry and no-to-low freeze-wet) in 198 out of 206 Canadian weather stations available for the MEPDG. However, for clarity, exceptionally high longitudinal cracking (2007 m/km) that occurs in the rest of the weather stations located at the high freeze-dry zone is not shown in the figure. The average values of longitudinal cracking for different climate zones are 11, 99, 5 and 8 m/km respectively. These phenomena indicate that the effects of longitudinal cracking on pavement performance are prominent in a high-freeze zone.

3.9 Variation of Pavement Performances Across Latitude and Longitude

The effects of latitude and longitude on pavement performances of 206 Canadian weather stations available for the MEPDG application were investigated. In order to

achieve this goal, the relationships among pavement distresses (IRI, AC layer deformation and total permanent pavement deformation) and latitude and longitude are discussed below:

3.9.1 IRI

Figure 3.17 (a) and (b) shows the distribution of IRI with latitude and longitude respectively.

Figure 3.17: Variation of IRI with Latitude and Longitude

(a)

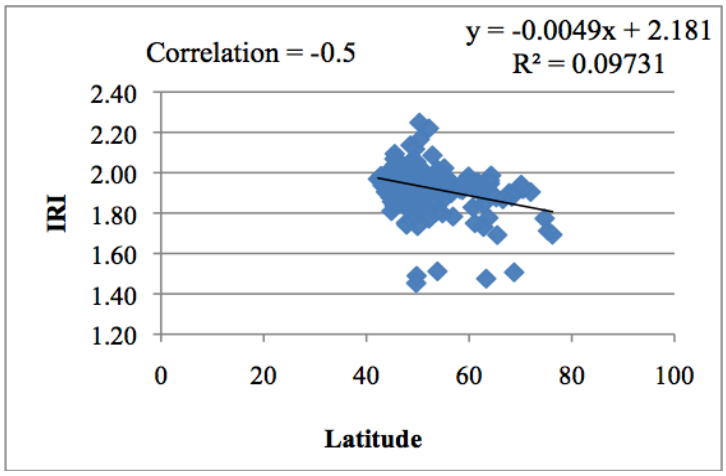

(b)

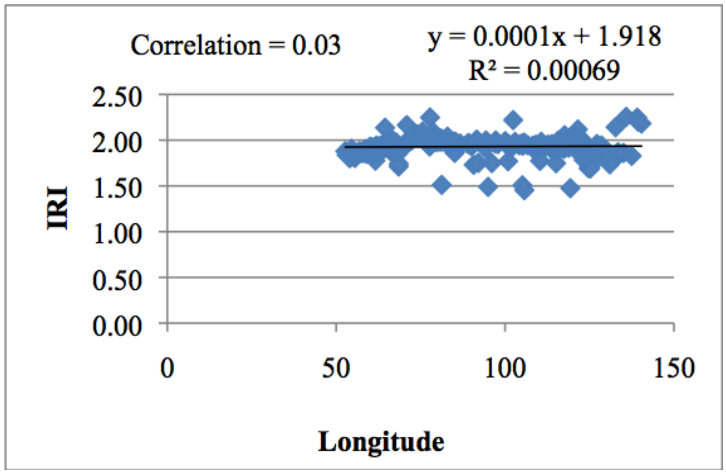

Figure 3.17(a) demonstrates a negative correlation between the latitude of available Canadian weather stations and IRI (correlation -0.5). This negetive correlation indicate that the value of IRI decreases as latitiude increases (negative slope of the

fitted line shown in Figure 3.17(a)). The latitude of Canadian weather stations increases from south to north in Canada but the air temperature decreases from south to north. The values of IRI increase as the temperatures increase, which was also demonstrated in the previous section. This illustrates the effects of temperature on IRI. However, the correlation value between the longitude of Canadian weather stations available for the MEPDG and IRI is very low (correlation 0.03) as shown in 3.17(b). This states that there is no considerable effect of longitude of Canadian weather stations on IRI. Longtitude increases from east to west in Canada. However, no increasing or decreasing trend of climate parameters (temperature, precipitation, etc.) is observed from east to west in Canada.

3.9.2 AC Layer Deformation

The dot plot of AC layer deformation with latitude and longitude is illustrated in Figure 3.18 (a) and (b) respectively.

Figure 3.18: Variation of AC Layer Deformation with Latitude and Longitude

(a)

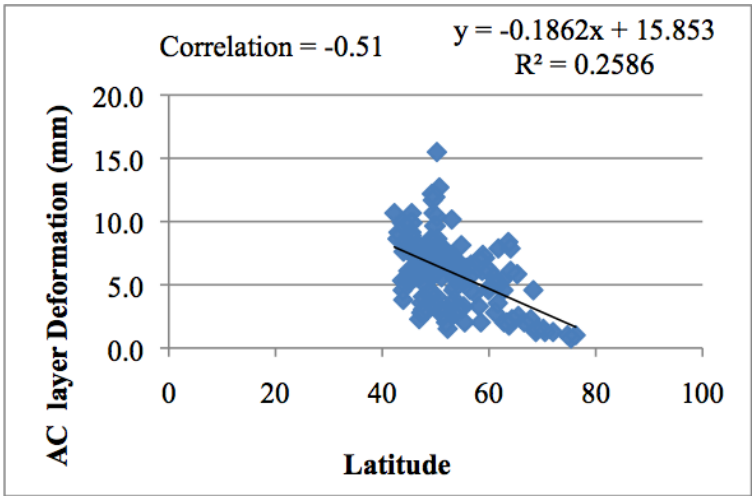

(b)

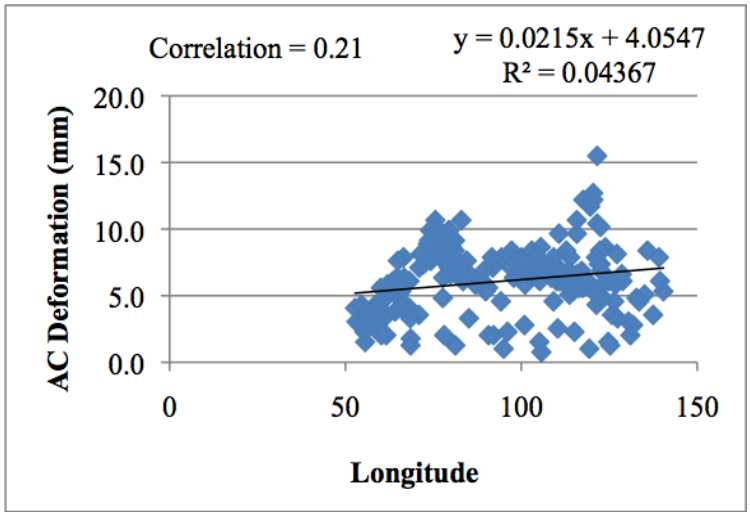

The primary observation in Figure 3.18(a) and (b), is that change in AC layer deformation is much more prominent across latitude than longitude. The correlation value between AC layer deformation and latitude is -0.51 whereas the correlation value between AC layer deformation and longitude is 0.21. A regression line was fitted using the points in Figure 3.18(a) and 3.18(b). The moderate negative correlation (correlation value -0.51) and negative slope of the fitted line between the latitude of available Canadian weather stations and AC rutting observed in Figure 3.18(a) specifies that AC rutting decreases as latitiude increases. As mentioned earlier, latitude increases from south to north in Canada but air temperature decreases

from south to north. This states that values of AC rutting decrease as temperatures decrease which was also demonstrated in the previous section. This shows that the effects of temperature are proportional to AC rutting.

However, the correlation value between the longitude of Canadian weather stations available for the MEPDG and AC rutting is very low (correlation 0.21) as shown in Figure 3.18(b). This states that the effect of longitude on AC rutting is not very significant. So although longtitude increases from east to west of Canada, there is no observable trend of the values of AC rutting in the weather stations.

3.9.3 Total Permanent Pavement Deformation

Figure 3.19 (a) and (b) shows the trend of total permanent pavement deformation with latitude and longitude respectively.

Figure 3.19: Variation of Total Permanent Pavement Deformation with Latitude and Longitude

(a)

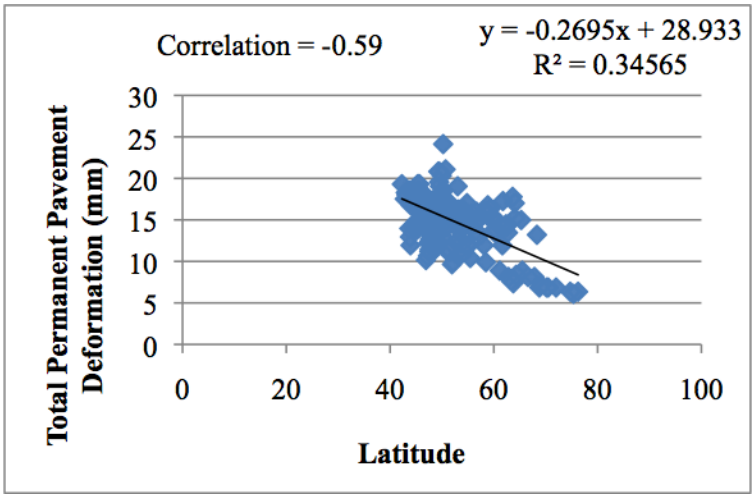

(b)

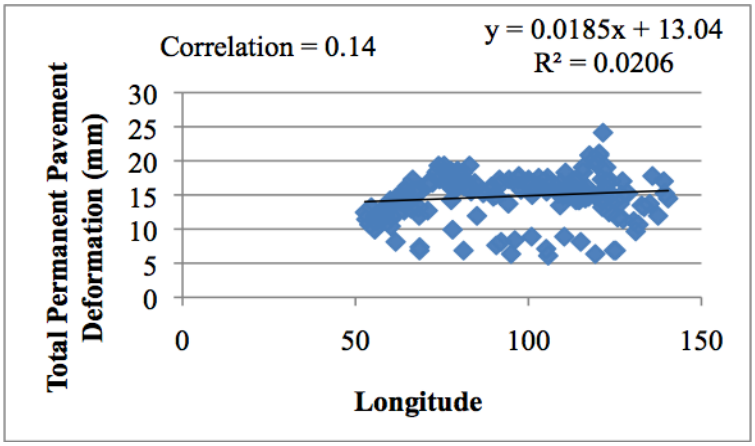

Figure 3.19(a) shows that TPPD is negatively correlated with latitude and somewhat positively correlated with longitude of Canadian weather stations available for the MEPDG application. The slope of the fitted line in Figure 3.19(a) turned out to be negative which indicates that value of TPPD decreases as latitiude increases. As mentioned earlier, air temperature is negatively correlated with latitude of Canadian weather stations available for the MEPDG application. The values of TPPD decrease as temperatures decrease, which was also demonstrated in the previous section.

Although the correlation value between the longitude of Canadian weather stations available for the MEPDG application and TPPD shown in Figure 3.19(b) is positive , the absolute value is low (correlation 0.14). This shows the minimal effect of longitude of Canadian weather stations on TPPD. Longtitude increases from east to west in Canada. However, no remarkable increasing or decreasing trend of climate parameters (temperature, precipitation, etc.) is found across east to west in Canada.

3.9.4 Longitudinal Cracking

Figure 3.20 (a) and (b) shows distribution of longitudinal cracking with latitude and longitude respectively. Few exceptionally high values (6 out of 206 weather stations) of longitudinal cracking are not shown in Figure 3.20(a) and (b) to observe the linear relationship between reasonable values of longitudinal cracking and latitude /longitude.

Figure 3.20: Variation of Longitudinal Cracking with Latitude and Longitude

(a)

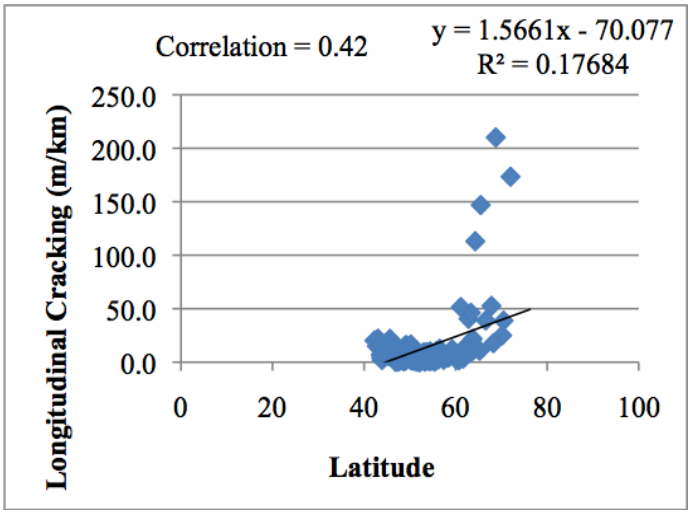

(b)

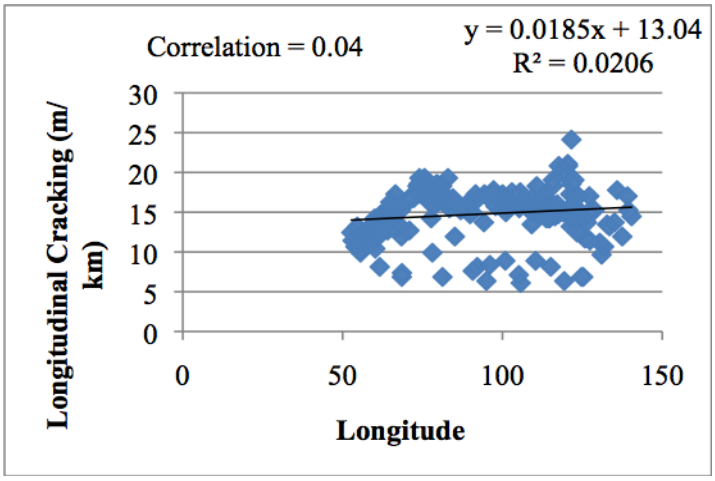

Both Figure 3.20(a) and 3.20(b) show a positive correlation between latitude and longitiude of Canadian weather stations available for the MEPDG application and longitudinal cracking respectively. These indicate that the value of longitudinal cracking increases as both latitiude and longitude increase (positive slope of the fitted line shown in both Figure 3.20(a) and 3.20(b)). However, the low correlation value (0.04) between the longitude of Canadian weather stations and longitudinal cracking indicates that the increasing trend of longitudinal cracking across east to west in Canadian weather stations is not significant. The reason could be the insignificant

change observed in climatic parameters (temperature, precipitation etc.) across Canada east to west.

On the contrary, a moderate positive correlation between latitude and longitudinal cracking indicates that values of longitudinal cracking decrease as temperature increases (temperature is negatively correlated with latitude), which supports the fact illustrated in the previous section. As discussed earlier, due to high freezing index in the permafrost or a high freeze zone located in the north of Canada, the sub-grade becomes very stiff, tending to cause a larger tensile strain at the surface layer resulting in high longitudinal surface cracking.

3.10 Verification of Virtual Climatic Data

To ensure the accuracy of future pavement design, it is essential to check that the derived virtual data are accurate and represent the specific climate conditions. In this study, to evaluate the accuracy of the MEPDG-generated Virtual Weather Station (VWS) data, the MEPDG software was used to compare pavement performance using both climate data from corresponding weather stations and VWS data of that project site. In this study, VWS was created by interpolating different combinations of weather stations from the 6 nearest stations.

Table 3.14 shows the IRI, AC rutting and total permanent pavement deformation results obtained from both weather station climate data and VWS climate data for a few representative stations from different Canadian provinces (and territories).

Table 3.14: Comparison of Pavement Distress Using Weather Station Climate Data and VWS Climate Data

Station Name	IRI (m/km)			AC rutting (mm)			Total Permanent Pavement Deformation (mm)		
	Stan. clim.	VWS clim.	Diff. between Stan & VWS clim.	Stan. clim.	VWS clim.	Diff. between Stan & VWS clim.	Stan. clim.	VWS clim.	Diff. between Stan & VWS clim.
Cold Lake Airport, AB	1.9	1.9	0.0	6.4	6.1	0.3	15.2	15.0	0.2
Edson, AB	1.9	1.9	0.0	5.6	6.1	0.5	14.5	15.2	0.7

Station Name	IRI (m/km)			AC rutting (mm)			Total Permanent Pavement Deformation (mm)		
	Stan. clim.	VWS clim.	Diff. between Stan & VWS clim.	Stan. clim.	VWS clim.	Diff. between Stan & VWS clim.	Stan. clim.	VWS clim.	Diff. between Stan & VWS clim.
Quesnel Airport, BC	2.0	1.9	0.1	10.2	7.1	3.1	19.1	15.7	3.4
Gimli Airport, MB	2.0	1.9	0.1	7.1	7.1	0.0	16.3	15.7	0.6
Saint John Airport, NB	1.9	2.0	0.1	5.3	7.4	2.1	14.2	16.5	2.3
Shelburne, NS	1.9	1.9	0.0	5.3	4.8	0.5	14.0	13.5	0.5
Fort Resolution Airport, NT	1.9	1.9	0.0	5.1	4.8	0.3	14.2	13.5	0.7
Ennadai Lake, NU	1.8	1.9	0.1	2.8	4.8	2.0	8.9	13.5	4.6
Earlton Airport, ON	2.0	1.9	0.1	6.6	4.8	1.8	16.3	13.5	2.8
Summerside Airport, PEI	1.9	1.9	0.0	5.6	4.8	0.8	14.5	13.5	1.0
Bagotville Airport QC	2.0	1.9	0.1	7.1	4.8	2.3	16.5	13.5	3.0
Broadview Airport, SK	1.9	1.9	0.0	6.6	4.8	1.8	16.0	13.5	2.5

Note: (Abbreviation) Stan.= Station, clim.= Climate

From Table 3.14, it can be observed that the difference of the predicted IRI, AC rutting and total permanent pavement deformation created by VWS data and station climate data varies from 0.0 to 0.1 m/km, 0.3 to 3.1 mm, and 0.2 to 4.6 mm, respectively. The results indicate that VWS data is quite close to representing the actual IRI using a particular station's data. However, in predicting AC rutting and total permanent pavement deformation, VWS data is not consistent enough in some

stations. The reason for these differences can be the selection of nearby weather stations, which range from a 3 to 100 km distance from the specified station. In dealing with long distances, there is a high probability of changing climates and consequent change in predicted pavement performance. Other reasons which may lead to differences in pavement performance include the following: climatic change at the micro level, meaning two stations can be closely located and have different climate conditions; incomplete hourly data in some selected weather stations; or low quality of climate data available in the surrounding weather stations, weather data record of surrounding stations in different time periods.

3.11 Summary and Conclusions

A comprehensive study was conducted to evaluate the effects of climate on pavement performances using the Canadian climate files available for the MEPDG. The quality of the Canadian climate database was reviewed. Pavement performances were analyzed for 206 weather stations in Canada which are applicable for the MEPDG. The effects of climate on pavement distresses (IRI, AC layer and total permanent pavement deformation) were analyzed at three levels: province, different climate zone and geography (across latitude and longitude). It was found that the climate has a reasonable impact on predicted pavement rutting. The outcomes of the study presented in this chapter are summarized as follows:

i) There are 206 Canadian climatic files for the MEPDG throughout Canada. Canadian climate data files contain various quantities of climate data ranging from 20 to 240 months. In this study, it was found that 31 weather station files have climate data for less than 10 years, and 13 stations have climate data for less than 5 years.

ii) The 75^{th} percentile of the difference of the annual air temperature and precipitation data recorded by two different sources (MEPDG used and publicly available data recorded by Environment Canada) was less than 0.5ºC and 0.5 mm for all 13 randomly selected weather stations in Canada respectively. This shows that data collected by the Transportation Association of Canada (TAC) for MEPDG show consistency with the Environment Canada data in terms of temperature and precipitation.

iii) Alligator cracking varies from 0.7 to 3.4% which is much lower than its allowable limiting value (25%). It shows a small range of variation due to different environmental factors. It indicates that alligator cracking models need calibration for local Canadian climate conditions.

iv) Transverse cracking values are same (0.2 m/km) for 196 out of 206 weather station files, although the climate is different for different weather station files. Therefore, transverse cracking is not showing realistic results.

v) The IRI for all 206 Canadian stations varies between 1.5 to 2.3 m/km at the end of its 20-year analysis period. However, the value of IRI lies between 1.8 to 2.1 m/km in more than 85% of weather stations. It shows that the IRI value for this type of pavement considered in this study was not very sensitive to climate change, or it needs recalibration.

vi) The IRI does not change reasonably in different climatic zones. However, AC layer deformation, TPPD, and longitudinal cracking change in different climate zones. IRI, AC layer deformation and TPPD were observed more at high temperature and low precipitation than low temperature and high precipitation regions. The interaction effects of temperature and precipitation on pavement distresses prevail. Based on MEPDG analyses, temperature has effects on longitudinal cracking; however precipitation does not affect longitudinal cracking.

vii) AC rutting and total permanent pavement deformation values vary between 0 to 15 mm and 6 to 24 mm, respectively, at the end of a 20-year pavement design life in this study for 206 Canadian weather stations that are applicable to MEPDG. These differences can be attributed to climate change.

viii) Pavement distresses (IRI, AC layer deformation and total permanent pavement deformation) decrease as latitiude increases but longitudinal cracking increases with increase of latitude. However, the longitude of Canadian weather stations available for the MEPDG application does not have considerable effect on pavement distresses.

ix) Longitudinal cracking was observed more at the permafrost regions where the mean annual air temperature is less than the freezing point of water. Due to a high freezing index in the permafrost zones located in the north part of Canada,

the subgrade becomes very stiff which tends to cause a larger tensile strain at the surface layer resulting in high longitudinal surface cracking.

x) VWS verification results showed that difference in total permanent pavement deformation using actual weather station and VWS can be up to 4.6 mm. The reason of this difference may be low quality of data in nearby station or the particular station has low quality of data. The selection of a combination of nearby stations was also found to be an important factor in generating VWS data.

Chapter 4

4. A Comparative Study: Alberta Transportation Pavement Design Method and MEPDG

4.1 Introduction

Alberta Transportation Pavement Design (ATPD) [28] method is an empirical method based on the American Association of State Highway and Transportation Official (AASHTO)-1993 [23] Guide for Design of Pavement Structure with some modifications. ATPD reflects past Alberta Transportation & Utilities (AT & U) pavement design practices adjusted to Alberta environmental, traffic and materials conditions [28]. When it was developed in 1997, the ATPD method claimed that it offered the most appropriate design methodologies and strategies adapted for Alberta conditions and practices [28]. However, the ATPD method has several inherent limitations similar to the AASHTO-1993 Guide that was developed from the AASHO Road Test. As mentioned in the literature review in Chapter 2, the AASHO Road Test was conducted in one location with limited pavement materials and traffic volumes. Since then, traffic has increased significantly in terms of volume and configurations. Limitations and deficiencies of the AASHTO Guide motivated the development of a Mechanistic Empirical Pavement Design Guide (MEPDG) under the National Cooperative Highway Research Program (1-37 NCHRP, 2004) [47].

The MEPDG aims at providing the highway community with a modern practice tool for designing, analyzing and managing new as well as rehabilitated pavement structures. The MEPDG and its associated software DARWinME are suitable for analyzing and predicting performance of flexible and rigid pavements. The MEPDG analyzes input data such as traffic, climate, materials and predicts pavement structure using mechanistic-empirical models. The performance models estimate accumulated damage over the service life of pavement. Moisture and temperature variations within the pavement structure are also calculated using the Enhanced Integrated Climatic Model (EICM).

If additional efforts and resources are employed, the MEPDG will provide better pavement analysis, design, and management [10]. Currently, many transportation

agencies are considering implementation of the MEPDG for the design and evaluation of pavement structures. However, implementation of the MEPDG is a costly and time consuming task. Therefore, initial studies are necessary to evaluate the MEPDG versus empirical pavement design methods such as AASHTO-1993 Guide. Several comparative studies of different empirical and MEPDG pavement design and analysis methods are available in the literatures discussed in the following Literature Review section. However, no study is available in the literature which has attempted a comparison of ATPD and MEPDG.

In this study, an effort has been made to explore the use of the MEPDG for designing pavements at Alberta in the future. To achieve this goal, a comparative study was conducted between existing ATPD and the MEPDG methods. Pavements were designed for different traffic levels and subgrade conditions by the ATPD method and then those pavement structures were evaluated by the MEPDG method. Pavement performance in terms of International Roughness Index (IRI) was evaluated by the ATPD method and then compared with the MEPDG method.

4.2 Literature Review

Different literatures on pavement design and analysis methods including the AASHTO and MEPDG were reviewed in Chapter 2. In some literature, authors have conducted studies to compare AASHTO and MEPDG methods. Those literatures were also reviewed. Some of that literature is provided in this section because they are related to the topic of this chapter.

Gedafa *et al*. [48] conducted a comparative analysis between AASHTO-1993 and MEPDG pavement design methods for typical Portland Cement Concrete (PCC) and Asphalt Concrete (AC) pavements in Kansas. Five in-service Jointed Plain Concrete Pavement (JPCP) projects were reanalyzed as equivalent JPCP and AC projects using both the AASHTO-1993 Guide and MEPDG at 90% reliability level. This study also has investigated the effect of change in performance criteria on the thickness of the pavement using the MEPDG software versions 1.0 and 1.1. The outcomes of this study include: the MEPDG procedure results in much thinner AC and PCC sections compared to AASHTO-1993 Design Guide methodology; MEPDG software version 1.1 produced higher or equal AC thickness and PCC slab thickness compared to MEPDG software version 1.0.

El-Badawy *et al.* [47] redesigned several pavement sections in Idaho using AASHTO-1993 and MEPDG methods that were designed according to the Idaho Transportation Department (ITD) design method. ITD design procedure is the most common empirical design method used in the Northwest region of the USA and is based on R-value. Their study revealed that the AASHTO-1993 Guide and MEPDG produced reasonably similar pavement structures. A comparative analysis between ITD, AASHTO-1993 and MEPDG design procedures was conducted on six different existing roads located in different regions in the state of Idaho. Performances of the pavement structures obtained from different design methods were predicted by nationally calibrated MEPDG software (version 1.1). The following conclusions were drawn from this study: (a) all three design methods, ITD, AASHTO-1993 and MEPDG, yielded reasonably similar thicknesses for the asphalt layers; (b) predicted alligator cracking, fatigue cracking, thermal cracking and IRI were much less than the MEPDG predicted threshold values for the sections selected for the experiment.

Schwartz et al. [10] demonstrated that different designs at the same serviceability in the AASHTO-1993 methodology had different performance predictions when evaluated using the MEPDG. Results of their experiments indicate that the AASHTO-1993 Guide possibly overestimates the performance (or underestimates the required pavement thickness) for warm locations. Authors mentioned that traffic has always been a source of uncertainty in the AASHTO-1993 Guide, especially for high traffic levels. Results found that the performance predicted by the MEPDG declined as traffic increased. The results illustrated that performance prediction variability increased with increasing traffic level. Authors showed that the AASHTO-1993 Guide may overestimate performance (or underestimate required pavement thickness) when traffic levels are well beyond those in the AASHO Road Test (2 million Equivalent Single Axle Load (ESAL)).

4.3 Objectives

The main objective of this chapter was to compare the existing pavement design practice of Alberta, Canada with the MEPDG method. The following tasks were carried out in this chapter.

- Comparison of ATPD with the MEPDG method in terms of predicted pavement distress (IRI);
- Evaluation of pavement performances (IRI and total rutting) using the MEPDG.

This comparative study will help the transportation agencies in Alberta to implement the MEPDG to design and analyze the pavement structure in the near future.

4.4 Differences between the ATPD and MEPDG Method

In this section, main differences between the pavement design method of ATPD and the MEPDG are discussed as follows.

- The MEPDG characterizes materials based on the principles of engineering mechanics, namely stress and strain, for the pavement analysis. The MEPDG is able to input different material characteristics in the design model that helps to predict the performance of the pavement [49]. However, ATPD follows empirical relations to design pavement structure based on serviceability loss and not based on stress strain in pavement layers.
- ATPD has been made based on the AASHTO-1993 Guide that predicts pavement condition as a function of distresses translated into one single index, PSI. On the other hand, the MEPDG predicts directly the structural distresses observed in the pavement section such as IRI, AC rutting, longitudinal cracking, and total permanent pavement deformation.
- ATPD directly computes the pavement layer thicknesses. The MEPDG evaluates the suitability of a pavement section for a given condition. In the MEPDG, a trial pavement section is defined and then evaluated by its predicted performance against the design criteria. If the result is not satisfactory, the section is modified and reanalyzed until an acceptable performance is reached.
- The MEPDG requires more input parameters than the ATPD, especially environmental and material properties. It also allows user to choose different quality levels of input parameters depending upon the level of information and resources available, technical issues, and the importance of the project.
- In the ATPD method that follows the AASHTO-1993 Guide, the seasonally adjusted subgrade resilient modulus and the layer drainage coefficients are the

only variables that account, to some extent, for environmental conditions. The MEPDG utilizes a set of project-specific climate data (air temperature, precipitation, wind speed, relative humidity, etc.) to adjust material properties for temperature and moisture influences.

- ATPD uses the concept of ESALs to define traffic levels, whereas the MEPDG defines traffic by vehicle class and load distributions in terms of traffic load spectra. In the MEPDG each load application is analyzed individually to compute pavement responses. These responses are used to predict distresses and damage increments that are accumulated over load applications and time [10].

Direct comparison of pavement performances by these two methods is difficult since they define pavement performance and reliability in different ways. The necessary steps and methodologies adopted for comparison of the ATPD and MEPDG methods in this study are discussed in the following section.

4.5 Methodologies

To compare the ATPD and the MEPDG methods, it is essential that the inputs of these two procedures be comparable to the highest possible level. General inputs in both methods include traffic data, subgrade, base layer and asphalt layer properties. Three different levels of traffic (low, medium and high), two different types of subgrade (poor and good) and the same base properties were considered for both the ATPD and MEPDG methods.

Based on the above considerations, the following steps were conducted to compare the ATPD and MEPDG methods which are as follows:

(1) Pavement structures were designed using the ATPD method for three different traffic and two subgrade strength levels;

(2) Using the designed pavement structures by the ATPD method, pavement distresses such as IRI and total permanent pavement deformation or total rutting were determined at the end of a 20-year analysis period using the MEPDG method;

(3) Terminal Present Serviceability Index (PSI) from the ATPD method was converted to IRI using an empirical formula suggested by Al-Omari and

Darter [50], and they were compared with IRI predicted by the MEPDG method.

4.6 Pavement Design by the ATPD Method

In order to capture the effects of different traffic levels and subgrade strength on pavement performances, pavements were designed for three traffic levels and two types of subgrade by the ATPD method. Traffic input used in the ATPD method is ESAL. The typical values for different traffic and subgrade strength levels according to ATPD are given below:

- Poor Subgrade: Subgrade modulus is 25 MPa.
- Good Subgrade: Subgrade modulus is 50 MPa.
- Low Traffic: 0.3 Million design ESAL
- Medium Traffic: 4 Million design ESAL
- High Traffic: 20 Million design ESAL.

Therefore, pavements structures were designed by the ATPD method for six different cases as defined below:

- Case 1: Poor subgrade – low traffic
- Case 2: Poor subgrade – medium traffic
- Case 3: Poor subgrade – high traffic
- Case 4: Good subgrade – low traffic
- Case 5: Good subgrade – medium traffic
- Case 6: Good subgrade – high traffic

Except for traffic and subgrade, other pavement design input parameters for six pavement structures were assumed according to ATPD as described in the manual [28] which are as follows:

- Pavement design life = 20 years
- Initial serviceability = 4.2
- Terminal serviceability = 2.5
- Standard deviation (So) = 0.45

- Layer coefficients for asphalt layer was a_1 = 0.40 and for granular base layers was a_2 = 0.14
- Reliability for low and medium traffic level = 85% and for high traffic level = 95%

Pavement structures were designed for all six cases based on required Structural Number (SN) required for each pavement structure. Final design thicknesses of the asphalt layer and granular base layer computed by the ATPD method for six different cases considered in this study are summarized in Table 4.1.

Table 4.1: Pavement Design Thicknesses by ATPD Method for Different Pavement Cases

Different Pavement Case	Structural Number (SN)	Asphalt layer thickness (mm)	Granular Base layer thickness (mm)
Case-1: Poor subgrade – low traffic	87	140	220
Case-2: Poor subgrade – medium traffic	135	180	450
Case-3: Poor subgrade – high traffic	170	250	500
Case-4: Good subgrade – low traffic	70	105	200
Case-5: Good subgrade – medium traffic	108	160	320
Case-6: Good subgrade – high traffic	148	240	370

Table 4.1 shows that the required pavement structure was highest for Case 3 (Poor subgrade – high traffic) and lowest for Case 4 (Good subgrade – low traffic) based on SN value. Table 4.1 shows that with an increase of traffic, SN value increases. Also for the same traffic level, pavement structure may need more SN value for the pavement with lower subgrade strength. The computed layer thicknesses by the ATPD method for all six pavement cases were used as input in the MEPDG method to evaluate the pavement performances.

4.7 Pavement Performance Evaluation by the MEPDG Method

The aim of the MEPDG analyses was to evaluate the pavement distresses and reliability at the end of 20-year analysis period. A reliability term has been

incorporated in the MEPDG for each predicted distress type in order to come up with an analytical solution that allows the design of a pavement with an acceptable level of distress at the end of the analysis period [48]. All of the inputs used in the MEPDG were considered as Level 3 inputs (the inputs consist of default or user-selected values obtained from national and regional experiences such as Long Term Pavement Performance (LTTP) sites). The following key pavement design input parameters are required for pavement performance prediction using the MEPDG:

- Analysis period
- Climatic parameters
- Traffic level information
- Reliability for pavement distresses
- Pavement layer thicknesses
- Material properties

The above parameters are discussed in brief in the following paragraphs.

4.7.1 Analysis Period

The Pavement analysis period was considered similar to the design life as assumed in the ATPD method that is 20-year. Therefore, pavement performances and distress reliabilities were evaluated at the end of 20 years.

4.7.2 Climatic Parameters

Climatic information is an essential input in the MEPDG. To facilitate the implementation of the MEPDG in Canada, climate files are required based on specific format for the locations of pavement analysis. Transportation Association of Canada (TAC) hired a consultant company to develop Canadian weather station files for the MEPDG in Canada. The Canadian climate files for the MEPDG includes a total of 232 weather station files. Out of the 232 weather station files, 206 weather stations files in Canada were found to have complete climate data that can be used by the MEPDG. It is noted that a complete climate data file requires information about hourly precipitation, air temperature, wind speed, percentage sunshine and relative humidity for a minimum of 24 months of period for the MEPDG computational purposes [3]. There are twenty seven (27) weather stations files in Alberta that can be

used for the MEPDG. These 27 weather stations are distributed all over Alberta. Figure 4.1 illustrates the distribution of these 27 different weather stations in Alberta on Google Earth Map.

Figure 4.1: Location of Weather Station Files for MEPDG in Alberta

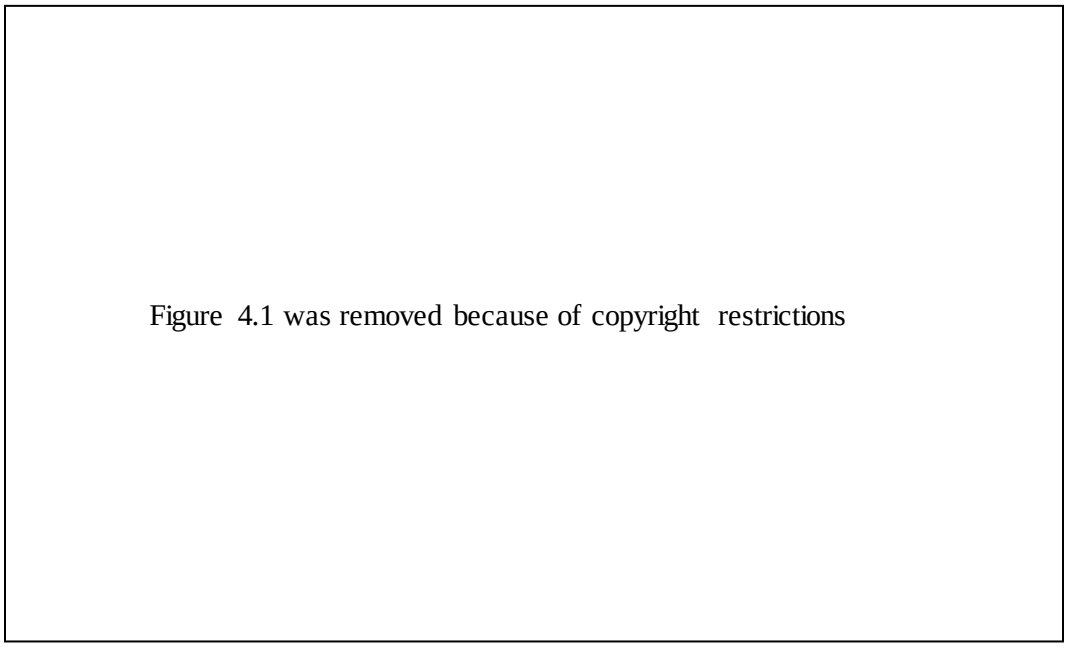

The climatic information details (station name, location, latitude, longitude, mean annual air temperature, mean annual precipitation, start and end date of climate data record and number of available months of climate data) of 206 Canadian weather files including 27 weather station files of Alberta are presented in the Appendix A.1.1.

Pavement structures which were designed based on ATPD were analyzed for all 27 weather station files in Alberta and all six pavement structure cases as considered in ATPD design. The MEPDG software version 1.1 was run for all cases and as a consequence, 162 analyses (27 x 6) were performed. Each run of MEPDG took approximate one hour. Therefore, analysis of six pavement cases for all weather station files took around 162 hour of analysis time.

4.7.3 Traffic Consideration in the MEPDG

ATPD uses ESAL as traffic unit, whereas MEPDG uses Average Annual Daily Traffic (AADT) or Average Annual Daily Truck Traffic (AADTT). To make a fair comparison between ATPD and MEPDG, it is necessary to use an equivalent traffic unit in both methods. To convert ESAL to AADT or AADTT, the following considerations were made according to ATPD [28] :

- The number of lane in design direction = 1 for low and medium traffic and 2 for high traffic as a divided road.
- % of truck in design direction = 50
- % of truck in design lane = 100 for low and medium traffic as undivided road and 85 for high traffic.
- % of single Unit Truck (SUT) in all truck traffic = 70
- % of Tractor Trailer Combination (TTC) in all truck traffic = 30

In Alberta, it is assumed that 15% AADT are attributed to heavy vehicles. MEPDG software converts AADT to AADTT using percentage of heavy vehicle. The conversion of ESALs per day per direction to AADT is given in the following Equation according to ATPD [28].

$$ESAL/day/direction = \frac{AADT}{2}\left[\frac{(\%SUT)}{2}\times 0.881 + \frac{(\%TTC)}{2}\times 2.073\right] \qquad (4.1)$$

In the Equation (4.1), the factors 0.881 and 2.073 refer to load equivalency factors for SUT and TTC respectively. The converted AADT and AADTT for three traffic levels are provided in Table 4.2.

Table 4.2: Traffic Information for Three Cases Used in the MEPDG

Traffic Levels	AADT	AADTT
Low traffic	267	40
Medium traffic	3364	535
High traffic	17822	2673

Traffic volume adjustment factor in terms of monthly adjustment, vehicle class distribution values and hourly distribution were kept as default values in the MEPDG. Axle load distribution factor and general traffic inputs were also kept as default values in the MEPDG.

4.7.4 Pavement Layer Thickness

The pavement layers thicknesses for all six cases are one of the required inputs in the MEPDG. Those pavement layer thicknesses were taken from ATPD output that is provided in Table 4.1.

4.7.5 Reliability

Pavements design deals with many factors that lead to a considerable amount of uncertainty. Even though mechanistic concepts provide a more accurate and realistic methodology for pavement design, a practical method to consider the uncertainties and variations in design is needed so that a new or rehabilitated pavement can be designed for a desired level of reliability [13]. Recommended levels of reliability for predicted distresses by the MEPDG [13] are based on the functional class of the roadway that is explained in Table 2.1 in Chapter 2, Literature Review. Following the guideline of MEPDG, the design reliability was taken as 85% in all distresses for 162 analyses in this study. 85% is also a default value in the MEPDG software.

4.7.6 Material Properties

Designed pavement structures consist of two layers (bound and unbound) and subgrade. The properties of those layers and subgrade considered in the MEPDG are explained below.

4.7.6.1 Subgrade and unbound base layer properties

Similar to ATPD inputs, two types of subgrade (poor and good) and the same base layer were considered for all MEPDG analyses. The other properties (Poisson's ratio, coefficients of lateral earth pressure (K_0), material gradation, liquid limit, plastic limit etc.) of subgrade and base layer were kept as default values of the MEPDG software. For instance, Poisson's ratio was considered as 0.35, coefficients of lateral earth pressure K_0 was considered as 0.5, for both subgrade and base layers. The base and

subgrade material were classified as A-1-a and A-6 respectively according to AASHTO soil classification system [51].

4.7.6.2 Asphalt layer properties

In the MEPDG, Hot Mix Asphalt (HMA) design properties including asphalt mix/gradation and thermal properties were taken as default values. In order to select asphalt binder type for specific weather station, first the high temperature climatic zone based on Alberta Transportation (AT) design bulletin #13 [52] was used for the location of each weather station files in Alberta. Different high temperature zones of Alberta are shown in Figure 4.2.

Figure 4.2: High Temperature Zones for Mix Type Selection

Source: AT Design Bulletin # 13 [52]

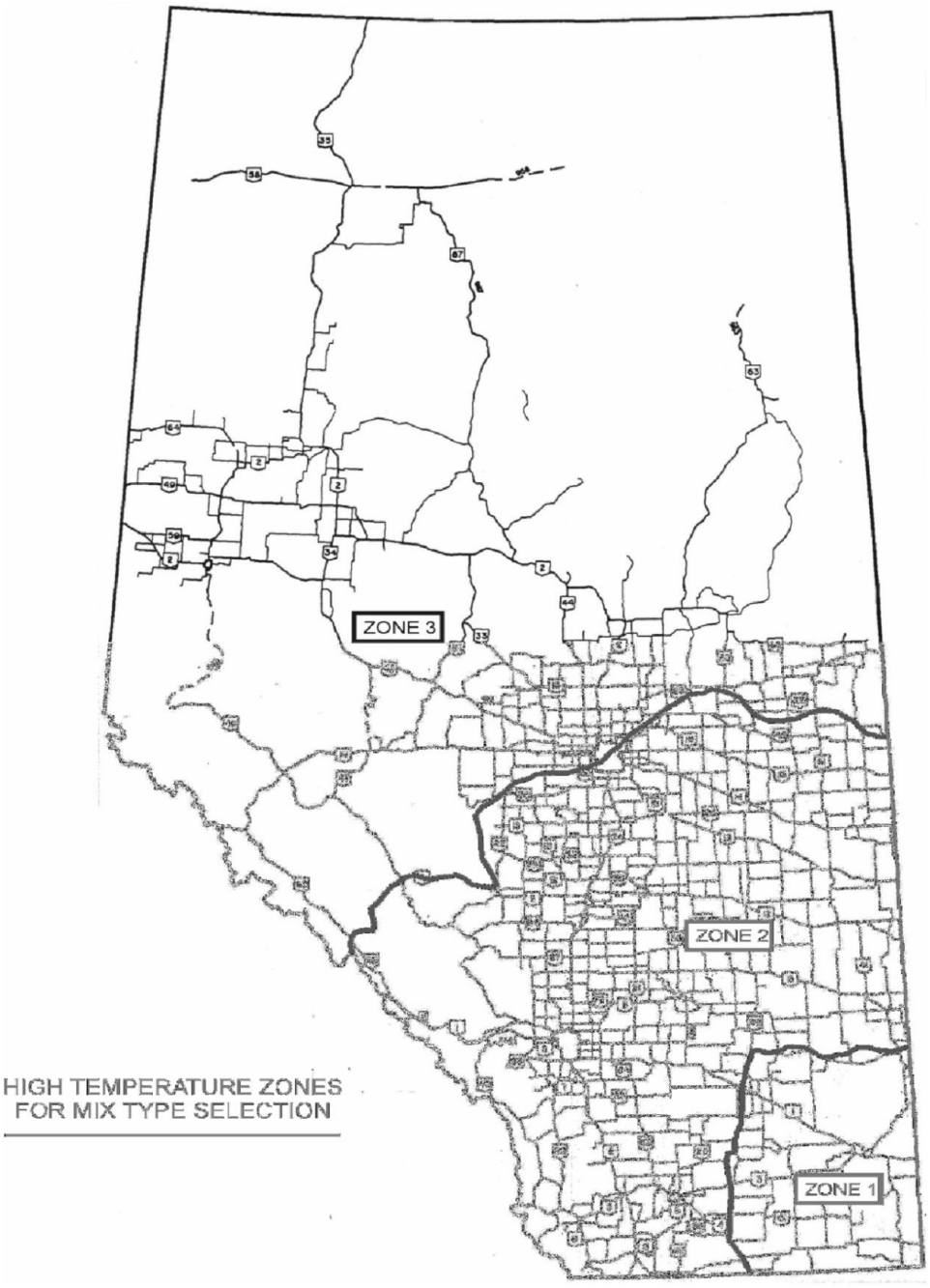

Table 4.3 provides the distribution of 27 Alberta weather files available into different high temperature zones classified by AT design bulletin #13 [52].

Table 4.3: Distribution of Weather Stations of Alberta in Different High Temperature Zones

High Temperature Zone	Weather Stations	Number of Stations
1	Medicine Hat	1
2	Namao Airport, Vermillion, Rocky Mountain House, Coronation Airport, Calgary Int. Airport, Spring Bank Airport, Cowley Airport, Pincher Creek, Leth Bridge Airport, Lloyd Minster Airport	10
3	High Level, Fort Chipewyan, Embarras Airport, Fort McMurray, Cold lake Airport, Peace River Airport, Grande Prairie Airport, Slave Lake Airport, Lec La Biche 1, Lec La Biche 2, White Court Airport, White Court, City Centre Airport, Edmonton International Airport, Edson, Edson Airport	16

Table 4.4 provides selection of conventional asphalt grades according to high temperature zone and design ESAL as defined by AT design bulletin #13 [52]. Among all asphalt grades mentioned in this table, the MEPDG software does not allow 150-200A asphalt binder. Based on engineering judgment, a PG 58-28 was selected instead of a 150-200A grade asphalt binder.

Table 4.4: Selection of Conventional Asphalt Grades based on AT Design Bulletin #13 [52]

High Temperature Zone	Design ESAL (millions)				
	< 1.0	1.0 to < 3.0	3.0 to < 6.0	6.0 to < 10.0	≥ 10.0
1	150-200A	150-200A	150-200A	120-150A	120-150A
2	200-300A	200-300A	150-200A	150-200A	120-150A
3	200-300A	200-300A	150-200A	150-200A	150-200A

The selected asphalt grades for different pavement design cases are provided in Table 4.5.

Table 4.5: Binders of Asphalt for Different Pavement Cases and Zones Used in the MEPDG

Different Pavement Cases	Zone 1	Zone 2	Zone 3
Case-1: Poor subgrade – low traffic	PG 58-28	200-300A	200-300A
Case-2: Poor subgrade – medium traffic	PG 58-28	PG 58-28	PG 58-28
Case-3: Poor subgrade – high traffic	120-150A	120-150A	PG 58-28
Case-4: Good subgrade – low traffic	PG 58-28	200-300A	200-300A
Case-5: Good subgrade – medium traffic	PG 58-28	PG 58-28	PG 58-28
Case-6: Good subgrade – high traffic	120-150A	120-150A	PG 58-28

Table 4.5 shows that in Zone 1 for low and medium traffic, asphalt binder is the same whereas high traffic pavement needs a different asphalt binder. In Zone 2, required asphalt binders are different for different traffic levels. However, in Zone 3 required asphalt binder is the same for medium and high traffic and different for low traffic.

4.8 Results and Discussions

Based on the input parameters described in the previous section, the MEPDG software version 1.1 was run and 162 analyses were performed. The failure criteria or allowable limits of the distresses for all analyses were considered as per MEPDG default values. The main outputs of the MEPDG are the different pavement distresses such as IRI, AC rutting, total permanent pavement deformation, longitudinal cracking, alligator cracking and transverse cracking. The detailed outputs of these distresses for all six pavement structures and 27 weather stations are provided in Appendix 2.1. The outputs of MEPDG analyses are illustrated below.

Table 4.6 shows the summary of all cracking (longitudinal, alligator and transverse) and their corresponding allowable limit by the MEPDG. The summary of IRI and total rutting predicted by the MEPDG and their allowable limits for failure are given in Table 4.7. The MEPDG output does not provide AC rutting values with design reliability separately. AC rutting is included within total rutting. Therefore, AC rutting is not discussed in this study.

Table 4.6: Summary of Pavement Distresses (Longitudinal, Alligator and Transverse Cracking) for Different Pavement Cases Predicted by the MEPDG

Pavement Distresses	Case	Distresses by the MEPDG at the end of 20 year design period at 85% reliability			
		Min.	Max.	Mean	Allowable limits
Longitudinal Cracking (m/km)	Case-1: Poor subgrade - low traffic	42.05	53.01	45.52	378.6
	Case-2: Poor subgrade - medium traffic	41.05	49.54	45.11	
	Case-3: Poor subgrade - high traffic	41.05	61.38	49.89	
	Case-4: Good subgrade – low traffic	293.00	341.70	314.39	
	Case-5: Good subgrade - medium traffic	150.65	228.00	177.03	
	Case-6: Good subgrade - high traffic	47.11	67.80	55.01	
Alligator Cracking (%)	Case-1: Poor subgrade - low traffic	1.48	1.56	1.52	25.0
	Case-2: Poor subgrade - medium traffic	2.30	2.72	2.48	
	Case-3: Poor subgrade - high traffic	1.35	2.35	2.09	
	Case-4: Good subgrade – low traffic	4.51	7.56	5.78	
	Case-5: Good subgrade - medium traffic	12.80	15.71	14.51	
	Case-6: Good subgrade - high traffic	2.95	4.94	3.76	
Transverse Cracking (m/km)	Case-1: Poor subgrade - low traffic	12.95	12.95	12.95	189.03
	Case-2: Poor subgrade - medium traffic	12.95	12.95	12.95	
	Case-3: Poor subgrade - high traffic	12.95	12.95	12.95	
	Case-4: Good subgrade – low traffic	12.95	473.42	64.11	
	Case-5: Good subgrade - medium traffic	12.95	12.95	12.95	
	Case-6: Good subgrade - high traffic	12.95	12.95	12.95	

4.8.1 Longitudinal Cracking

Table 4.6 shows that the values of longitudinal cracking varied from 0 to 67.8 m/km for all weather stations of Case 1, 2, 3 and 6 pavement structures i.e. in 108 out of 162 analyses (67%). However, longitudinal cracking values were observed between 150.6 to 341.7 m/km for 54 weather stations that are included in Case 4 and 5 pavement structures. The values of longitudinal cracking at each station for all pavement cases are provided in Appendix A.2.1. Among the six cases, Case 3 and 6 of pavement structures which represent pavements designed with high traffic value, whereas Case 4 represents low traffic condition. Analyses results showed that longitudinal cracking values are low in high traffic and comparatively high in low traffic road which is unrealistic. This unrealistic prediction of the longitudinal cracking model in the MEPDG also was previously demonstrated by Ali [17]. Ali has mentioned that longitudinal cracking is not well defined in the MEPDG from a mechanistic viewpoint. The study conducted by Ali produced fluctuating and unstable trends of longitudinal cracking in Canada. Schwartz *et al*. [10] and Velasquez *et al*. [29] also mentioned that the existing models for longitudinal cracking or top-down cracking incorporated in the MEPDG are immature and did not appear to produce reasonable predictions.

4.8.2 Alligator Cracking

Table 4.6 illustrates that the values of alligator cracking varied from 1.35 to 7.56% for 135 analyses of Case 1, 2, 3, 4 and 6 pavement structures i.e., in. However, in Case 5 of pavement at 27 weather stations, the alligator cracking values were observed between 12.8 to 15.71%. Case 4 represents medium traffic-good subgrade road. Results demonstrated that the alligator cracking values created in high traffic condition, for both poor and good subgrade levels are less than the medium traffic-good subgrade roads. These results are unrealistic and hence alligator cracking models need calibration for local Canadian climate condition. The similar findings also were demonstrated in the US study conducted by Johanneck and Khazanovich [3].

4.8.3 Transverse Cracking

Transverse cracking values were the same (12.95 m/km) for 159 out of 162 analyses as shown in Table 4.6. Very few exceptionally high values (473.42 m/km) were found in only three out of 162 analyses as provided in Appendix A.2.1. Although all the 162 analyses are different in terms of climate, traffic and subgrade, but transverse cracking values are not changing reasonably. These observations indicate that transverse cracking model is not very sensitive to Alberta environment, traffic and material and hence it needs calibration for local condition.

On the other hand, the MEPDG predicts expected values for the other three distresses (IRI, AC rutting and total rutting) at the end of analyses period as shown in Appendix 4.1.

4.8.4 Evaluation of the MEPDG Predicted IRI and Total Rutting and Comparison with Their Allowable Limits

The desired level of reliability is related to the acceptable level of distress at the end of the analysis period in defining performance requirements for a pavement design [13]. As mentioned in section 4.7, the reliability in the MEPDG analyses was considered as 85% for all distresses. Before discussing the results in detail for predicted distresses and reliability values at the end of the 20-year analysis period, an understanding of how the MEPDG estimates and presents the results is required. In order to understand that, one example is discussed below.

4.8.4.1 Sample Distress Plots

Results of MEPDG software version 1.1 for Case-3, Calgary Int. Airport are provided in Figure 4.3 and 4.4. These two figures show distresses (IRI and rutting) versus pavement age (month). The MEPDG uses the imperial system; however, for the purpose of this thesis all results were converted to metric system.

Figure 4.3: IRI Predictions for Calgary Int. Airport for Case 3 Pavement Structure

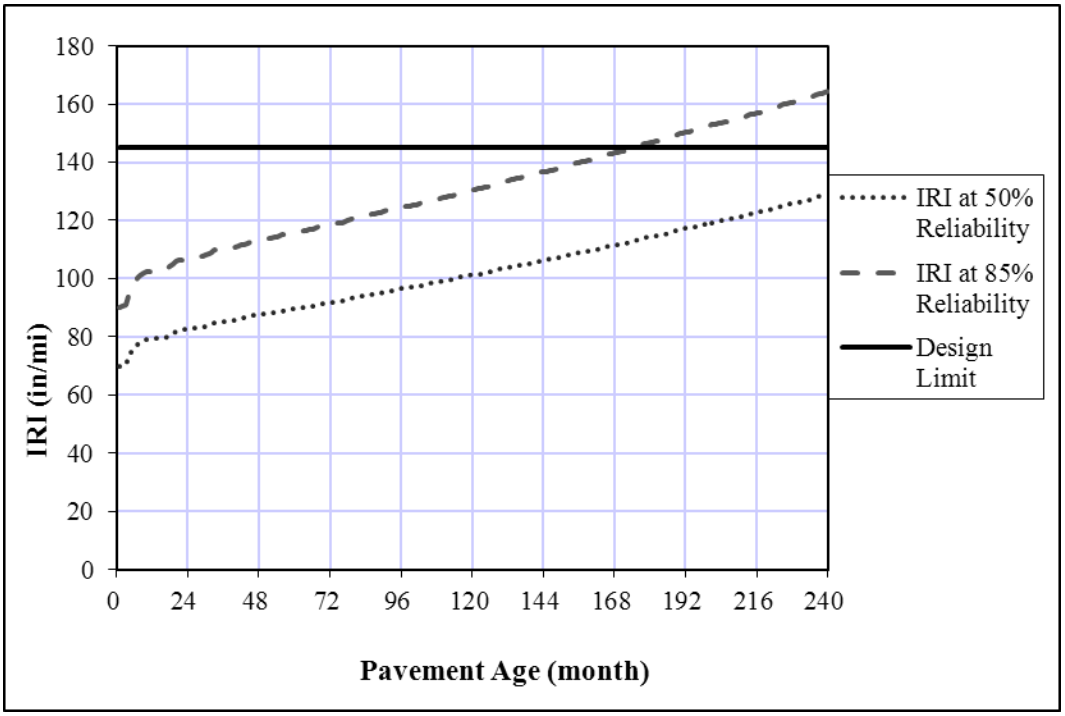

Figure 4.3 shows predicted IRI over the 20-year analysis period with failure criteria of IRI as 145 inches/mile. This figure also shows IRI at 50% reliability, as well as at the selected reliability in the analysis.

Figure 4.3 illustrates that the value of IRI at 85% reliability is 164.29 in/mi and at 50% reliability the value is 128.9 in/mile at the end of the 20-year analysis period. The predicted reliability at the end of the 20-year analysis period is 68.2%.

Figure 4.4: Permanent Deformation (Total Rutting) Predictions for Calgary Int. Airport for Case 3 Pavement Structure

Figure 4.4 shows predicted rutting depth over the 20 year-design period. The figure shows the user specified failure criteria for rutting: 0.25 inches for HMA layer and 0.75 inches in total pavement rutting (also on graph as total rutting design limit line). These limits are briefly discussed under the "Results and Discussion" section of this chapter. The total rutting at 50% reliability as well as at selected design reliability are displayed on the. The selected design reliability corresponds to the level specified by the designer.

Figure 4.4 also describes that the value of total rutting at design reliability (85%) is 0.93 inch and at 50% reliability the value is 0.81 inch at the end of the 20 year analysis period. The predicted reliability after 20 year is 30.6%.

4.8.4.1 Summary and Discussion on the MEPDG Distress Outputs (IRI and Total Rutting)

The maximum, minimum, and mean values of IRI and total rutting for each of the six pavement cases of 27 weather stations are provided in Table 4.7.

Table 4.7: Summary of Pavement Distresses (IRI and Total Rutting) for Different Pavement Cases Predicted by the MEPDG

Pavement Distresses	Pavement Case	Distresses by the MEPDG at the end of 20 year analysis period at 85% reliability			
		Min.	Max.	Mean	Allowable limits
IRI (m/km)	Case-1: Poor subgrade - low traffic	2.45	2.53	2.51	2.29
	Case-2: Poor subgrade - medium traffic	2.58	2.62	2.60	
	Case-3: Poor subgrade - high traffic	2.59	2.90	2.66	
	Case-4: Good subgrade – low traffic	2.40	2.80	2.46	
	Case-5: Good subgrade - medium traffic	2.50	2.54	2.52	
	Case-6: Good subgrade - high traffic	2.49	2.57	2.53	
Total rutting (mm)	Case-1: Poor subgrade - low traffic	18.80	20.58	19.97	19.05
	Case-2: Poor subgrade - medium traffic	22.39	24.30	23.01	
	Case-3: Poor subgrade - high traffic	23.11	32.11	25.31	
	Case-4: Good subgrade – low traffic	16.14	17.95	17.28	
	Case-5: Good subgrade - medium traffic	18.67	20.62	19.36	
	Case-6: Good subgrade - high traffic	19.05	22.52	20.66	

Note: Min. = Minimum, Max. = Maximum

The minimum and maximum predicted IRI values among all six cases are 2.40 and 2.90 m/km respectively. The minimum value is observed at Calgary Int. Airport in Case 4 (Good subgrade - low traffic) and maximum value is observed at High Level Airport in Case 3 (Poor subgrade-high traffic). The difference between maximum and minimum IRI is nearly 21% and this difference is the result of different traffic, subgrade as well as climatic factors. The IRI values in all pavement cases exceed the allowable limit of 2.29 m/km. Since the IRI values in all cases provided in Table 4.7 were observed at 85% reliability; the pavement structure designed by the ATPD method will not meet the MEPDG allowable limit with 85% design reliability at the

end of the 20-year analysis period. Therefore, it is necessary to evaluate the exact reliability for the ATPD designed pavement structure in each case.

Table 4.7 illustrates that total rutting values vary from 16.14 to 32.11 mm in all cases. The allowable limit is considered as 19.05 mm. The mean total rutting values in all cases exceed the MEPDG allowable limit, except Case 4 which represents the best road condition (Good subgrade-low traffic). The maximum total rutting value is found in Case 3, which is the worst case (high traffic and poor subgrade). From the above results it can be concluded that most of the pavement will fail at the given failure criteria after 20-year with 85% reliability. Therefore, it is essential to evaluate the exact reliability values at the end of the 20-year design period since achieving higher reliability within all the project constraints is highly expected. The predicted distress reliabilities are discussed below.

The design reliability in the MEPDG method was considered as 85%, which is the default value in the MEPDG software version 1.1 [13]. From the above discussion, we can see that in many cases pavement structures fails with 85% reliability value. Therefore, it is necessary to evaluate the exact reliability at the end of the 20-year design period with the given allowable limit of each distress. The predicted reliabilities by the MEPDG for IRI and total rutting for six case at all 27 weather station files are summarized and presented in Table 4.8.

Table 4.8: Summary of Pavement Distress Reliability at the End of 20-Year Analysis Period predicted by the MEPDG

Pavement Distresses	Pavement Case	MEPDG predicted distress reliability at the end of 20 year analysis period (%)		
		Min.	Max.	Mean
IRI	Case-1: Poor subgrade - low traffic	71.6	76.3	73.1
	Case-2: Poor subgrade - medium traffic	66.2	69.2	67.7
	Case-3: Poor subgrade - high traffic	50.0	68.2	64.2
	Case-4: Good subgrade – low traffic	55.9	79.3	74.3
	Case-5: Good subgrade - medium traffic	71.2	74.0	72.5
	Case-6: Good subgrade - high traffic	69.3	74.3	71.6
Total rutting	Case-1: Poor subgrade - low traffic	67.0	87.2	74.7
	Case-2: Poor subgrade - medium traffic	22.7	42.4	35.0
	Case-3: Poor subgrade - high traffic	0.4	34.7	18.1
	Case-4: Good subgrade – low traffic	93.3	99.0	96.0
	Case-5: Good subgrade - medium traffic	67.6	88.3	81.7
	Case-6: Good subgrade - high traffic	46.0	82.4	66.8

Note: Min. = Minimum, Max. = Maximum

Table 4.8 shows that in all six cases the minimum, maximum and mean IRI reliability predicted by the MEPDG is less than design reliability of 85%. The lowest average IRI reliability is observed as 64.2% in Case 3 (Poor subgrade and high traffic condition). Therefore, it can be said that designed pavement section by the ATPD method needs more thickness to satisfy the IRI failure criteria by the MEPDG to reach 85% reliability.

Table 4.8 also illustrates that the mean total rutting reliability predicted by the MEPDG is less than 85% in all cases except Case 4. Case 4 (Good subgrade-low traffic) represents the best case among all the six cases considered in this study where the MEPDG predicted total rutting reliably exceeds 90%. The mean total rutting values in Case 2 and 3 pavement structures (poor subgrade - medium & high traffic) are 35 and 21%, which are much lower than the design reliability. Therefore, it can be concluded that except in very good road conditions (Case-4), the total rutting reliability predicted by the MEPDG does not meet the design reliability for the given

failure criteria or allowable limit. Therefore, to satisfy the allowable limits of total rutting, the pavement section used in the MEPDG analyses needs more thickness. However, for Case 4 pavement structure, the designed pavement section is overestimated according to MEPDG analysis since the average reliability is 96 %.

In any pavement structure case, the difference among minimum, maximum and mean reliability reflects the effects of different climatic conditions in 27 weather stations. For instance, with the same pavement structure in Case 3 pavement structure the minimum, average and maximum IRI reliabilities predicted by the MEPDG are 61%, 65% and 75%.

4.9 Comparison of ATPD with the MEPDG Method in Terms of Roughness (IRI)

Direct comparison of pavement performances by the ATPD and MEPDG methods is difficult since they define pavement performances and reliability in different ways. Therefore, it is essential to keep the inputs and performance criteria similar for both methods. In methodology (section 4.5) common inputs for these two methods have already been discussed. However, performance criteria are also important to make a valid comparison which is discussed below.

ATPD computes pavement performances in terms of PSI at the end of design life. On the other hand, MEPDG predicts pavement performances in terms of pavement distresses such as IRI, AC rutting, total permanent pavement deformation, alligator cracking, transverse cracking and longitudinal cracking. MEPDG distress prediction models, for example, fatigue cracking, permanent deformation and thermal cracking are empirically correlated to smoothness. The smoothness model considers other distresses as well, such as potholes, longitudinal cracking outside the wheel path, and block cracking if there is potential of occurrence [13]. Road roughness index such as IRI is a useful indicator of the level of the pavement smoothness. Lower IRI means less deviation in the pavement's surface; an IRI of zero represents a perfectly smooth pavement. IRI and PSI are both performances indices that can be used as indicators of road roughness and serviceability.

As serviceability ratings are dominated by vehicle ride perception, a strong correlation between serviceability (PSI) and roughness (IRI) prevails which has been

discussed in the literature [50, 53, 54]. An empirical formula showing the relationship between PSI and IRI was suggested by Al-Omari and Darter [48],

$$PSI = 5 * e^{(-0.26*IRI)} \quad (4.2)$$

Where, IRI is in meter per kilometer

This correlation was employed to compare the pavement performances predicted by the ATPD and MEPDG methods in this study. The terminal PSI was considered as 2.5 for all pavements in six cases based on the ATPD method [13] and then converted to IRI using equation 4.2. The converted IRI is 2.67 m/km in the ATPD method. The IRI for six cases and 27 weather stations were received from output distress files of 162 analyses which were performed by the MEPDG software version 1.1. In the MEPDG method the design reliability was assumed as 85%. The maximum, minimum and average IRI of 27 weather stations for all six cases predicted by the MEPDG at the end of the 20-year analysis period are tabulated and compared with ATPD predicted IRI which are given below.

Table 4.9: Comparison of IRI computed by ATPD or AASHTO and MEPDG Method for Different Subgrade and Traffic Level

Pavement Case	IRI (m/km) after 20 years predicted by			
	ATPD	MEPDG with design reliability of 85%		
		Minimum	Maximum	Average
Case-1: Poor subgrade - low traffic	2.67	2.45	2.53	2.51
Case-2: Poor subgrade - medium traffic		2.58	2.62	2.60
Case-3: Poor subgrade - high traffic		2.47	2.70	2.64
Case-4: Good subgrade – low traffic		2.40	2.80	2.46
Case-5: Good subgrade - medium traffic		2.50	2.54	2.52
Case-6: Good subgrade - high traffic		2.49	2.57	2.53

Table 4.9 shows that average MEPDG predicted IRI for all cases varies from 2.46 to 2.64 m/km. However, IRI which is equivalent to terminal PSI in the ATPD method is 2.67 m/km. The IRI found from both methods are fairly close since variation in IRI values is between 1.1 to 7.8%. According to equivalent terminal PSI, ATPD method considers failure criteria for IRI as 2.67 m/km, whereas MEPDG considers 2.29 m/km which is a default value as provided in Table 4.7. However, the user has the option to change the default value and provide different failure limits. With 2.29 m/km allowable limit in the MEPDG method, pavement sections were observed to fail in IRI criteria and could not reach design reliability that was discussed in the previous section 4.8.1. However, Table 4.9 demonstrates that the IRI values at 85% reliability at the end of the 20-year analysis period in the MEPDG method are pretty close (<8 % difference) to the allowable limit of 2.67 m/km of ATPD method. From the above analyses it can be concluded that with same allowable limits both method shows comparable pavement distress as well as design life since the predicted distresses are close enough in terms of IRI. Therefore, allowable limits play an important role to carry out pavement design and its performance evaluation. Since no correlation exists in literature to compare other MEPDG distresses (e.g. rutting or cracking) with PSI, the above comments are made based on smoothness criteria only.

4.10 Comparison of IRI from ATPD and the MEPDG with Field Observed Values

Pavement performance in terms of IRI predicted by ATPD and MEPDG were compared with field data from Alberta Transportation Pavement Management System (PMS) survey data available online [55]. To compare field data with ATPD and MEPDG predictions, all pavement sections in the PMS which had a service life of 20 years must be selected; however it was not possible to find any pavement section which had not any rehabilitation in 20 years after construction. It was possible to find several sections with 19 years life without any rehabilitation. These sections have been listed in Appendix A.2.2, these pavement sections have different traffic levels. It was found that the average IRI for 19-year sections from PMS have the same IRI value at an average of 2.4 m/km. Comparison of measured IRI by the PMS survey with ATPD and MEPDG method is demonstrated in Table 4.10.

Table 4.10: Comparison of average IRI values Found from ATPD and MEPDG with PMS Survey Data Collected by Alberta Transportation

Traffic level	Mean IRI (m/km) from different sources		
	MEPDG	PMS	ATPD
Low	2.46	2.40	2.67
Medium	2.52		
High	2.53		

From Table 4.10, it is observed that the mean IRI from the MEPDG, ATPD and PMS survey data are close (maximum difference 11.3%). The maximum difference is noticed between field observed IRI with ATPD considered IRI, whereas the MEPDG predicted IRI is fairly close (maximum difference 5.4%) to field measured IRI. The difference between IRI predictions by the MEPDG method, and field observations could be the reason of different traffic level considerations. Traffic level of low, medium and high was defined as 267, 3564 and 17822 AADT respectively for all pavements considered in the MEPDG. One difficulty in comparison of IRI from pavement design methods and field data was that most of pavement sections from PMS, are related to two highways (24:02 and 845:40) which have traffic levels of 1000 and 2320 AADT (112 and 326 ESAL/day) respectively as provided in Appendix A.2.2. It can be concluded that it is difficult to compare the pavement performance prediction parameters with field data due to limited road sections with the same attributes.

4.11 Summary and Conclusions

This study attempted to compare the ATPD which is based on the AASHTO-1993 and the MEPDG method. In order to make such comparison, first of all, predicted distresses by the MEPDG in terms of IRI and total rutting were evaluated. Then the ATPD method was compared with the MEPDG in terms of IRI. Several conclusions from this study are given below.

- The ATPD and MEPDG method predicts close IRI distress (<10% difference) at the end of the 20-year analysis period with similar design inputs.
- The comparative study between the ATPD and the MEPDG methods explored that if the allowable limit of the MEPDG analysis is increased from 2.29 m/km to 2.67 m/km, all the pavement cases (162 analyses) will meet 85% reliability at the end of 20-year analysis period. Therefore, allowable limits play an important role in carrying out pavement design and its performance evaluation.
- In this study, 162 MEPDG analyses indicated that all pavements fail in IRI with an allowable limit of 2.29 m/km. Pavements designed with this allowable limit reached minimum 50% and maximum 79.3% reliability at the end of the 20-year analysis period. Therefore, in no case does the pavement structure designed by the ATPD method meet the MEPDG, considering a design reliability of 85%.
- The maximum difference between the lowest and highest predicted IRI by the MEPDG method reaches 21%, which reflects the effects of different input parameters in terms of traffic, subgrade as well as climatic parameters for 27 weather station files.
- This study has concluded that the ATPD method cannot be said to overestimate or underestimate pavement design when compared to the MEPDG method, rather the estimation completely depends on different cases (traffic and subgrade condition).
- According to the MEPDG analysis, ATPD designed pavement structures have been underestimated for total rutting in poor subgrade- medium and high traffic conditions. However, for good subgrade-low traffic the ATPD designed structure is overestimated according to MEPDG distress analyses.
- Based on the MEPDG prediction, Case 3 pavement structure (high traffic-poor subgrade), was the only pavement structure that failed in both IRI and total rutting. Therefore, ATPD designed Case 3 pavement structure needs strengthening to satisfy the failure criteria in the MEPDG method.
- It is difficult to compare the pavement performance prediction parameters with field data due to limited road sections with the same attributes.

Chapter 5

5. Summary, Conclusions, Contributions and Future Works

This chapter describes work summary, conclusions, contributions of this study and future research directions.

5.1 Work Summary

Currently, most of the provincial transportation agencies in Canada use the American Association of State Highway Transportation Official (AASHTO)-1993 pavement design Guide for pavement design and rehabilitation. Several studies demonstrated that the AASHTO-1993 overestimates or underestimates pavement designs (thicknesses) in various situations. The current Mechanistic Empirical Pavement Design Guide (MEPDG) incorporates effects of climate, traffic and materials on pavement performances in a more comprehensive manner than the AASHTO method. In this thesis, an effort has been made to explore the implementation of the MEPDG in Canada, especially in Alberta.

In this study the accuracy of Canadian climate data files developed for the MEPDG was extensively evaluated for 206 weather stations files and 206 MEPDG analyses were performed to evaluate the effects of climatic factors on pavement performances.

In addition, a comparative study was carried out between the Alberta Transportation Pavement Design (ATPD) method and the MEPDG. Three different traffic levels and two different types of subgrade at 27 weather station files were considered for the analysis in Alberta. As a consequence, 162 analyses were performed by the MEPDG. The conclusions from this study are discussed in the following section.

5.2 Conclusions

The conclusions that were made from each of the objectives of this study are mentioned below. The bold fonts indicate specific objectives, and conclusions from the related study are given under each objective.

(a) Evaluating of the accuracy of Canadian Climatic Database used for the MEPDG:

i) Differences between climatic parameters (temperature and precipitation) of the MEPDG database and those parameters of the Environment Canada database were negligible. Results showed that 75th percentile of the differences for temperature and precipitation were 0.5^{0}C and 0.5 mm respectively.

ii) The differences of freezing index computed by the MEPDG and other sources were less than 100^{0}C-days, except in a few stations located in permafrost zones such as Inuvik Airport of NT, Baker Lake of NU and so on.

iii) The differences between frost depth computed by the MEPDG and Modified Berggren methods were less than 0.6 m except in few stations located in permafrost zones.

iv) In permafrost zones, the freezing index and frost depth values were overestimated by the MEPDG method in comparison to other available sources and hence, the freezing index and frost depth calculating models in the MEPDG needs calibration for locations in permafrost regions.

v) The comparison of Virtual Weather Station (VWS) data and actual weather station data demonstrates that both of these data predict close IRI values (< 0.1 m/km difference). However, in predicting AC rutting and total rutting, VWS data did not produce consistent results (difference was up to 4.6 mm) in some stations.

(b) Evaluating the Effects of Canadian Climate on Pavement Performances using the MEPDG:

i) AC rutting and total permanent pavement deformation values vary between 0 to 15 mm and 6 to 24 mm, respectively, at the end of a 20-year pavement design life in 206 available Canadian weather stations for MEPDG. These differences can be attributed to climate change.

ii) IRI was less sensitive to environmental factors as the predicted IRI by the MEPDG for 85% of weather stations was between 1.8 - 2.1 m/km.

iii) Predicted Alligator cracking values predicted by the MEPDG were unrealistic since alligator cracking varied from 0.7 to 3.4% among 206 weather stations, which is much lower than its allowable limiting value of 25%.

iv) Transverse cracking predicted by the MEPDG were the same (0.2 m/km) for 196 out of 206 weather station files. Therefore, predicted transverse cracking by the MEPDG is not showing realistic results.

v) Extensive longitudinal cracking (up to 2007 m/km) was predicted by the MEPDG for weather stations located in northern Canada where the mean annual air temperatures are less than zero.

vi) Unrealistic output of MEPDG for alligator and transverse cracking indicates that associated models need calibration for local Canadian climatic conditions.

(c) Comparison between the AASHTO-1993 based ATPD Method and the MEPDG:

i) The ATPD and MEPDG methods predict close IRI distress (<8% difference) at the end of the 20-year analysis period with similar design inputs for 27 weather stations files in Alberta.

ii) The comparative study between ATPD and the MEPDG methods explored that if the allowable limit of the MEPDG analysis is increased from 2.29 m/km to 2.67 m/km, all the pavement cases (162 analyses) will meet 85% reliability at the end of the 20-year analysis period.

iii) In this study, 162 MEPDG analyses indicated that all pavements fail in IRI with an allowable limit of 2.29 m/km. Pavements designed with this allowable limit reached the minimum 50% and maximum 79.3% reliability levels at the end of the 20-year analysis period. Therefore, in no case does the pavement structure designed by the ATPD method meet the MEPDG, considering a design reliability of 85%

iv) The maximum difference between the lowest and highest predicted IRI by the MEPDG method was 21%, which reflects the effects of all variables considered in this study for traffic levels, subgrade types, as well as climatic parameters for 27 weather station files.

v) Comparing the two pavement design methods, ATPD and the MEPDG, it was concluded that the ATPD method overestimated or underestimated performance of pavement as a function of pavement structures, traffic levels, and subgrade types.

vi) According to the MEPDG analysis, ATPD designed pavement structures have been underestimated for total rutting in poor subgrade- medium and high traffic conditions. However, for good subgrade-low traffic the ATPD designed structure is overdesigned according to MEPDG distress analyses.

vii) Pavement structure with high traffic and poor subgrade, Case 3, was the only pavement structure that failed in both considered distresses (IRI and total rutting) by the MEPDG method. Therefore, ATPD underestimates thickness to satisfy failure criteria in the MEPDG method.

viii) It is difficult to compare the pavement performance prediction parameters with field data due to limited road sections with the same attributes.

5.3 Contributions

Some contributions of this study are as follows:

- This study attempted a primary effort to explore the implementation of MEPDG in Canada. An earlier similar study was conducted only for the USA [3].
- This study is a first attempt in evaluation of the quality of Canadian climate data files for use in the MEPDG.
- This study evaluated the effects of Canadian climate files for the MEPDG on pavement performances that might help transportation agencies of Canada to review the feasibility of MEPDG application in Canadian local condition.
- This study is an initial effort to compare the AASHTO-1993 based ATPD and the MEPDG methods. This comparative study might help Alberta Transportation to evaluate the benefits of the MEPDG over ATPD method.

5.4 Future Works

Some issues were identified for future research to evaluate the sensitivity of the MEPDG inputs as well as to assess the benefits of the MEPDG over empirical methods:

- IRI, alligator and transverse cracking models used in the MEPDG were found to be less or insensitive to Canadian climate files in this study. Calibrating of the

existing IRI, alligator and transverse cracking models in the MEPDG are strongly recommended.

- Effects of climatic files on pavement performances were studied only for flexible pavement. A similar study for rigid pavement is proposed for future work.
- As only one pavement structure was considered to study the effects of climatic data files, it is recommended that more pavement structures be studied in the future.
- Extend the comparative study between current pavement design practices with MEPDG for other provinces of Canada.

References

1. Smith J. T., Tighe S. L. and Andrey J. and Mills B., "Temperature and Precipitation Sensitivity Analysis on Pavement Performance," Transportation Research Circular, E-C126, pp. 558 -571, June 2008.
2. Dore. G., Drouin. P., Pierre. P. and Pierre. D., "Estimations of the Relationships of Road Deterioration to Traffic and Weather in Canada," Final Report, Transport Canada, BPR Project Number: M-61-04-07, May, 2005.
3. Johanneck L. and Khazanovich L., "A Comprehensive Evaluation of the Effect of Climate in MEPDG Prediction," In *Transportation Research: Journal of the Transportation Research Board*, No 2170, Transportation Research Board of the National Academies, Washington, D.C., P.P.45-55, 2010.
4. Selezneva O. I., Jiang Y. J., Larson G., and Puzin T., "LTPP Computed Parameter: Frost Penetration," Publication FHWA-HRT-08-057. FHWA, U.S. Department of Transportation, 2008.
5. Richter C. A., "Seasonal Variations in the Moduli of Unbound Pavement Layers," Publication FHWA-HRT-04-079. FHWA, U.S. Department of Transportation, 2006.
6. http://www.nrc-cnrc.gc.ca/eng/ibp/irc/cbd/building-digest-182.html, Accessed: August 2011.
7. Nix F., Weight-Distance taxes, prepared for Canadian Trucking Alliance, p.34, 2001.
8. Saint-Laurent D. and Gervais C. L, "impact des restrictions de charge en periode de degal," Innovation Transport, no. 18, p.25-31, 2003.
9. Canadian Strategic Highway Research Program (C-SHRP), "Pavement Structural Design Practices Across Canada," C-SHRP Technical Brief # 23, April 2002, ISBN 1-55187-068-1. (http://www.cshrp.org/products/techbr-23.pdf; Accessed: July 2011).
10. Schwartz C. W, Carvalho R. L., "Implementation of the NCHRP 1-37A Design Guide Final Report Volume 2: Evaluation of Mechanistic-Empirical Design Procedure," Maryland State Highway Administration, University of Maryland Project No. SP0077B41 UMD FRS No. 430572, February, 2007.

11. Nantung T. E., "Implementing the Mechanistic – Empirical Pavement Design Guide for Cost Savings in Indiana," Indiana Department of Transportation, TR News 271 November – December 2010.
12. Oh J., Ryu D., Fernando E.G., and Lytton R. L.,"Estimation of Expected Moisture Contents for Pavements by Soil and Water Characteristics," In *Transportation Research: Journal of the Transportation Research Board*, No 1967, Transportation Research Board of the National Academies, Washington, D.C., P.P.135-147, 2006.
13. Guide for Mechanistic Empirical Design of New and Rehabilitated Pavement Structures, Final Report NCHRP, USA, 2004.
14. Larson G., and Dempsey B. J.," Enhanced *Integrated Climatic Model (Version 2.0)*," Report No. DTFA MN/DOT 72114, University of Illinois at Urbana-Champaign, Urbana, IL, 1997.
15. *Independent Review of the Mechanistic-Empirical Design Guide and Software*. NCHRP Research Results Digest No. 307, National Cooperative Highway Research Program, Transportation Research Board of the National Academies, Washington, D.C., 2006.
16. Yoder E. J., and Matthew W., Principles of pavement design. Wiley, 2nd Edition, 1975.
17. Ali O., Evaluation of the Mechanistic Empirical Pavement Design Guide (NCHRP-1-37A), RR-216, September 2005.
18. http://training.ce.washington.edu/wsdot/Modules/06_structural_design/06-3_body.htm. Accessed: June 2011.
19. National Crushed Stone Association, "Flexible *Pavement Design Guide for Highways*", NCSA Publication, Washington D.C., 1972.
20. Department of Transportation U.S. *AASHO Interim Guide for the Design of Rigid and Flexible Pavements*. Published by the American Association of State Highway Officials, Washington D.C., 1961.
21. Department of Transportation, U.S. *AASHTO Interim Guide for the Design of Pavement Structures*. Published by the American Association of State Highway and Transportation Officials, Washington D.C. 1972.

22. Department of Transportation, U.S. *AASHTO Guide for the Design of Pavement Structures*. Published by the American Association of State Highway and Transportation Officials, Washington D.C. 1986.
23. Department of Transportation, U.S. AASHTO Guide for Design of Pavement Structures (1993). American Association of State Highway and Transportation Officials, Washington, D.C. 1993.
24. Taamneh M. M., "Long Term Monitoring and Evaluation of Drainable Bases at I-90 Test Road," PhD Thesis, The University of Akron, August, 2009.
25. Timm D. H., Newcomb D. E. and Birgisson B., "Development of a Mechanistic-Empirical Design Procedure for Minnesota," In *Transportation Research: Journal of the Transportation Research Board*, No 1629, Transportation Research Board of the National Academies, Washington, D.C., pp. 181-188, 1998.
26. Transportation Association of Canada (TAC), Canadian Strategic Highway Research Program (C-SHRP), Pavement Structural Design Practices Across Canada, C-SHRP Technical Brief No. 23, Ottawa, Ontario, April 2002.
27. http://www.ce.memphis.edu/4901/Calculating an Effective Resilient Modulus.pdf. Accessed: April 2011.
28. Pavement Design Manual, Alberta Transportation and Utilities, Edition 1, June 1997.
29. Velasquez R., Hoegh K., Yut I., Funk N., Cochran G., Marasteanu M., and Khazanovich L., " Implementation of the MEPDG for New and Rehabilitated Pavement Structures for Design of Concrete and Asphalt Pavements in Minnesota," June 2009.
30. Mamlouk M. S., and Zaniewski J. P., Materials for Civil and Construction Engineers, 2nd Edition, Pearson Education Company, Inc., Upper Saddle River, New Jersey, 2006.
31. Zapata C. E., and Houston W. N., "Calibration and Validation of the Enhanced Integrated Climatic Model for Pavement Design," NCHRP Report No. 602, National Cooperative Highway Research Program, Transportation Research Board of the National Academies, Washington, D.C., 2008.
32. Birgisson B., Ovik J., and Newcomb D. E., "Analytical Predictions of Seasonal Variations in Flexible Pavements," In *Transportation Research: Journal of the*

Transportation Research Board, No 1730, Transportation Research Board of the National Academies, Washington, D.C., pp. 81-90, 2000.

33. Richter C. A., Seasonal Variations in the Moduli of Unbound Pavement Layers, Publication FHWA-HRT-04-079. FHWA, U.S. Department of Transportation, 2006.
34. Guide for Mechanistic-Empirical Design of New and Rehabilitated Structures, NCHRP Report I-37A. TRB, National Research Council, Washington, D. C., Part 2, Ch.3, 2004.
35. Yang H. H. Pavement Analysis and Design. Prentice Hall, Englewood Cliffs, New Jersey 1993.
36. Hudson W. R., Haas R., and Uddin W., Infrastructure Management: Integrating Design, Construction, Maintenance, Rehabilitation, and Reconstruction, McGraw-Hill, New York, 1997.
37. Breakah T. M., Williams R. C., Herzmann D. E. and Takle E. S., "Effects of Using Accurate Climate Conditions for Mechanistic – Empirical Pavement Design," Journal of Transportation Engineering, ASCE, pp. 84 – 90, January, 2011.
38. Tighe S. L. and Smith J., "Using the MEPDG to Assess Climate Change Impacts on Southern Canadian Roads," 7th International Conference on Managing Pavement Assets, pp. 1 - 10, 2008.
39. http://sis.agr.gc.ca/cansis/glossary/freezing_index,_f.html. Accessed: June 2011.
40. http://nsidc.org/data/nsidc-0063.html. Accessed: June 2011.
41. Tech Solutions 605.0 calculating insulation needs to fight frost heave by comparing freezing index and frost depth, (http://msdssearch.dow.com/PublishedLiteratureDOWCOM/dh_01f6/0901b803801f6296.pdf?filepath=styrofoam/pdfs/noreg/178-00754. Pdf & from Page =GetDoc). Accessed: February 2011.
42. David P. O., and Irwin L. H., "Seasonal Variations of In Situ Materials Properties in New York State ," Final Report, June 2007.
43. TM 5-852-6/AFR 88-19 (VOL. 6), Technical Manual, Arctic and Subarctic Construction-Calculation Methods for Determination of Depths of Freeze and Thaw in Soils. Accessed: February 2011.
44. http://en.wikipedia.org/wiki/Permafrost. Accessed: February 2011.

45. Part 3_Chaper 3_Design of New and Reconstructed Pavements, Guide for Mechanistic Empirical Design.
46. http://www.fhwa.dot.gov/pavement/ltpp/pubs/06121/chapt6.cfm. Accessed: February 2011.
47. El-Badawy S. M., Bayomy F. M, Santi M., and Clawson. C.W, "Comparison of Idaho Pavement Design Procedure with AASHTO 1993 and MEPDG Methods," T & DI Congress 2011: Integrated Transportation and Development for Better Tomorrow, pp. 586-595, ASCE 2011.
48. Gedafa D. S., Mulandi J., Hossain M., and Schieber. G., "Comparison of Pavement Design Using AASHTO 1993 and NCHRP Mechanistic–Empirical Pavement Design Guides," T & DI Congress 2011: Integrated Transportation and Development for better tomorrow, pp. 538-547, ASCE 2011.
49. VDOT Preparation Plan for the Implementation of The Mechanistic-Empirical Guide for Design of New and Rehabilitated Pavement Structures January 2007
50. Al-Omari O., and Darter M. I., "Relationship Between International Roughness Index and Present Serviceability Rating," Transportation Research Record 1435, TRB, Washington DC, pp. 130-136, 1994.
51. http://en.wikipedia.org/wiki/AASHTO_Soil_Classification_System. Accessed: August 2011.
52. Design Bulletin # 13, Pavement Design Manual, Alberta Transportation and Utilities.
53. Reid R. A. and Clark T. M.,"Roughness on Virginia's Roads," Annual Roughness Report. July 2003.
54. Latif A. B. AB., "Relationship between International Roughness index (IRI) and Present Serviceability index (PSI)," Master Thesis, Universiti Teknologi Malaysia, 2009.
55. http://www.transportation.alberta.ca/629.htm. Accessed: March, 2011

Appendix 1

A.1.1 List of Complete Weather Stations

Provinces of Canada	Weather Stations	Lat.	Long.	Elev. (m)	Mean Annual Air Temp. (°C)	Mean Annual Precp. (cm)	Average annual freezing index (°C-days)	Start date of Data	End date of data	No of available months	Climt. Zones
Alberta	Calgary Int. Airport	51.114	-114.02	330	4.7	42.6	982.7	7/1/1987	6/30/2007	240	2
	Cold Lake Airport	54.417	-110.28	165	2.3	43.0	1672.6	7/1/1987	6/30/2007	240	2
	Coronation Air port	52.067	-111.45	241	2.6	36.1	1609.0	4/1/1957	3/31/1977	240	2
	Cowley Airport	49.633	-114.08	360	3.9	51.0	1067.0	1/1/1953	7/31/1960	91	4
	Namao Airport	53.667	-113.46	210	3.6	46.2	1293.2	2/1/1975	1/31/1995	240	2
	City Centre Airport	53.573	-113.51	204	4.2	47.2	1188.0	4/1/1974	3/31/1994	240	2
	Edmonton Int. Airport	53.317	-113.58	220	3.0	47.8	1381.6	7/1/1987	6/30/2007	240	2
	Edson Airport	53.583	-116.47	283	2.2	56.9	1416.9	8/1/1971	7/31/1991	240	4
	Edson	53.583	-116.42	282	1.8	53.4	1556.0	3/1/1960	4/30/1970	122	4
	Embarras Airport	58.2	-111.38	72	-0.9	39.3	2547.0	1/1/1953	10/31/1967	178	2
	Fort Chipewyan	58.717	-111.15	69	-2.2	42.7	2972.1	11/1/1962	10/31/1967	60	2
	Fort Mcmurray Airport	56.65	-111.22	113	2.1	45.7	1819.1	7/1/1987	6/30/2007	240	2
	Grande Prairie Airport	55.18	-118.88	204	2.5	45.8	1549.7	7/1/1987	6/30/2007	240	2
	High Level Airport	58.621	-117.16	103	-0.4	36.0	2411.7	7/1/1987	6/30/2007	240	2
	Lac La Biche	54.767	-111.97	170	2.7	46.8	1502.6	12/1/1955	9/30/1958	34	2
	Lac La Biche 1	54.767	-112.02	173	1.3	46.7	1860.9	10/1/1958	5/31/1971	152	2
	Lethbridge Airport	49.63	-112.80	283	6.2	39.4	876.3	4/1/1974	3/31/1994	240	2
	Lloydminster Airport	53.309	-110.07	204	2.4	40.3	1614.5	7/1/1987	6/30/2007	240	2
	Medicine Hat Airport	50.019	-110.72	219	6.2	34.0	1013.6	1/1/1976	12/31/1995	240	2
	Peace River Airport	56.227	-117.45	174	2.0	39.7	1684.1	7/1/1987	6/30/2007	240	2

Provinces of Canada	Weather Stations	Lat.	Long.	Elev. (m)	Mean Annual Air Temp. (°C)	Mean Annual Precp. (cm)	Average annual freezing index (°C-days)	Start date of Data	End date of data	No of available months	Climt. Zones
	Pincher Creek	49.5	-113.95	352	4.8	53.3	993.2	9/1/1960	11/30/1973	159	4
	Rocky Mtn House	52.383	-114.92	309	2.8	51.5	1350.2	1/1/1954	8/31/1969	188	4
	Slave Lake Airport	55.3	-114.78	177	1.9	49.9	1604.1	6/1/1972	5/31/1992	240	2
	Springbank Airport	51.103	-114.37	366	3.0	49.7	1187.7	8/1/1988	5/31/2002	166	2
	Vermilion Airport	53.35	-110.83	189	1.8	42.8	1824.9	3/1/1962	2/28/1982	240	2
	Whitecourt	54.133	-115.67	226	1.5	54.6	1677.0	8/1/1958	7/31/1978	240	4
	Whitecourt Airport	54.144	-115.78	238	2.7	58.3	1374.6	12/1/1979	6/30/1997	211	4
British Columbia	Abbotsford Airport	49.025	-122.36	18	10.4	152.8	55.7	7/1/1987	6/30/2007	240	3
	Beatton River Airport	57.383	-121.38	256	-1.1	44.7	2271.3	1/1/1953	3/31/1967	171	2
	Cape St. James	51.933	-131.02	28	8.4	164.2	17.1	9/1/1972	8/31/1992	240	3
	Castlegar Airport	49.296	-117.63	151	7.9	73.7	328.1	1/1/1966	11/30/1981	191	3
	Comox Airport	49.717	-124.9	8	10.1	112.3	27.7	7/1/1987	6/30/2007	240	3
	Cranbrook Airport	49.612	-115.78	287	6.3	38.2	687.5	7/1/1987	6/30/2007	240	2
	Fort Nelson Airport	58.836	-122.59	116	-0.3	44.4	2375.6	7/1/1987	6/30/2007	240	2
	Fort St John Airport	56.238	-120.74	212	2.5	44.6	1470.7	7/1/1987	6/30/2007	240	2
	Kamloops Airport	50.702	-120.44	105	9.3	29.0	333.2	7/1/1987	6/30/2007	240	1
	Kelowna Airport	49.956	-119.38	131	7.2	32.6	443.9	6/1/1972	8/31/1976	51	2
	Kimberley Airport	49.733	-115.78	279	5.0	36.0	853.3	1/1/1953	3/31/1969	195	2
	Lytton1	50.233	-121.57	53	9.5	46.8	345.3	1/1/1953	1/31/1970	205	1
	Lytton2	50.233	-121.58	70	8.9	30.5	385.8	11/1/1971	3/31/1974	29	1
	Nanaimo Airport	49.052	-123.87	9	9.2	104.8	74.7	1/1/1954	10/31/1967	166	3
	Penticton Airport	49.463	-119.60	105	9.8	34.2	201.5	7/1/1987	6/30/2007	240	1
	Port Hardy Airport	50.68	-127.36	7	8.6	192.3	23.5	7/1/1987	6/30/2007	240	3
	Prince Geoge Airport	53.891	-122.68	211	4.6	58.7	830.7	7/1/1987	6/30/2007	240	4

Provinces of Canada	Weather Stations	Lat.	Long.	Elev. (m)	Mean Annual Air Temp. (°C)	Mean Annual Precp. (cm)	Average annual freezing index (°C-days)	Start date of Data	End date of data	No of available months	Climt. Zones
	Prince Rupert Airport	54.293	-130.45	11	7.3	253.4	128.2	2/1/1975	1/31/1991	192	3
	Princeton Airport	49.468	-120.51	213	5.4	35.5	696.8	1/1/1953	1/31/1969	193	2
	Quesnel Airport	53.026	-122.51	166	4.6	52.4	895.5	4/1/1969	3/31/1989	240	4
	Sandspit Airport	53.254	-131.81	2	8.4	143.5	31.0	7/1/1974	6/30/1994	240	3
	Smith River Airport	59.9	-126.43	205	-2.8	46.8	2808.0	1/1/1953	9/30/1969	201	2
	Smithers Airport	54.825	-127.18	159	4.3	50.6	755.4	7/1/1987	6/30/2007	240	4
	Terrace Airport	54.466	-128.58	66	6.4	137.6	331.4	7/1/1987	6/30/2007	240	3
	Tofino Airport	49.081	-125.78	7	8.7	308.5	19.7	1/1/1960	4/30/1978	220	3
	Vancouver Int. Airport	49.195	-123.18	1	10.6	117.0	34.2	1/1/1987	12/31/2006	240	3
	Gonzales Heights	48.417	-123.32	21	9.5	70.1	21.3	1/1/1953	4/30/1968	184	3
	Williams Lake Airport	52.183	-122.05	287	4.4	44.8	830.7	6/1/1975	5/31/1995	240	2
Manitoba	Bird	56.5	-94.2	26	-5.5	50.3	3617.0	11/1/1957	12/31/1963	74	4
	Brandon Airport	49.917	-99.95	125	2.5	45.6	1767.7	7/1/1987	6/30/2007	240	2
	Dauphin Airport	51.1	-100.05	93	2.6	51.6	1767.8	7/1/1974	6/30/1994	240	4
	Gimli	50.633	-97.02	68	1.9	53.7	1897.0	1/1/1972	10/31/1990	226	4
	Gimli Airport	50.633	-97.05	68	1.8	55.9	1953.7	1/1/1953	12/31/1971	228	4
	Lynn Lake Airport	56.864	-101.07	109	-3.0	48.1	2978.7	2/1/1974	1/31/1994	240	2
	Rivers Airport	50.017	-100.32	144	1.9	48.4	1936.6	1/1/1953	9/30/1970	213	2
	The Pas Airport	53.967	-101.10	82	0.8	43.1	2109.2	7/1/1987	6/30/2007	240	2
	Thompson Airport	55.803	-97.86	68	-2.2	49.8	2820.6	7/1/1987	6/30/2007	240	2
	Richardson Int. Airport	49.917	-97.23	73	3.3	50.9	1670.7	7/1/1987	6/30/2007	240	4
NB	Campbellton Airport	48	-66.67	2	4.2	99.1	1041.8	1/1/1953	11/30/1966	167	4
	Charlo Airport	47.983	-66.33	12	3.1	106.2	1270.5	6/1/1971	5/31/1991	240	4

Provinces of Canada	Weather Stations	Lat.	Long.	Elev. (m)	Mean Annual Air Temp. (°C)	Mean Annual Precp. (cm)	Average annual freezing index (°C-days)	Start date of Data	End date of data	No of available months	Climt. Zones
	Fredericton Airport	45.872	-66.53	6	5.6	115.5	936.0	3/1/1976	2/29/1996	240	4
	Moncton Airport	46.104	-64.69	22	5.5	117.2	850.7	7/1/1987	6/30/2007	240	4
	Saint John Airport	45.318	-65.89	33	5.1	142.4	803.1	11/1/1975	10/31/1995	240	4
	St. Leonard Airport	47.158	-67.83	74	3.2	108.6	1372.5	4/1/1985	4/30/1995	121	4
Newfoundland & Labrador	Argentia Airport	47.3	-54.00	4	5.5	100.9	288.9	9/1/1953	7/31/1969	194	3
	Battle Harbourlor	52.25	-55.60	3	0.3	95.1	1154.0	10/1/1961	9/30/1981	240	4
	Bonavista Airport	48.667	-53.11	8	4.2	106.2	555.8	9/1/1975	8/31/1995	240	4
	Buchans Airport	48.85	-56.83	84	2.9	102.5	936.7	1/1/1953	5/31/1965	149	4
	Burgeo	47.617	-57.62	3	4.2	167.0	572.5	10/1/1971	9/30/1991	240	4
	Cape Harrison	54.767	-58.45	3	-0.6	71.3	1625.1	1/1/1953	9/30/1959	81	4
	Cartwright Airport	53.708	-57.03	4	-0.5	102.5	1670.7	7/1/1987	6/30/2007	240	4
	Churchill Falls Airport	53.55	-64.10	134	-3.5	93.2	2732.5	2/1/1973	1/31/1993	240	4
	Gander Int. Airport	48.946	-54.58	46	4.2	126.5	778.2	7/1/1987	6/30/2007	240	4
	Goose Bay Airport	53.317	-60.42	15	0.2	91.8	1918.0	7/1/1987	6/30/2007	240	4
	Hopedale Airport	55.45	-60.22	4	-2.1	82.1	1944.8	8/1/1964	7/31/1984	240	4
	Mary's Harbour Airport	52.304	-55.83	4	0.4	90.3	1408.3	11/1/1983	1/31/1988	51	4
	Port Aux Basques Airport	47.574	-59.15	12	4.0	151.7	583.1	9/1/1971	8/31/1991	240	4
	St. Andrews	47.767	-59.33	3	4.9	110.9	511.7	1/1/1953	5/31/1966	161	4
	St.Anthony	51.367	-55.58	5	1.8	87.2	934.1	1/1/1953	12/31/1965	156	4
	St.Anthony Airport	51.4	-56.08	9	2.5	96.1	783.4	4/1/1967	9/30/1970	42	4
	St.Anthony1	51.367	-55.60	4	0.2	111.9	1426.9	11/1/1970	6/30/1977	80	4
	St. John's Airport	47.622	-52.74	43	4.9	148.7	534.3	7/1/1987	6/30/2007	240	4
	St. Lawrence	46.917	-55.38	15	4.7	143.9	381.7	3/1/1966	3/31/1983	205	3
	Stephenville Airport	48.533	-58.55	8	5.0	136.9	666.8	7/1/1987	6/30/2007	240	4

Provinces of Canada	Weather Stations	Lat.	Long.	Elev. (m)	Mean Annual Air Temp. (°C)	Mean Annual Precp. (cm)	Average annual freezing index (°C-days)	Start date of Data	End date of data	No of available months	Climt. Zones
NovaScotia	Copper Lake	45.383	-61.97	30	5.5	130.8	661.1	1/1/1953	2/28/1962	110	4
	Debert Airport	45.417	-63.45	13	6.0	128.1	637.6	1/1/1953	9/30/1960	93	4
	Eddy Point	45.517	-61.25	20	5.8	141.8	560.7	1/1/1972	3/31/1985	159	4
	Greenwood Airport	44.983	-64.92	9	7.6	113.3	539.4	7/1/1987	6/30/2007	240	4
	Halifax	44.65	-63.57	10	7.4	124.7	376.9	1/1/1953	8/31/1963	128	3
	Stanfield Int. Airport	44.883	-63.52	44	6.6	128.8	590.3	7/1/1987	6/30/2007	240	4
	Sable Island Airport	43.932	-60.01	2	7.5	139.5	185.1	11/1/1971	10/31/1991	240	3
	Shearwater Airport	44.633	-63.50	16	6.6	138.2	498.0	10/1/1975	9/30/1995	240	4
	Shelburne	43.717	-65.25	9	7.3	135.6	383.5	3/1/1982	12/31/1986	58	3
	Sydney Airport	46.167	-60.05	19	6.0	146.5	558.8	7/1/1987	6/30/2007	240	4
	Truro	45.367	-63.27	12	5.7	111.2	693.4	1/1/1960	3/31/1977	207	4
	Yarmouth Airport	43.831	-66.09	13	7.2	127.0	346.1	7/1/1987	6/30/2007	240	3
Northwest Territory	Cape Parry Airport	70.167	-124.72	26	-11.8	15.7	4792.7	8/1/1972	7/31/1992	240	2
	Fort Reliance	62.717	-109.17	51	-6.6	27.3	3824.8	10/1/1977	10/31/1990	157	2
	Fort Resolution Airport	61.181	-113.69	49	-4.1	36.2	3256.8	1/1/1954	1/31/1970	193	2
	Fort Simpson	61.867	-121.35	40	-4.3	37.9	3461.8	4/1/1955	4/30/1963	97	2
	Fort Simpson Airport	61.76	-121.24	52	-2.4	38.7	3010.4	3/1/1987	2/28/2007	240	2
	Hay River Airport	60.84	-115.78	50	-2.3	33.9	2739.4	1/1/1953	7/31/1960	91	2
	Inuvik Airport	68.304	-133.48	21	-7.4	21.7	4108.8	7/1/1987	6/30/2007	240	2
	Mould Bay Airport	76.233	-119.33	4	-17.7	11.5	5000.0	4/1/1981	4/30/1987	73	2
	Norman Wells Airport	65.283	-126.80	22	-4.9	29.4	3649.6	7/1/1987	6/30/2007	240	2
	Sachs Harbour Airport	72	-125.27	26	-13.9	13.6	5524.1	11/1/1970	9/30/1977	83	2
	Yellowknife	62.463	-114.44	63	-4.0	29.4	3288.5	7/1/1987	6/30/2007	240	2

Provinces of Canada	Weather Stations	Lat.	Long.	Elev. (m)	Mean Annual Air Temp. (°C)	Mean Annual Precp. (cm)	Average annual freezing index (°C-days)	Start date of Data	End date of data	No of available months	Climt. Zones
	Airport										
Nunavut	Baker Lake Airport	64.299	-96.08	5	-12.1	24.7	5299.1	11/1/1962	9/30/1979	203	2
	Cambridge Bay Airport	69.108	-105.14	8	-14.5	14.0	5000.0	4/1/1975	3/31/1995	240	2
	Cape Dyer Airport	66.583	-61.62	120	-10.4	61.4	4174.1	3/1/1970	2/28/1990	240	4
	Chesterfield	63.333	-90.72	2	-11.9	22.8	5062.9	11/1/1962	4/30/1968	66	2
	Clyde River Airport	70.486	-68.52	8	-12.7	24.6	5000.0	8/1/1984	12/31/1989	65	2
	Contwoyto Lake	65.483	-110.37	138	-12.1	30.7	5314.3	2/1/1959	8/31/1962	43	2
	Coppermine	67.833	-115.12	3	-11.2	25.5	4927.3	4/1/1970	12/31/1977	93	2
	Ennadai Lake	61.133	-100.90	99	-9.6	30.1	4645.2	6/1/1956	9/30/1966	124	2
	Hall Beach Airport	68.776	-81.24	2	-14.2	21.6	5000.0	4/1/1975	3/31/1995	240	2
	IqaluitAirport	63.75	-68.55	10	-9.5	42.2	4130.4	1/1/1976	12/31/1995	240	2
	Rankin Inlet Airport	62.817	-92.12	9	-11.3	30.6	4931.0	3/1/1981	2/28/1997	192	2
	Rea Point Airport	75.367	-105.72	5	-17.5	6.9	5000.0	1/1/1972	6/30/1977	66	2
	Resolute Airport	74.717	-94.98	20	-16.3	16.3	5000.0	1/1/1978	12/31/1997	240	2
Ontario	Armstrong Airport	50.294	-88.91	98	-0.5	73.6	2285.7	1/1/1953	6/30/1968	186	4
	Atikokan	48.75	-91.62	120	2.0	75.8	1790.1	10/1/1966	9/30/1986	240	4
	Big Trout Lake	53.833	-89.87	68	-2.4	63.0	2771.2	1/1/1970	12/31/1989	240	4
	Chapleau	47.833	-83.43	131	1.8	83.3	1748.2	11/1/1965	3/31/1976	125	4
	Earlton Airport	47.7	-79.85	74	2.3	81.7	1687.1	10/1/1959	9/30/1979	240	4
	Geraldton	49.7	-86.95	101	0.2	74.1	2146.7	11/1/1967	3/31/1977	113	4
	Geraldton Airport	49.783	-86.93	106	0.2	74.1	2146.7	7/1/1987	6/30/2007	240	4
	Gore Bay Airport	45.883	-82.57	59	5.6	78.5	878.1	10/1/1971	9/30/1991	240	4
	Graham Airport	49.267	-90.58	153	0.5	81.3	2057.2	1/1/1953	12/31/1966	168	4
	Hamilton Airport	43.172	-79.93	72	7.9	89.5	616.7	8/1/2002	5/31/2006	46	4

Provinces of Canada	Weather Stations	Lat.	Long.	Elev. (m)	Mean Annual Air Temp. (°C)	Mean Annual Precp. (cm)	Average annual freezing index (°C-days)	Start date of Data	End date of data	No of available months	Climt. Zones
	Kapuskasing Airport	49.414	-82.47	69	1.5	84.3	1859.4	7/1/1987	6/30/2007	240	4
	Kenora Airport	49.79	-94.36	125	3.3	70.3	1609.1	7/1/1987	6/30/2007	240	4
	Killaloe	45.567	-77.42	53	5.0	66.1	1148.9	1/1/1953	7/31/1972	235	4
	London Airport	43.033	-81.15	85	7.7	100.0	582.8	2/1/1974	1/31/1994	240	4
	Mount Forest	43.983	-80.75	126	5.5	91.3	861.8	1/1/1962	7/31/1976	175	4
	Nakina Airport	50.183	-86.70	99	0.0	78.6	2136.8	1/1/1953	10/31/1967	178	4
	North Bay Airport	46.364	-79.42	113	4.0	100.1	1275.5	2/1/1974	1/31/1994	240	4
	Ottawa Rockcliffe Airport	45.45	-75.63	17	6.3	86.5	995.9	1/1/1953	3/31/1964	135	4
	Macdonald-Cartier Int. Airport	45.323	-75.67	35	6.5	92.4	920.6	7/1/1987	6/30/2007	240	4
	Petawawa Airport	45.95	-77.32	40	4.6	80.5	1206.2	7/1/1973	6/30/1993	240	4
	Saulte Marie Airport	46.483	-84.51	59	5.1	89.9	919.4	7/1/1987	6/30/2007	240	4
	Simcoe	42.85	-80.27	73	7.8	87.9	569.3	1/1/1962	7/31/1977	187	4
	Sioux Lookout Airport	50.117	-91.90	117	2.3	77.2	1776.4	7/1/1987	6/30/2007	240	4
	Stirling	44.317	-77.63	42	6.7	75.6	787.5	1/1/1953	11/30/1968	191	4
	Sudbury Airport	46.625	-80.79	106	4.2	93.4	1249.3	7/1/1987	6/30/2007	240	4
	Thunder Bay Airport	48.369	-89.33	61	3.0	69.1	1423.6	1/1/1974	12/31/1993	240	4
	Victor Power Airport	48.57	-81.37	90	1.7	84.9	1795.1	7/1/1974	6/30/1994	240	4
	Buttonville Airport	43.862	-79.37	60	7.9	82.9	583.6	7/1/1987	6/30/2007	240	4
	Lester B. Pearson Int. Airport	43.677	-79.63	53	8.3	76.7	511.0	7/1/1987	6/30/2007	240	4
	Trenton Airport	44.117	-77.53	26	7.3	86.9	681.2	6/1/1974	5/31/1994	240	4
	White River	48.6	-85.28	115	0.7	83.5	1932.0	1/1/1956	12/31/1975	240	4
	Wiarton Airport	44.746	-81.11	68	6.3	105.2	704.7	7/1/1975	6/30/1995	240	4

Provinces of Canada	Weather Stations	Lat.	Long.	Elev. (m)	Mean Annual Air Temp. (°C)	Mean Annual Precp. (cm)	Average annual freezing index (°C-days)	Start date of Data	End date of data	No of available months	Climt. Zones
	Windsor Airport	42.276	-82.96	58	9.3	92.4	453.8	7/1/1975	6/30/1995	240	4
	Winisk Airport	55.233	-85.12	4	-5.4	51.4	3241.3	2/1/1959	6/30/1965	77	4
PEI (Prince Edward Island)	Charlottetown Airport	46.289	-63.13	15	5.8	112.7	741.1	7/1/1987	6/30/2007	240	4
	Summerside Airport	46.439	-63.83	6	5.5	107.4	791.5	7/1/1971	6/30/1991	240	4
Quebec	Bagotville Airport	48.333	-71.00	48	3.0	92.6	1513.7	7/1/1987	6/30/2007	240	4
	Baie-Comeau Airport	49.133	-68.20	7	2.0	99.3	1350.5	2/1/1974	1/31/1994	240	4
	Gaspe Airport	48.777	-64.48	10	3.6	109.0	1130.4	7/1/1987	6/30/2007	240	4
	Gatineau Airport	45.517	-75.57	20	5.6	0.0	1096.9	10/1/1987	9/30/1991	48	2
	Grindstone Island	47.383	-61.87	18	4.5	97.2	696.4	4/1/1968	1/31/1983	178	4
	Inukjuas Airport	58.467	-78.08	7	-6.6	48.9	3305.2	9/1/1976	9/30/1992	193	2
	Kuujjuaq Airport	58.1	-68.42	12	-4.9	51.1	3068.2	7/1/1987	6/30/2007	240	4
	La Grande Riviere Airport	53.633	-77.70	59	-2.3	68.0	2608.2	7/1/1987	6/30/2007	240	4
	Maniwaki U Airport	46.302	-76.01	59	3.3	97.7	1414.5	1/1/1990	9/30/1992	33	4
	Mont-Joli Airport	48.6	-68.22	16	3.8	89.3	1116.4	7/1/1987	6/30/2007	240	4
	St-Hubert Airport	45.517	-73.42	8	6.4	101.5	934.4	5/1/1974	4/30/1994	240	4
	Mirabel Int. Airport	45.667	-74.03	25	5.7	106.4	1027.7	7/1/1987	6/30/2007	240	4
	Pierre Elliottrudeau Int. Airport	45.467	-73.75	11	7.1	99.2	840.7	7/1/1987	6/30/2007	240	4
	Nitchequon	53.2	-70.90	163	-3.8	85.4	2855.2	12/1/1965	11/30/1985	240	4
	Jean Lesage Int. Airport	46.8	-71.38	23	4.8	54.3	1111.5	7/1/1987	6/30/2007	240	4
	Roberval Airport	48.517	-72.27	54	2.9	85.3	1564.2	7/1/1987	6/30/2007	240	4
	Rouyn Airport	48.217	-78.83	92	2.4	0.0	1663.1	7/1/1987	6/30/2007	240	2
	Sept-Iles Airport	50.217	-66.27	17	1.6	87.3	1460.5	7/1/1987	6/30/2007	240	4

Provinces of Canada	Weather Stations	Lat.	Long.	Elev. (m)	Mean Annual Air Temp. (°C)	Mean Annual Precp. (cm)	Average annual freezing index (°C-days)	Start date of Data	End date of data	No of available months	Climt. Zones
	Ste Agathe DesS Monts	46.05	-74.28	120	3.5	117.5	1303.7	6/1/1972	5/31/1992	240	4
	Val-D'or Airport	48.056	-77.78	103	1.7	90.7	1775.3	12/1/1975	11/30/1995	240	4
Saskatchewan	Broadviewi Airport	50.368	-102.57	183	2.5	41.5	1708.2	1/1/1975	12/31/1994	240	2
	Broadview Airport	50.25	-102.53	189	2.0	41.4	1809.2	1/1/1953	1/31/1965	145	2
	Estevan Airport	49.217	-102.97	177	3.9	41.9	1449.8	7/1/1987	6/30/2007	240	2
	Hudson Bay	52.867	-102.40	113	0.1	45.2	2276.9	2/1/1955	3/31/1974	230	2
	Kindersley Airport	51.517	-109.18	212	3.2	32.6	1517.3	7/1/1987	6/30/2007	240	2
	La Ronge Airport	55.15	-105.27	115	0.7	48.7	2088.0	7/1/1987	6/30/2007	240	2
	Moose Jaw Airport	50.333	-105.55	176	4.1	36.0	1440.4	12/1/1977	11/30/1997	240	2
	North Battleford Airport	52.772	-108.26	167	2.4	36.9	1709.0	9/1/1985	8/31/2005	240	2
	Prince Albert Airport	53.217	-105.67	131	1.8	40.8	1869.4	7/1/1987	6/30/2007	240	2
	Regina Airport	50.433	-104.67	176	3.2	38.4	1590.9	7/1/1987	6/30/2007	240	2
	Diefenbaker Int. Airport	52.167	-106.72	154	2.8	34.2	1667.5	7/1/1987	6/30/2007	240	2
	Stony Rapids Airport	59.25	-105.83	75	-3.1	43.5	3015.3	7/1/1987	6/30/2007	240	2
	Uranium City Airport	59.567	-108.48	97	-3.2	34.0	3104.6	6/2/1966	6/1/1986	240	2
	Wynyard Airport	51.767	-104.20	171	1.9	41.2	1844.2	9/1/1969	8/31/1989	240	2
	Yorkton Airport	51.267	-102.47	152	2.0	43.7	1806.4	7/1/1985	6/30/2005	240	2
Yukon	Aishihik Airport	61.65	-137.48	294	-4.5	23.9	3004.6	1/1/1953	9/30/1966	165	2
	Dawson	64.05	-139.43	98	-5.4	33.7	3690.5	3/1/1960	12/31/1975	190	2
	Dawson Airport	64.043	-139.13	113	-4.4	33.3	3405.5	2/1/1976	10/31/1987	141	2
	Mayo Airport	63.617	-135.87	154	-2.6	32.0	2893.8	5/1/1974	9/30/1988	173	2
	Snag Airport	62.367	-140.40	179	-5.7	37.5	3686.8	1/1/1953	8/31/1966	164	2
	Teslin Airport	60.174	-132.74	215	-2.0	32.3	2367.0	6/1/1955	5/31/1975	240	2

Provinces of Canada	Weather Stations	Lat.	Long.	Elev. (m)	Mean Annual Air Temp. (°C)	Mean Annual Precp. (cm)	Average annual freezing index (°C-days)	Start date of Data	End date of data	No of available months	Climt. Zones
	Watson Lake Airport	60.118	-128.82	210	-2.0	41.1	2665.5	7/1/1987	6/30/2007	240	2
	Whitehorse Airport	60.71	-135.07	215	0.2	21.7	1825.3	7/1/1987	6/30/2007	240	2

Note:Lat.= Latitude, Long. =Longitude, Elv. = Elevation, Temp.= Temperature, Precp= Precipitation, Climt.= Climate

A.1.2 Sample of Climate Data Input File

The field designations of a climate data input file are Date(yyyy/mm/dd/hr),air temperature(°F), precipitation(inch),wind speed(mile/hr), percent sunshine, relative humidity. A sample of data records are given below.

1974020100,-0.9,6,70,0,55

1974020101,-4,4,100,0,62

1974020102,-4,3,0,0,60

1974020103,-5.1,7,0,0,59

1974020104,-8,5,60,0,62

1974020105,-9.9,4,30,0,60

1974020106,-11,3,40,0,61

1974020107,-13,3,90,0,58

1974020108,-14.1,3,90,0,58

1974020109,-11,3,90,0,58

1974020110,-9.9,7,20,0,56

1974020111,-8,3,50,0,50

1974020112,-5.1,3,60,0,48

1974020113,-4,4,50,0,50

1974020114,-2,8,40,0,43

1974020115,-0.9,7,20,0,46

1974020116,-0.9,6,40,0,48

1974020117,-2,3,80,0,50

1974020118,-4,5,40,0,46

1974020119,-6,3,40,0,50

1974020120,-8,3,80,0,52

1974020121,-9,4,80,0,55

1974020122,-11,9,80,0,57

1974020123,-11.9,10,100,0,59

1974020200,-13,10,100,0,56

1974020201,-13,9,100,0,56

1974020202,-13,7,100,0,56

1974020203,-14.1,7,100,0,57

1974020204,-15,7,100,0,53

1974020205,-15,7,100,0,54

1974020206,-16.1,9,100,0,54

1974020207,-17,7,100,0,55

1974020208,-17,8,90,0,56

1974020209,-16.1,9,70,0,52

1974020210,-14.1,8,80,0,47

1974020211,-11,7,70,0,45

1974020212,-9,6,70,0,42

1974020213,-7.1,6,20,0,42

1974020214,-6,6,30,0,41

1974020215,-5.1,8,20,0,41

A.1.3 List of Climate Data Records found from MEPDG and Environment Canada for Calgary Airport

MEPDG data				Environment Canada Data		Difference in two methods	
Month (Year)	Average Temp. (ºC)	Total Precp. (mm.)	Max. Frost (m.)	Mean Temp (°C)	Total Precp. (mm)	Diff in mean temp. (ºC)	Diff in Total Precp. (mm)
9/1987	13.8	29.0	0.00	13.6	29.2	0.2	0.2
10/1987	7.1	2.0	0.12	7.1	2.0	0.0	0.0
11/1987	2.2	5.6	0.44	2.0	5.4	0.2	0.2
12/1987	-2.4	4.8	1.02	-2.9	4.9	0.5	0.1
1/1988	-8.2	4.3	1.64	-8.5	4.3	0.3	0.0
2/1988	-4.2	4.3	2.05	-3.9	4.3	0.3	0.0
3/1988	1.2	19.8	2.07	0.9	19.8	0.3	0.0
4/1988	6.9	1.5	0.07	6.4	1.5	0.5	0.0
5/1988	13.1	16.3	0.00	12.4	16.0	0.7	0.3
6/1988	16.5	84.6	0.00	16.3	84.6	0.2	0.0
7/1988	16.8	47.0	0.00	16.5	46.8	0.3	0.2
8/1988	15.2	150.1	0.00	15.0	163.9	0.2	13.8
9/1988	10.7	43.4	0.02	10.7	43.5	0.0	0.1
10/1988	7.1	8.1	0.37	6.8	8.0	0.3	0.1
11/1988	-0.3	7.4	0.77	-0.3	7.1	0.0	0.3
12/1988	-4.4	5.1	1.14	-5.0	4.9	0.6	0.2
1/1989	-6.7	23.9	1.60	-7.1	23.4	0.4	0.5
2/1989	-11.7	12.4	2.00	-12.2	12.4	0.5	0.0
3/1989	-6.7	8.9	2.33	-7.0	N.A.	0.3	8.9
4/1989	4.7	22.9	2.35	4.4	22.8	0.3	0.1
5/1989	9.6	41.4	0.02	9.0	41.2	0.6	0.2
6/1989	14.8	80.5	0.00	14.3	80.7	0.5	0.2
7/1989	17.8	50.5	0.00	17.7	50.6	0.1	0.1
8/1989	15.2	61.7	0.00	15.4	61.6	0.2	0.1
9/1989	11.6	41.7	0.00	11.6	41.4	0.0	0.3
10/1989	5.9	6.1	0.14	5.7	6.0	0.2	0.1
11/1989	-0.2	17.3	0.64	-0.7	17.2	0.5	0.1
12/1989	-3.6	21.6	1.15	-4.5	21.8	0.9	0.2
1/1990	-4.5	5.8	1.27	-4.6	5.6	0.1	0.2
2/1990	-6.2	6.4	1.81	-6.5	6.4	0.3	0.1
3/1990	1.0	8.4	1.82	0.9	8.7	0.1	0.3

MEPDG data				Environment Canada Data		Difference in two methods	
Month (Year)	Average Temp. (ºC)	Total Precp. (mm.)	Max. Frost (m.)	Mean Temp (°C)	Total Precp. (mm)	Diff in mean temp. (ºC)	Diff in Total Precp. (mm)
4/1990	4.6	21.6	0.51	4.7	21.2	0.1	0.4
5/1990	9.1	100.8	0.02	9.0	100.2	0.1	0.6
6/1990	14.1	62.0	0.00	13.9	61.3	0.2	0.7
7/1990	16.4	84.1	0.00	16.2	83.7	0.2	0.4
8/1990	16.9	58.2	0.00	16.7	58.3	0.2	0.1
9/1990	14.0	7.6	0.00	14.1	7.5	0.1	0.1
10/1990	4.3	13.2	0.15	4.1	12.9	0.2	0.3
11/1990	-3.6	20.8	0.86	-4.0	20.7	0.4	0.1
12/1990	-10.3	12.4	1.45	-10.7	11.7	0.4	0.7
1/1991	-8.4	7.9	1.95	-8.8	7.4	0.4	0.5
2/1991	1.1	15.5	2.01	0.9	14.9	0.2	0.6
3/1991	-3.3	21.1	2.07	-3.5	21.0	0.2	0.1
4/1991	5.8	7.4	2.04	5.4	7.1	0.4	0.3
5/1991	9.6	96.5	0.07	9.4	96.1	0.2	0.4
6/1991	12.7	113.3	0.00	13.0	113.2	0.3	0.1
7/1991	16.7	30.0	0.00	16.4	29.6	0.3	0.4
8/1991	18.1	64.5	0.00	18.1	64.2	0.0	0.3
9/1991	11.4	26.2	0.00	11.5	25.9	0.1	0.3
10/1991	2.5	16.5	0.68	2.2	15.8	0.3	0.7
11/1991	-2.2	9.7	0.82	-2.6	9.6	0.4	0.1
12/1991	-2.0	1.8	0.98	-2.0	1.8	0.0	0.0
1/1992	-0.4	2.3	1.16	-1.1	2.2	0.7	0.1
2/1992	-2.3	3.8	1.45	-2.5	3.6	0.2	0.2
3/1992	3.1	8.1	0.26	3.1	7.9	0.0	0.2
4/1992	6.4	25.1	0.47	6.4	24.6	0.0	0.5
5/1992	9.6	46.0	0.05	9.5	46.2	0.1	0.2
6/1992	14.8	177.5	0.00	14.8	177.2	0.0	0.3
7/1992	14.4	76.5	0.00	14.2	76.2	0.2	0.3
8/1992	14.3	42.2	0.02	14.1	41.5	0.2	0.7
9/1992	9.4	47.8	0.03	9.5	48.1	0.1	0.3
10/1992	5.0	14.7	0.29	5.3	14.6	0.3	0.1
11/1992	-0.9	38.9	0.67	-1.4	38.8	0.5	0.1
12/1992	-11.8	14.5	1.45	-11.8	14.0	0.0	0.5
1/1993	-10.6	5.8	2.02	-11.4	5.8	0.8	0.0
2/1993	-6.9	12.4	2.23	-7.1	12.5	0.2	0.1
3/1993	-0.2	17.8	2.34	-0.3	17.8	0.1	0.0
4/1993	5.2	6.6	2.34	4.8	6.5	0.4	0.1

MEPDG data				Environment Canada Data		Difference in two methods	
Month (Year)	Average Temp. (ºC)	Total Precp. (mm.)	Max. Frost (m.)	Mean Temp (°C)	Total Precp. (mm)	Diff in mean temp. (ºC)	Diff in Total Precp. (mm)
5/1993	11.8	62.2	0.00	11.5	61.9	0.3	0.3
6/1993	13.2	118.4	0.00	12.8	118.4	0.4	0.0
7/1993	13.1	87.6	0.00	13.3	87.0	0.2	0.6
8/1993	13.8	92.7	0.00	13.8	92.3	0.0	0.4
9/1993	10.6	24.4	0.02	10.5	24.3	0.1	0.1
10/1993	6.1	9.4	0.21	6.3	9.0	0.2	0.4
11/1993	-2.4	10.4	0.88	-2.9	10.4	0.5	0.0
12/1993	-1.9	3.8	1.00	-1.9	3.6	0.0	0.2
1/1994	-9.7	10.9	1.70	-9.4	10.6	0.3	0.3
2/1994	-13.2	9.9	2.11	-13.5	9.6	0.3	0.3
3/1994	2.6	8.4	2.30	2.5	8.1	0.1	0.3
4/1994	6.0	12.7	2.29	5.8	12.6	0.2	0.1
5/1994	10.8	63.0	0.00	10.5	62.5	0.3	0.5
6/1994	13.8	68.6	0.00	13.3	68.4	0.5	0.2
7/1994	17.7	38.1	0.00	17.4	38.0	0.3	0.1
8/1994	16.1	84.8	0.00	16.2	84.4	0.1	0.4
9/1994	13.1	10.4	0.01	13.1	10.4	0.0	0.0
10/1994	4.6	31.2	0.13	4.6	31.4	0.0	0.2
11/1994	-2.8	14.0	0.84	-3.3	13.9	0.5	0.1
12/1994	-5.9	5.1	1.20	-5.8	5.2	0.1	0.1
1/1995	-7.3	2.8	1.73	-7.3	2.8	0.0	0.0
2/1995	-5.2	2.0	1.91	-5.2	2.1	0.0	0.1
3/1995	-2.6	7.4	2.12	-3.0	7.3	0.4	0.1
4/1995	2.9	32.0	2.12	3.3	31.8	0.4	0.2
5/1995	9.6	72.1	0.05	9.3	71.9	0.3	0.2
6/1995	14.3	43.7	0.00	14.1	43.4	0.2	0.3
7/1995	15.4	133.4	0.00	15.6	133.4	0.2	0.1
8/1995	13.5	34.8	0.00	13.6	34.2	0.1	0.6
9/1995	11.8	27.9	0.04	11.9	27.9	0.1	0.0
10/1995	4.1	14.7	0.36	4.2	14.4	0.1	0.3
11/1995	-4.9	23.1	0.90	-4.8	22.7	0.1	0.4
12/1995	-11.1	23.1	1.57	-11.0	22.9	0.1	0.2
1/1996	-15.6	27.9	2.12	-15.7	27.8	0.1	0.1
2/1996	-5.7	3.3	2.42	-5.6	3.0	0.1	0.3
3/1996	-5.9	35.3	2.61	-6.0	35.4	0.1	0.1
4/1996	5.1	18.3	2.67	4.9	18.5	0.2	0.2
5/1996	6.3	52.1	0.19	6.4	51.5	0.1	0.6

MEPDG data				Environment Canada Data		Difference in two methods	
Month (Year)	Average Temp. (ºC)	Total Precp. (mm.)	Max. Frost (m.)	Mean Temp (°C)	Total Precp. (mm)	Diff in mean temp. (ºC)	Diff in Total Precp. (mm)
6/1996	13.7	59.4	0.00	13.4	59.2	0.3	0.2
7/1996	16.6	42.2	0.00	16.4	41.9	0.2	0.3
8/1996	17.1	21.1	0.00	16.8	21.0	0.3	0.1
9/1996	9.1	46.5	0.04	9.1	46.4	0.0	0.1
10/1996	4.3	23.4	0.42	4.2	23.4	0.1	0.0
11/1996	-9.6	30.2	1.22	-9.7	30.0	0.1	0.2
12/1996	-13.7	18.5	1.76	-14.3	18.3	0.6	0.2
1/1997	-12.1	18.5	2.24	-12.5	18.5	0.4	0.0
2/1997	-2.8	3.8	2.45	-2.8	3.7	0.0	0.1
3/1997	-4.0	17.0	2.63	-4.0	17.1	0.0	0.1
4/1997	2.3	12.7	2.71	2.2	12.6	0.1	0.1
5/1997	9.5	100.6	0.02	9.3	100.7	0.2	0.1
6/1997	13.8	138.4	0.00	13.8	138.4	0.0	0.0
7/1997	16.3	16.8	0.00	16.0	16.9	0.3	0.1
8/1997	15.7	58.2	0.00	15.9	57.8	0.2	0.4
9/1997	12.9	37.8	0.02	13.1	37.8	0.2	0.0
10/1997	4.7	15.2	0.14	4.7	14.8	0.0	0.4
11/1997	-1.3	0.5	0.69	-1.5	0.6	0.2	0.1
12/1997	-2.2	6.4	0.98	-2.6	6.3	0.4	0.0
1/1998	-13.4	16.0	1.82	-13.6	15.6	0.2	0.4
2/1998	-2.7	4.1	1.97	-2.9	4.0	0.2	0.1
3/1998	-4.2	59.7	2.23	-4.6	59.4	0.4	0.3
4/1998	6.2	41.1	2.23	6.4	41.2	0.2	0.1
5/1998	12.5	86.4	0.00	12.2	86.4	0.3	0.0
6/1998	12.6	110.5	0.00	12.5	110.4	0.1	0.1
7/1998	17.8	130.0	0.00	17.8	132.2	0.0	2.2
8/1998	18.0	18.0	0.00	17.8	18.0	0.2	0.0
9/1998	12.7	26.2	0.00	12.7	26.0	0.0	0.2
10/1998	6.7	11.4	0.07	7.0	11.4	0.3	0.0
11/1998	-2.3	14.0	0.62	-2.6	14.1	0.3	0.1
12/1998	-8.2	19.3	1.30	-8.4	19.0	0.2	0.3
1/1999	-8.1	11.4	1.81	-7.9	11.3	0.2	0.1
2/1999	-1.6	0.0	1.90	-1.5	0.0	0.1	0.0
3/1999	-0.8	6.6	2.07	-0.8	6.4	0.0	0.2
4/1999	4.7	72.4	1.59	4.8	72.8	0.1	0.4
5/1999	8.7	52.8	0.07	8.7	52.8	0.0	0.0
6/1999	11.9	95.3	0.00	11.9	95.4	0.0	0.2

MEPDG data				Environment Canada Data		Difference in two methods	
Month (Year)	Average Temp. (ºC)	Total Precp. (mm.)	Max. Frost (m.)	Mean Temp (°C)	Total Precp. (mm)	Diff in mean temp. (ºC)	Diff in Total Precp. (mm)
7/1999	13.9	103.6	0.00	13.7	103.8	0.2	0.2
8/1999	15.8	87.6	0.00	15.9	89.2	0.1	1.6
9/1999	10.2	9.1	0.06	10.3	9.1	0.1	0.0
10/1999	5.8	3.8	0.13	5.7	3.6	0.1	0.2
11/1999	1.3	12.4	0.56	1.3	12.4	0.0	0.0
12/1999	-0.2	2.0	0.91	-0.6	1.8	0.4	0.2
1/2000	-9.7	10.4	1.49	-9.7	10.2	0.0	0.2
2/2000	-6.2	20.8	1.84	-6.7	20.6	0.5	0.2
3/2000	-0.4	25.4	2.03	-0.4	25.5	0.0	0.1
4/2000	4.1	17.5	0.76	4.1	17.0	0.0	0.5
5/2000	9.0	29.0	0.03	8.8	28.8	0.2	0.2
6/2000	12.7	110.2	0.01	12.5	109.8	0.2	0.4
7/2000	17.1	66.8	0.00	16.7	66.8	0.4	0.0
8/2000	15.4	63.5	0.00	15.6	63.9	0.2	0.4
9/2000	10.6	53.6	0.12	10.7	53.6	0.1	0.0
10/2000	5.1	1.8	0.16	5.4	1.8	0.3	0.0
11/2000	-3.1	5.6	0.74	-3.3	5.8	0.2	0.2
12/2000	-9.8	9.1	1.50	-9.9	8.8	0.1	0.3
1/2001	-1.2	2.3	1.58	-1.5	2.0	0.3	0.3
2/2001	-10.2	8.1	2.02	-10.5	7.7	0.3	0.4
3/2001	-0.3	12.4	2.15	-0.1	12.3	0.2	0.1
4/2001	4.1	19.6	2.19	4.0	19.2	0.1	0.4
5/2001	11.6	30.7	0.03	11.2	30.5	0.4	0.2
6/2001	12.4	121.7	0.00	12.2	121.4	0.2	0.3
7/2001	17.1	58.7	0.00	16.8	58.8	0.3	0.1
8/2001	18.6	14.2	0.00	18.0	14.2	0.6	0.0
9/2001	13.0	13.2	0.00	13.2	13.0	0.2	0.2
10/2001	3.8	18.0	0.18	4.0	17.9	0.2	0.1
11/2001	0.1	16.8	0.83	-0.2	16.6	0.3	0.2
12/2001	-8.0	4.8	1.27	-8.2	4.8	0.2	0.0
1/2002	-6.0	11.7	1.55	-6.5	11.4	0.5	0.3
2/2002	-2.9	9.4	1.79	-3.2	9.4	0.3	0.0
3/2002	-12.2	16.3	2.28	-12.2	16.6	0.0	0.3
4/2002	0.8	20.8	2.38	1.1	20.5	0.3	0.3
5/2002	7.2	33.5	0.20	6.6	34.0	0.6	0.5
6/2002	14.9	58.7	0.00	14.4	58.6	0.5	0.1
7/2002	18.6	35.1	0.00	18.3	34.6	0.3	0.5

MEPDG data				Environment Canada Data		Difference in two methods	
Month (Year)	Average Temp. (ºC)	Total Precp. (mm.)	Max. Frost (m.)	Mean Temp (°C)	Total Precp. (mm)	Diff in mean temp. (ºC)	Diff in Total Precp. (mm)
8/2002	14.3	57.2	0.00	14.2	57.4	0.1	0.3
9/2002	10.0	58.4	0.00	10.1	58.2	0.1	0.2
10/2002	1.6	23.9	0.54	1.9	23.6	0.3	0.3
11/2002	2.7	9.9	0.53	2.7	10.0	0.0	0.1
12/2002	-2.7	10.2	0.99	-2.9	10.2	0.2	0.0
1/2003	-6.3	5.8	1.48	-6.3	5.6	0.0	0.2
2/2003	-6.7	21.6	1.81	-7.2	21.7	0.5	0.1
3/2003	-4.6	16.5	2.17	-4.8	15.8	0.2	0.7
4/2003	3.7	81.8	2.23	3.5	81.8	0.2	0.0
5/2003	8.6	34.8	0.05	8.3	34.5	0.3	0.3
6/2003	13.8	104.9	0.00	13.7	104.8	0.1	0.1
7/2003	17.8	42.4	0.00	17.5	42.2	0.3	0.2
8/2003	17.8	39.1	0.00	18.0	39.3	0.2	0.2
9/2003	10.8	39.9	0.01	11.2	39.6	0.4	0.3
10/2003	7.2	30.7	0.39	7.5	30.8	0.3	0.1
11/2003	-5.5	13.5	0.90	-5.8	13.2	0.3	0.3
12/2003	-4.8	0.8	1.19	-4.9	0.7	0.1	0.1
1/2004	-10.3	16.8	1.71	-10.5	16.9	0.2	0.1
2/2004	-3.1	2.3	2.07	-3.1	2.2	0.0	0.1
3/2004	1.3	11.2	2.10	2.0	10.9	0.7	0.3
4/2004	6.3	18.0	0.09	6.1	18.0	0.2	0.0
5/2004	8.1	55.6	0.00	8.1	55.6	0.0	0.0
6/2004	13.2	98.0	0.00	13.1	98.2	0.1	0.2
7/2004	16.9	54.6	0.00	17.0	54.2	0.1	0.4
8/2004	15.1	58.2	0.00	15.5	58.6	0.4	0.4
9/2004	9.7	30.5	0.01	9.9	30.4	0.2	0.1
10/2004	4.1	24.4	0.30	4.0	24.1	0.1	0.3
11/2004	1.4	4.1	0.53	1.6	3.4	0.2	0.7
12/2004	-4.3	14.7	1.04	-4.7	14.3	0.4	0.4
1/2005	-9.1	10.2	1.79	-8.9	10.2	0.2	0.0
2/2005	-2.8	10.7	1.91	-3.1	10.6	0.3	0.1
3/2005	0.3	14.7	1.94	0.2	14.6	0.1	0.1
4/2005	6.0	8.6	0.15	5.8	8.4	0.2	0.2
5/2005	11.0	18.8	0.09	10.7	18.8	0.3	0.0
6/2005	12.3	247.7	0.00	12.4	247.6	0.1	0.0
7/2005	16.7	19.6	0.00	16.4	19.8	0.3	0.2
8/2005	13.9	98.6	0.00	13.8	98.2	0.1	0.4

MEPDG data				Environment Canada Data		Difference in two methods	
Month (Year)	Average Temp. (ºC)	Total Precp. (mm.)	Max. Frost (m.)	Mean Temp (°C)	Total Precp. (mm)	Diff in mean temp. (ºC)	Diff in Total Precp. (mm)
9/2005	9.2	71.9	0.03	9.4	86.0	0.2	14.1
10/2005	5.7	11.2	0.12	5.9	10.8	0.2	0.4
11/2005	0.8	12.4	0.50	0.4	12.2	0.4	0.2
12/2005	-4.2	2.5	1.13	-4.4	2.4	0.2	0.1
1/2006	-1.3	6.4	1.13	-1.5	6.2	0.2	0.1
2/2006	-5.3	20.1	1.53	-5.6	20.0	0.3	0.1
3/2006	-4.3	7.4	1.89	-4.4	7.2	0.1	0.2
4/2006	7.0	29.7	1.92	6.8	29.4	0.2	0.3
5/2006	11.8	37.3	0.04	11.2	37.0	0.6	0.3
6/2006	15.1	122.7	0.00	14.7	122.8	0.4	0.1
7/2006	18.5	51.6	0.00	18.4	51.4	0.1	0.2

Note: Max. = Maximum, Temp. = Temperature, Precp. = Precipitation

A.1.3.1 Literature on Frost Depth Computation by Modified Berggren Method (Source: TM 5-852-6/AFR 88-19 (VOL. 6), Technical Manual, Arctic and Subarctic Construction-Calculation Methods for Determination of Depths of Freeze and Thaw in Soils)

CHAPTER 3

ONE-DIMENSIONAL LINEAR AND PERIODIC HEAT FLOW

3-1. Thermal regime.

The seasonal depths of frost and thaw penetration in soils depends upon the thermal properties of the soil mass, the surface temperature (upper boundary condition) and the thermal regime of the soil at the start of the freezing or thawing season. Many methods are available to estimate frost and thaw penetration depths and surface temperatures. Some of these are summarized in appendix B. This chapter concentrates on some techniques that require only relatively simple hand calculations. For the computational methods discussed below, the initial ground temperature is assumed to uniformly equal the mean annual air temperature of the particular site under consideration. The upper boundary condition is represented by the surface freezing (or thawing) index.

3-2. Modified Berggren equation.

a. The depth to which 32°F temperatures will penetrate into the soil mass is based upon the "modified" Berggren equation, expressed as:

$$X = \lambda \frac{48\,K\,nF}{L}$$

or (eq 3-1)

$$X = \lambda \frac{48\,K\,nI}{L}$$

where

X = depth of freeze or thaw (ft)

K = thermal conductivity of soil (Btu/ft hr °F)

L = volumetric latent heat of fusion (Btu/ft^3)

n = conversion factor from air index to surface index (dimensionless)

F = air freezing index (°F-days)

I = air thawing index (°F-days)

λ = coefficient that considers the effect of temperature changes in the soil mass (dimensionless).

The λ coefficient is a function of the freezing (or thawing) index, the mean annual temperature of the site, and the thermal properties of the soil. Freeze and thaw of low-moisture-content soils in the lower latitudes is greatly influenced by this coefficient. It is determined by two factors: the thermal ratio α and the fusion parameter μ. These have been defined in paragraph 2-1. Figure 3-1 shows λ as a function of α and μ.

b. A complete development of this equation and a discussion of the necessary assumptions and simplifications made during its development are not presented here. A few of the more important assumptions and some of the equation limitations are discussed below. The assumptions and limitations apply regardless of whether the equation is used to determine the depth of freeze or the depth of thaw.

(1) *Assumptions.* The mathematical model assumes one-dimensional heat flow with the entire soil mass at its mean annual temperature (MAT) prior to the start of the freezing season. It assumes that when the freezing season starts, the surface temperature changes suddenly (as a step function) from the mean annual temperature to a temperature v_s degrees below freezing and that it remains at this new temperature throughout the entire freezing season. Latent heat affects the model by acting as a heat sink at the moving frost line, and the model assumes that the soil freezes at a temperature of 32°F.

(2) *Limitations.* The modified Berggren equation is able to determine frost penetration in areas where the ground below a depth of several feet

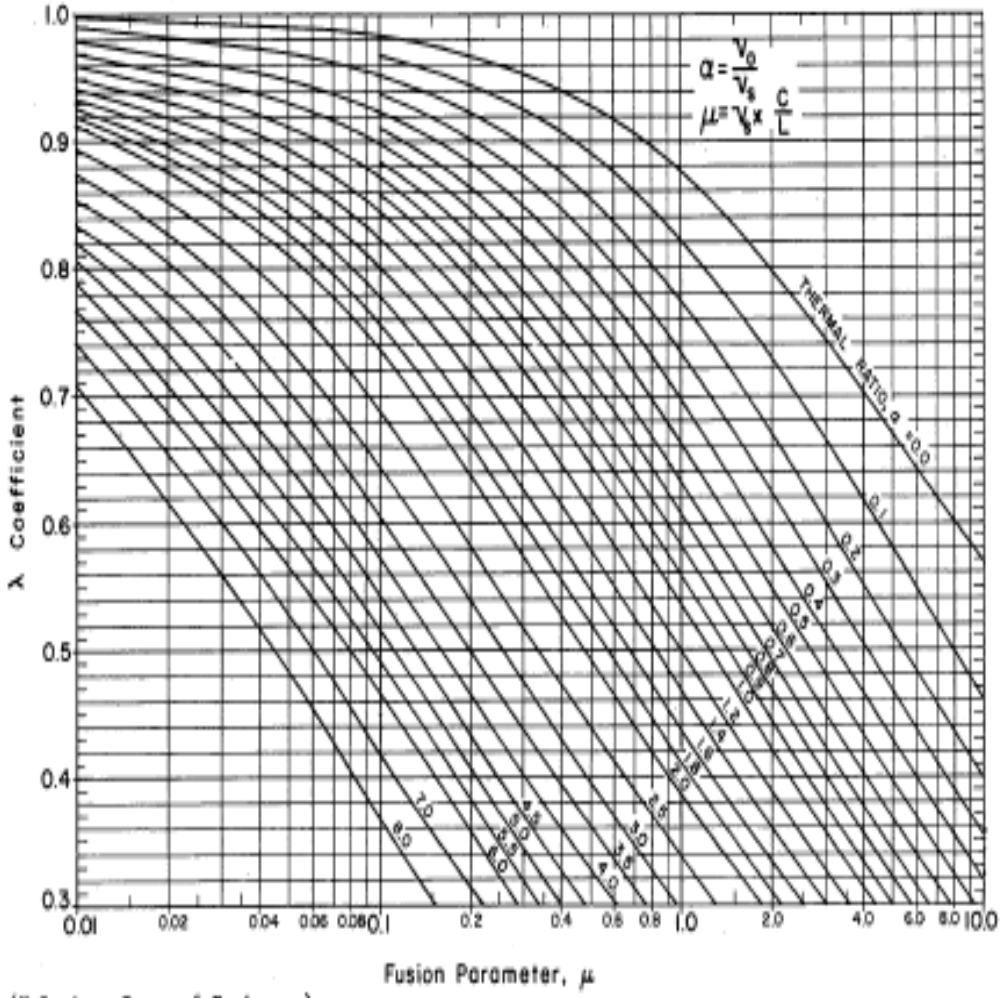

(U.S. Army Corps of Engineers)

remains permanently thawed, or to determine thaw penetration in areas where the ground below a depth of several feet remains permanently frozen. These two conditions are similar in that the temperature gradients are of the same shape, although reversed with respect to the 32°F line. No simple analytical method exists to determine the depth of thaw in seasonal frost areas or the depth of freeze in permafrost areas, and such problems should be referred to HQDA (DAEN-ECE-G) or HQ AFESC. Numerical techniques and computer programs are available to solve more complex problems. Appendix B discusses some thermal computer models for computing freeze and thaw depths. The modified Berggren equation cannot be used successfully to calculate penetration over parts of the season. The modified Berggren equation does not account for any moisture movement that may occur within the soil. This limitation would tend to result in overestimated frost penetration (if frost heave is significant) or underestimated thaw penetration.

(3) *Applicability.* The modified Berggren equation is most often applicable in either of two ways: to calculate the multi-year depth of thaw in permafrost areas or to calculate the depth of seasonal frost penetration in seasonal frost areas. It is also sometimes used to calculate seasonal thaw penetration (active layer thickness) in permafrost areas.

3-3. Homogeneous soils.

The depth of freeze or thaw in one layer of homogeneous soil may be determined by means of the modified Berggren equation. A thin bituminous concrete pavement will not affect the homogeneity of this layer in calculations, but a portland-cement-concrete pavement greater than 6 inches thick should be treated as a multilayered system. In this *example* for homogeneous soils, determine the depth of frost penetration into a homogeneous sandy silt for the following conditions:

—Mean annual temperature (MAT) = 37.2°F.

—Surface freezing index (nF) = 2500 degree-days.

—Length of freezing season (t) = 160 days.

—Soil properties: γ_d = 100 lb/ft^3, w = 15%.

The soil thermal properties are as follows:

—Volumetric latent heat of fusion,

$L = 144(100)(0.15) = 2160$ Btu/ft^3. (eq 3-2)

—Average volumetric heat capacity,

$C_{avg} = 100[0.17+(0.75 \times 0.15)]$
$= 28.3$ Btu/ft^3 °F. (eq 3-3)

—Average thermal conductivity,

$K_f = 0.80$ Btu/ft hr °F (fig. 2-3)

$K_u = 0.72$ Btu/ft hr °F (fig. 2-4)

$K_{avg} = 1/2\,(K_u + K_f) = 0.76$ Btu/ft hr °F.

The λ coefficient is as follows:

—Average surface temperature differential,

$v_s = nF/t = 2500/160$
$= 16.6$°F (16.6°F below 32°F). (eq 3-4)

—Initial temperature differential,

$v_o = MAT - 32 = 37.2 - 32.0 =$
5.2°F (5.2° above 32°F). (eq 3-5)

—Thermal ratio,

$\alpha = v_o/v_s = 5.2/16.6 = 0.33$. (eq 3-6)

—Fusion parameter,

$\mu = v_s\,(C/L) = 16.6(28.2/2160) = 0.20$. (eq 3-7)

—Lambda coefficient,

$\lambda = 0.89$ (fig. 3-1). (eq 3-8)

Estimated depth of frost penetration,

$$X = \lambda\sqrt{\frac{48\,K\,nF}{L}} = 0.89\sqrt{\frac{48(0.76)(2500)}{2160}} = 5.8 \text{ ft.} \quad \text{(eq 3-9)}$$

3-4. Multilayer soils.

A multilayer solution to the modified Berggren equation is used for nonhomogeneous soils by determining that portion of the surface freezing (or thawing) index required to penetrate each layer. The sum of the thicknesses of all the frozen (or thawed) layers is the depth of freeze (or thaw). The partial freezing (or thawing) index required to penetrate the top layer is given by

$$F_1 \text{ (or } I_1) = \frac{L_1 d_1}{24\lambda_1^2}\left(\frac{R_1}{2}\right) \quad \text{(eq 3-10)}$$

where

d_1 = thickness of first layer (ft)

$R_1 = d_1/K_1$ = thermal resistance of first layer.

The partial freezing (or thawing) index required to penetrate the second layer is

$$F_2 \text{ (or } I_2) = \frac{L_2 d_2}{24\lambda_2^2}\left(R_1 + \frac{R_2}{2}\right). \quad \text{(eq 3-11)}$$

The partial index required to penetrate the n^{th} layer is:

$$F_n \text{ (or } I_n) = \frac{L_n d_n}{24\lambda_n^2}\left(\Sigma R + \frac{R_n}{2}\right) \quad \text{(eq 3-12)}$$

where ΣR is the total thermal resistance above the n^{th} layer and equals

$$R_1 + R_2 + R_3 \cdots + R_{n-1}. \quad \text{(eq 3-13)}$$

The summation of the partial indexes,

$$F_1 + F_2 + F_3 \cdots + F_n (\text{or } I_1 + I_2 + I_3 \cdots + I_n) \quad \text{(eq 3-14)}$$

is equal to the surface freezing index thawing index).

a. In this *example*, determine the depth of thaw penetration beneath a bituminous concrete pavement for the following conditions:

—Mean annual temperature (MAT) = 12°F.

—Air thawing index (I) = 780 degree-days.

—Average wind speed in summer = 7.5 miles per hour (mph).

—Length of thaw season (t) = 105 days.

—Soil boring log:

Layer	Depth (ft)	Material*	Dry unit weight (lb/ft^3)	Water content (%)
1	0.0-0.4	Asphaltic concrete	138	--
2	0.4-2.0	GW-GP	156	2.1
3	2.0-5.0	GW-GP	151	2.8
4	5.0-6.0	SM	130	6.5
5	6.0-8.0	SM-SC	122	4.6
6	8.0-9.0	SM	116	5.2

*In accordance with Unified Soil Classification System.

Since a wind speed of 7-1/2 mph results in an n-factor of 2.0 (fig. 2-10), a surface thawing index nI of 1560 degree-days is used in the computations. The v_s, v_o and α values are determined in the same way as those for the homogeneous case:

$$v_s = 1560/105 = 14.8°F \quad \text{(eq 3-15)}$$

$$v_o = 12.0 - 32.0 = 20.0°F \quad \text{(eq 3-16)}$$

$$\alpha = 20.0/14.8 = 1.35. \quad \text{(eq 3-17)}$$

The thermal properties C, K and L of the respective layers are obtained from figures 2-1 through 2-8.

b. Table 3-1 facilitates solution of the multilayer problem, and in the following discussion, layer 3 is used to illustrate quantitative values. Columns 9, 10, 12 and 13 are self-explanatory. Column 11, $\overline{L}$, represents the average value of L for a layer and is equal to $\Sigma Ld/\Sigma d$ (2581/5.0 = 517). Column 14, $\overline{C}$, represents the average value of C and is obtained from $\Sigma Cd/\Sigma d$ (145/5.0 = 29). Thus $\overline{L}$ and $\overline{C}$ represent weighted values to a depth of thaw penetration given by Σd, which is the sum of all layer thicknesses to that depth.

The fusion parameter μ for each layer is determined from

$$v_s (\overline{C}/\overline{L}) = 14.8 (29/517) = 0.83. \quad \text{(eq 3-18)}$$

The λ coefficient is equal to 0.508 from figure 3-1. Column 18, R_n, is the ratio d/K and for layer 3 equals (3.0/2.0) or 1.5. Column 19, ΣR, represents the sum of the R_n values above the layer under consideration. Column 20, $\Sigma R + (R_n/2)$, equals the sum of the R_n values above the layer plus one-half the R_n value of the layer being considered. For layer 3 this is [1.32 + (1.50/2)] = 2.07. Column 21, nI, represents the number of degree-days required to thaw the layer being considered and is determined from

Table 3-1. Multilayer solution of modified Berggren equation (U.S. Army Corps of Engineers).

(1)	(2)	(3)	(4)	(5)	(6)	(7)	(8)	(9)	(10)	(11)	(12)	(13)	(14)	(15)	(16)	(17)	(18)	(19)	(20)	(21)	(22)
Layer	γ_d	w	d	Σd	C	K	L	Ld	ΣLd	$\bar{L}$	Cd	ΣCd	$\bar{C}$	μ	λ	λ^2	R_n	ΣR	$\Sigma R + \frac{R_n}{2}$	nI	ΣnI
1	138	--	0.4	0.4	28	0.86	0	0	0	--	12	12	--	--	--	--	0.46	0	0.23	--	--
2	156	2.1	1.6	2.0	29	1.85	470	751	751	376	46	58	29	1.15	0.455	0.207	0.86	0.46	0.89	134	134
3	151	2.8	3.0	5.0	29	2.00	610	1830	2581	517	87	145	29	0.83	0.508	0.258	1.50	1.32	2.07	612	746
4	130	6.5	1.0	6.0	28	1.65	1220	1220	3801	633	28	173	29	0.68	0.537	0.288	0.60	2.82	3.12	551	1297
5a	122	4.6	1.0	7.0	25	0.64	808	808	4609	658	25	198	28	0.63	0.552	0.305	1.56	3.42	4.20	465	1762
5b	122	4.6	0.6	6.6	25	0.64	808	485	4286	650	15	188	28	0.64	0.550	0.303	0.94	3.42	3.89	260	1557

$\alpha = 1.35$ $v_s = 14.8°F$ nI = 1560 degree-days

$$I_2 = \frac{(470)(1.6)}{(24)(0.207)}(0.89) = 134$$

$$I_3 = \frac{(610)(3.0)}{(24)(0.258)}(2.07) = 612$$

$$I_4 = \frac{(1220)(1.0)}{(24)(0.288)}(3.12) = 551$$

$$I_{5a} = \frac{(808)(1.0)}{(24)(0.305)}(4.20) = 465$$

$$I_{5b} = \frac{(808)(0.6)}{(24)(0.303)}(3.89) = 260$$

Total thaw penetration = 6.6 feet

Table 3-1. Multilayer solution of modified Berggren equation.

$$nI = \frac{Ld}{24\lambda^2}\left(\Sigma R + \frac{R_n}{2}\right). \qquad \text{(eq 3-19)}$$

For layer 3,

$$nI_3 = \frac{(610)(3.0)}{24(0.508)^2}(2.07) \qquad \text{(eq 3-20)}$$

$$= 612 \text{ degree-days}$$

The summation of the number of degree-days required to thaw layers 1 through 4 is 1297, leaving (1560 - 1297 =) 263 degree-days to thaw a portion of layer 5. A trial-and-error method is used to determine the thickness of the thawed part of layer 5. First, it is assumed that 1.0 feet of layer 5 is thawed (designated as layer 5a). Calculations indicate 465 degree-days are needed to thaw 1.0 foot of layer 5 or (465 - 263 =) 202 degree-days more than available. A new layer, 5b, is then selected by the following proportion

$$(263/465)1.0 = 0.57 \text{ ft (try 0.6 ft).} \qquad \text{(eq 3-21)}$$

This new thickness results in 260 degree-days required to thaw layer 5b or 3 degree-days less than available. Further trial-and-error is unwarranted and the total estimated thaw penetration would be 6.6 feet. A similar technique is used to estimate frost penetration in a multilayer soil profile.

A.1.4 Frost Depth Calculation for Multi-layer System in Modified Berggren Method

Partial freezing index required to penetrate nth layer is $F_n = L_n d_n/(24\lambda^2)+(\Sigma R+R_n/2)$

The summation of the partial freezing indexes, F1+F2+F3…+Fn is equal to the surface freezing indexes

Definition of used units:

d= dpth (ft), C= volumetric heat capacity

K = Thermal conductivity, L = Latent Heat

V_0 = Initial temperature differential= Mean cumulative monthly temp. - 32˚

V_s = Average surface temperature differential, V_s = nF/t = surface freezing index/length of freezing season

α = Thermal Ratio= V_0/V_s

μ = Fusion Parameter= V_s(C bar/L bar)

Station	layer	d	∑ d	C	k	L	Ld	∑ Ld	L bar	Cd	∑Cd	C bar	Frezing Index, nF	No of Freezing days (t)	Mean annual Temp. (MAT)	V_s	V_0	α	μ	λ	λ^2	R_n	∑R	∑R+R_n/2	nF	∑nF
		(ft)	(ft)	Btu/ft^3°F	Btu/ft hr °F	Btu/ft^3	Btu/ft^2	Btu/ft^3	Btu/ft^3	Btu/ft^2°F	Btu/ft^2°F	Btu/ft^3°F														
Calgary Int. Airport_AB	1	0.8	0.8	28.0	0.9	0.0	0.0	0.0	-	21.0	21.0	28.0	**1138.1**	84.0	43.3	13.5	11.3	0.8	-	-	-	0.9	0.0	0.4	-	-
	2	1.1	1.9	25.2	1.0	403.2	443.5	443.5	239.7	27.7	48.7	26.3	**1138.1**	84.0	43.3	13.5	11.3	0.8	1.5	0.5	0.3	1.1	0.9	1.4	100.7	100.7
	3	6.0	7.9	25.2	1.2	403.2	2419.2	2862.7	364.7	151.2	199.9	25.5	**1138.1**	84.0	43.3	13.5	11.3	0.8	0.9	0.7	0.4	5.0	2.0	4.5	1037.2	1137.9
Kamloops_ BC	1	0.8	0.8	28.0	0.9	0.0	0.0	0.0	-	21.0	21.0	28.0	**601.9**	56.0	49.3	10.7	17.3	1.6	-	-	-	0.9	0.0	0.4	-	-
	2	1.1	1.9	25.2	1.0	403.2	443.5	443.5	239.7	27.7	48.7	26.3	**601.9**	56.0	49.3	10.7	17.3	1.6	1.2	0.4	0.2	1.1	0.9	1.4	148.4	148.4
	3	2.0	3.9	25.2	1.2	403.2	806.4	1249.9	324.7	50.4	99.1	25.7	**601.9**	56.0	49.3	10.7	17.3	1.6	0.9	0.5	0.2	1.7	2.0	2.8	454.7	603.1
Gimli Airport, MB	1	0.8	0.8	28.0	0.9	0.0	0.0	0.0	-	21.0	21.0	28.0	**3129.0**	143.0	36.0	21.9	4.0	0.2	-	-	-	0.9	0.0	0.4	-	-
	2	1.1	1.9	25.2	1.0	403.2	443.5	443.5	239.7	27.7	48.7	26.3	**3129.0**	143.0	36.0	21.9	4.0	0.2	2.4	0.6	0.4	1.1	0.9	1.4	63.9	63.9
	3	12.9	14.7	25.2	1.2	403.2	5181.1	5624.6	382.6	323.8	372.5	25.3	**3129.0**	143.0	36.0	21.9	4.0	0.2	1.4	0.7	0.5	10.8	2.0	7.4	3065.1	3129.0
Saint John Airport_NB	1	0.8	0.8	28.0	0.9	0.0	0.0	0.0	-	21.0	21.0	28.0	**1523.2**	123.0	40.3	12.4	8.3	0.7	-	-	-	0.9	0.0	0.4	-	-
	2	1.1	1.9	25.2	1.0	403.2	443.5	443.5	239.7	27.7	48.7	26.3	**1523.2**	123.0	40.3	12.4	8.3	0.7	1.4	0.6	0.3	1.1	0.9	1.4	75.2	75.2
	3	7.1	9.0	25.2	1.2	403.2	2870.8	3314.3	369.5	179.4	228.1	25.4	**1523.2**	123.0	40.3	12.4	8.3	0.7	0.9	0.6	0.4	6.0	2.0	5.0	1446.4	1521.6
Argentia Airport_NF&L	1	0.8	0.8	28.0	0.9	0.0	0.0	0.0	-	21.0	21.0	28.0	**404.0**	74.0	43.0	5.5	11.0	2.0	-	-	-	0.9	0.0	0.4	-	-
	2	1.1	1.9	25.2	1.0	403.2	443.5	443.5	239.7	27.7	48.7	26.3	**404.0**	74.0	43.0	5.5	11.0	2.0	0.6	0.5	0.2	1.1	0.9	1.4	121.1	121.1
	3	1.8	3.6	25.2	1.2	403.2	705.6	1149.1	319.2	44.1	92.8	25.8	**404.0**	74.0	43.0	5.5	11.0	2.0	0.4	0.5	0.3	1.5	2.0	2.7	282.2	403.3
Halifax_NS	1	0.8	0.8	28.0	0.9	0.0	0.0	0.0	-	21.0	21.0	28.0	**513.0**	57.0	47.2	9.0	15.2	1.7	-	-	-	0.9	0.0	0.4	-	-
	2	1.1	1.9	25.2	1.0	403.2	443.5	443.5	239.7	27.7	48.7	26.3	**513.0**	57.0	47.2	9.0	15.2	1.7	1.0	0.4	0.2	1.1	0.9	1.4	138.4	138.4
	3	2.1	3.9	25.2	1.2	403.2	826.6	1270.1	325.7	51.7	100.4	25.7	**513.0**	57.0	47.2	9.0	15.2	1.7	0.7	0.5	0.3	1.7	2.0	2.8	373.7	512.1
Inuvik Airport_NT	1	0.8	0.8	28.0	0.9	0.0	0.0	0.0	-	21.0	21.0	28.0	**7169.6**	213.0	19.6	33.7	12.4	0.4	-	-	-	0.9	0.0	0.4	-	-
	2	1.1	1.9	25.2	1.0	403.2	443.5	443.5	239.7	27.7	48.7	26.3	**7169.6**	213.0	19.6	33.7	12.4	0.4	3.7	0.5	0.3	1.1	0.9	1.4	104.7	104.7

Station	layer	d	∑ d	C	k	L	Ld	∑ Ld	L bar	Cd	∑Cd	C bar	Frezing Index, nF	No of Freezing days (t)	Mean annual Temp. (MAT)	V_s	V_0	α	μ	λ	λ^2	R_n	∑R	∑R+R_n/2	nF	∑nF
		(ft)	(ft)	Btu/ft^3°F	Btu/ft hr °F	Btu/ft^3	Btu/ft^2	Btu/ft^3	Btu/ft^3	Btu/ft^2°F	Btu/ft^2°F	Btu/ft^3°F														
	3	15.5	17.4	25.2	1.2	403.2	6261.7	6705.2	385.8	391.4	440.1	25.3	**7169.6**	213.0	19.6	33.7	12.4	0.4	2.2	0.6	0.3	13.1	2.0	8.5	7060.4	7165.1
Bakr Lake A_NU	1	0.8	0.8	28.0	0.9	0.0	0.0	0.0	-	21.0	21.0	28.0	**9500.4**	255.0	10.0	37.3	22.0	0.6	-	-	-	0.9	0.0	0.4	-	-
	2	1.1	1.9	25.2	1.0	403.2	443.5	443.5	239.7	27.7	48.7	26.3	**9500.4**	255.0	10.0	37.3	22.0	0.6	4.1	0.4	0.2	1.1	0.9	1.4	159.6	159.6
	3	14.6	16.4	25.2	1.2	403.2	5870.6	6314.1	384.8	366.9	415.6	25.3	**9500.4**	255.0	10.0	37.3	22.0	0.6	2.5	0.5	0.2	12.2	2.0	8.1	9339.1	9498.7
Hamilton A_ON	1	0.8	0.8	28.0	0.9	0.0	0.0	0.0	-	21.0	21.0	28.0	**1288.4**	111.0	45.1	11.6	13.1	1.1	-	-	-	0.9	0.0	0.4	-	-
	2	1.1	1.9	25.2	1.0	403.2	451.6	451.6	241.5	28.2	49.2	26.3	**1288.4**	111.0	45.1	11.6	13.1	1.1	1.3	0.5	0.3	1.1	0.9	1.4	103.2	103.2
	3	5.2	7.0	25.2	1.2	403.2	2076.5	2528.1	360.1	129.8	179.0	25.5	**1288.4**	111.0	45.1	11.6	13.1	1.1	0.8	0.6	0.3	4.3	2.0	4.1	1185.5	1288.7
Charlottetown A_PEI	1	0.8	0.8	28.0	0.9	0.0	0.0	0.0	-	21.0	21.0	28.0	**1377.4**	121.0	41.6	11.4	9.6	0.8	-	-	-	0.9	0.0	0.4	-	-
	2	1.1	1.9	25.2	1.0	403.2	443.5	443.5	239.7	27.7	48.7	26.3	**1377.4**	121.0	41.6	11.4	9.6	0.8	1.3	0.5	0.3	1.1	0.9	1.4	89.8	89.8
	3	6.2	8.1	25.2	1.2	403.2	2511.9	2955.5	365.8	157.0	205.7	25.5	**1377.4**	121.0	41.6	11.4	9.6	0.8	0.8	0.6	0.4	5.2	2.0	4.6	1287.9	1377.7
Bagotville A_QC	1	0.8	0.8	28.0	0.9	0.0	0.0	0.0	-	21.0	21.0	28.0	**2754.4**	142.0	36.8	19.4	4.8	0.2	-	-	-	0.9	0.0	0.4	-	-
	2	1.1	1.9	25.2	1.0	403.2	443.5	443.5	239.7	27.7	48.7	26.3	**2754.4**	142.0	36.8	19.4	4.8	0.2	2.1	0.6	0.4	1.1	0.9	1.4	68.1	68.1
	3	11.3	13.2	25.2	1.2	403.2	4568.3	5011.8	380.3	285.5	334.2	25.4	**2754.4**	142.0	36.8	19.4	4.8	0.2	1.3	0.7	0.5	9.5	2.0	6.7	2687.3	2755.4
Broadview A_SK	1	0.8	0.8	28.0	0.9	0.0	0.0	0.0	-	21.0	21.0	28.0	**2832.3**	142.0	35.8	19.9	3.8	0.2	-	-	-	0.9	0.0	0.4	-	-
	2	1.1	1.9	25.2	1.0	403.2	443.5	443.5	239.7	27.7	48.7	26.3	**2832.3**	142.0	35.8	19.9	3.8	0.2	2.2	0.7	0.4	1.1	0.9	1.4	60.1	60.1
	3	12.1	14.0	25.2	1.2	403.2	4886.8	5330.3	381.6	305.4	354.1	25.4	**2832.3**	142.0	35.8	19.9	3.8	0.2	1.3	0.7	0.5	10.2	2.0	7.1	2770.5	2830.6
Aishihik A_YU	1	0.8	0.8	28.0	0.9	0.0	0.0	0.0	-	21.0	21.0	28.0	**5301.9**	201.0	23.7	26.4	8.3	0.3	-	-	-	0.9	0.0	0.4	-	-
	2	1.1	1.9	25.2	1.0	403.2	443.5	443.5	239.7	27.7	48.7	26.3	**5301.9**	201.0	23.7	26.4	8.3	0.3	2.9	0.6	0.3	1.1	0.9	1.4	86.5	86.5
	3	14.7	16.5	25.2	1.2	403.2	5919.0	6362.5	384.9	369.9	418.7	25.3	**5301.9**	201.0	23.7	26.4	8.3	0.3	1.7	0.6	0.4	12.3	2.0	8.1	5215.6	5302.1

A.1.5 A List of the MEPDG Input Parameters Used in the Analysis

Project: Calgary Int. Airport.dgp

General Information

Design Life	20 years
Base/Subgrade construction:	September, 2010
Pavement construction:	October, 2010
Traffic open:	November, 2010
Type of design	Flexible

Analysis Parameters

Performance Criteria

	Limit	Reliability
Initial IRI (in/mi)	63	
Terminal IRI (in/mi)	145	85
AC Surface Down Cracking (Long. Cracking) (ft/mile):	2000	85
AC Bottom Up Cracking (Alligator Cracking) (%):	25	85
AC Thermal Fracture (Transverse Cracking) (ft/mi):	1000	85
Permanent Deformation (AC Only) (in):	0.25	85
Permanent Deformation (Total Pavement) (in):	0.75	85
Reflective cracking (%):	100	

Location:	Edmonton
Project ID:	
Section ID:	
Date:	6/7/2009
Station/milepost format:	
Station/milepost begin:	
Station/milepost end:	
Traffic direction:	East bound

Default Input Level

Default input level — Level 3, Default and historical agency values.

Traffic

Initial two-way AADTT:	3200
Number of lanes in design direction:	1
Percent of trucks in design direction (%):	50
Percent of trucks in design lane (%):	100
Operational speed (mph):	60

Traffic -- Volume Adjustment Factors

Monthly Adjustment Factors (Level 3, Default MAF)

Month	Vehicle Class									
	Class 4	Class 5	Class 6	Class 7	Class 8	Class 9	Class 10	Class 11	Class 12	Class 13
January	1.00	1.00	1.00	1.00	1.00	1.00	1.00	1.00	1.00	1.00
February	1.00	1.00	1.00	1.00	1.00	1.00	1.00	1.00	1.00	1.00
March	1.00	1.00	1.00	1.00	1.00	1.00	1.00	1.00	1.00	1.00
April	1.00	1.00	1.00	1.00	1.00	1.00	1.00	1.00	1.00	1.00
May	1.00	1.00	1.00	1.00	1.00	1.00	1.00	1.00	1.00	1.00
June	1.00	1.00	1.00	1.00	1.00	1.00	1.00	1.00	1.00	1.00
July	1.00	1.00	1.00	1.00	1.00	1.00	1.00	1.00	1.00	1.00
August	1.00	1.00	1.00	1.00	1.00	1.00	1.00	1.00	1.00	1.00
September	1.00	1.00	1.00	1.00	1.00	1.00	1.00	1.00	1.00	1.00
October	1.00	1.00	1.00	1.00	1.00	1.00	1.00	1.00	1.00	1.00
November	1.00	1.00	1.00	1.00	1.00	1.00	1.00	1.00	1.00	1.00
December	1.00	1.00	1.00	1.00	1.00	1.00	1.00	1.00	1.00	1.00

Vehicle Class Distribution **Hourly truck traffic distribution**

(Level 3, Default Distribution)

AADTT distribution by vehicle class

Class 4	1.8%
Class 5	24.6%
Class 6	7.6%
Class 7	0.5%
Class 8	5.0%
Class 9	31.3%
Class 10	9.8%
Class 11	0.8%
Class 12	3.3%
Class 13	15.3%

by period beginning:

Midnight	2.3%	Noon	5.9%
1:00 am	2.3%	1:00 pm	5.9%
2:00 am	2.3%	2:00 pm	5.9%
3:00 am	2.3%	3:00 pm	5.9%
4:00 am	2.3%	4:00 pm	4.6%
5:00 am	2.3%	5:00 pm	4.6%
6:00 am	5.0%	6:00 pm	4.6%
7:00 am	5.0%	7:00 pm	4.6%
8:00 am	5.0%	8:00 pm	3.1%
9:00 am	5.0%	9:00 pm	3.1%
10:00 am	5.9%	10:00 pm	3.1%
11:00 am	5.9%	11:00 pm	3.1%

Traffic Growth Factor

Vehicle Class	Growth Rate	Growth Function
Class 4	5.0%	Compound
Class 5	5.0%	Compound
Class 6	5.0%	Compound
Class 7	5.0%	Compound
Class 8	5.0%	Compound
Class 9	5.0%	Compound
Class 10	5.0%	Compound
Class 11	5.0%	Compound

Class 12	5.0%	Compound
Class 13	5.0%	Compound

Traffic -- Axle Load Distribution Factors

Level 3: Default

Traffic -- General Traffic Inputs

Mean wheel location (inches from the lane marking): 18

Traffic wander standard deviation (in): 10

Design lane width (ft): 12

Number of Axles per Truck

Vehicle Class	Single Axle	Tandem Axle	Tridem Axle	Quad Axle
Class 4	1.62	0.39	0.00	0.00
Class 5	2.00	0.00	0.00	0.00
Class 6	1.02	0.99	0.00	0.00
Class 7	1.00	0.26	0.83	0.00
Class 8	2.38	0.67	0.00	0.00
Class 9	1.13	1.93	0.00	0.00
Class 10	1.19	1.09	0.89	0.00
Class 11	4.29	0.26	0.06	0.00
Class 12	3.52	1.14	0.06	0.00
Class 13	2.15	2.13	0.35	0.00

Axle Configuration

Average axle width (edge-to-edge) outside dimensions,ft): 8.5

Dual tire spacing (in): 12

Axle Configuration

Tire Pressure (psi) : 120

Average Axle Spacing

Tandem axle(psi):	51.6
Tridem axle(psi):	49.2
Quad axle(psi):	49.2

Climate

icm file:	C:\Documents and Settings\raj\Desktop\Jhuma MSc\MEPDG\Canadian project\Calgary.icm
Latitude (degrees.minutes)	51.114
Longitude (degrees.minutes)	-114.02
Elevation (ft)	330
Depth of water table (ft)	5

Structure--Design Features

HMA E* Predictive Model:	NCHRP 1-37A viscosity based model.
HMA Rutting Model coefficients:	NCHRP 1-37A coefficients
Endurance Limit (microstrain):	None (0 microstrain)

Structure--Layers

Layer 1 -- Asphalt concrete

Material type:	Asphalt concrete
Layer thickness (in):	9

General Properties

General

Reference temperature (F°):	70

Volumetric Properties as Built

Effective binder content (%):	10
Air voids (%):	8.5
Total unit weight (pcf):	150

Poisson's ratio: 0.35 (user entered)

Thermal Properties

Thermal conductivity asphalt (BTU/hr-ft-F°): 0.67

Heat capacity asphalt (BTU/lb-F°): 0.23

Asphalt Mix

Cumulative % Retained 3/4 inch sieve: 7

Cumulative % Retained 3/8 inch sieve: 30

Cumulative % Retained #4 sieve: 57.5

% Passing #200 sieve: 4

Asphalt Binder

Option: Superpave binder grading

A 11.0100 (correlated)

VTS: -3.7010 (correlated)

High temp. °C	Low temperature, °C						
	-10	-16	-22	-28	-34	-40	-46
46							
52							
58							
64							
70							
76							
82							

Thermal Cracking Properties

Average Tensile Strength at 14ºF: 493.26

Mixture VMA (%) 18.5

Aggreagate coeff. thermal contraction (in./in.) 0.000005

Mix coeff. thermal contraction (in./in./ºF): 0.000013

Load Time (sec)	Low Temp. -4ºF (1/psi)	Mid. Temp. 14ºF (1/psi)	High Temp. 32ºF (1/psi)
1	2.05E-07	3.87E-07	5.68E-07
2	2.31E-07	4.63E-07	7.64E-07
5	2.71E-07	5.89E-07	1.13E-06
10	3.05E-07	7.05E-07	1.53E-06
20	3.44E-07	8.45E-07	2.05E-06
50	4.03E-07	1.07E-06	3.04E-06
100	4.54E-07	1.29E-06	4.1E-06

Layer 2 -- A-1-a

Unbound Material: A-1-a
Thickness(in): 13

Strength Properties

Input Level: Level 3
Analysis Type: ICM inputs (ICM Calculated Modulus)
Poisson's ratio: 0.35
Coefficient of lateral pressure,Ko: 0.5
Modulus (input) (psi): 40000

ICM Inputs

Gradation and Plasticity Index

Plasticity Index, PI: 1
Liquid Limit (LL) 6
Compacted Layer Yes
Passing #200 sieve (%): 8.7

Passing #40	20
Passing #4 sieve (%):	44.7
D10(mm)	0.1035
D20(mm)	0.425
D30(mm)	1.306
D60(mm)	10.82
D90(mm)	46.19

Sieve	Percent Passing
0.001mm	
0.002mm	
0.020mm	
#200	8.7
#100	
#80	12.9
#60	
#50	
#40	20
#30	
#20	
#16	
#10	33.8
#8	
#4	44.7
3/8"	57.2
1/2"	63.1
3/4"	72.7
1"	78.8
1 1/2"	85.8
2"	91.6
2 1/2"	
3"	
3 1/2"	97.6
4"	97.6

Calculated/Derived Parameters

Maximum dry unit weight (pcf):	127.7 (derived)
Specific gravity of solids, Gs:	2.70 (derived)
Saturated hydraulic conductivity (ft/hr):	0.05054 (derived)
Optimum gravimetric water content (%):	7.4 (derived)
Calculated degree of saturation (%):	62.2 (calculated)

Soil water characteristic curve parameters: Default values

Parameters	Value
a	7.2555
b	1.3328
c	0.82422
Hr.	117.4

Layer 3 -- A-6

Unbound Material: A-6
Thickness(in): Semi-infinite

Strength Properties

Input Level: Level 3
Analysis Type: ICM inputs (ICM Calculated Modulus)
Poisson's ratio: 0.35
Coefficient of lateral pressure,Ko: 0.5
Modulus (input) (psi): 14500

ICM Inputs

Gradation and Plasticity Index

Plasticity Index, PI:	16
Liquid Limit (LL)	33
Compacted Layer	No
Passing #200 sieve (%):	63.2
Passing #40	82.4
Passing #4 sieve (%):	93.5

D10(mm)	0.000285
D20(mm)	0.0008125
D30(mm)	0.002316
D60(mm)	0.05364
D90(mm)	1.922

Sieve	Percent Passing
0.001mm	
0.002mm	
0.020mm	
#200	63.2
#100	
#80	73.5
#60	
#50	
#40	82.4
#30	
#20	
#16	
#10	90.2
#8	
#4	93.5
3/8"	96.4
1/2"	97.4
3/4"	98.4
1"	99
1 1/2"	99.5
2"	99.8
2 1/2"	
3"	
3 1/2"	100
4"	100

Calculated/Derived Parameters

Maximum dry unit weight (pcf):	107.9 (derived)
Specific gravity of solids, Gs:	2.70 (derived)
Saturated hydraulic conductivity (ft/hr):	1.95e-005 (derived)
Optimum gravimetric water content (%):	17.1 (derived)
Calculated degree of saturation (%):	82.1 (calculated)
Soil water characteristic curve parameters:	Default values

Parameters	Value
a	108.41
b	0.68007
c	0.21612
Hr.	500

Distress Model Calibration Settings - Flexible

AC Fatigue

Level 3: NCHRP 1-37A coefficients (nationally calibrated values)

k1	0.007566
k2	3.9492
k3	1.281

AC Rutting

Level 3: NCHRP 1-37A coefficients (nationally calibrated values)

k1	-3.35412
k2	1.5606
k3	0.4791
Standard Deviation Total Rutting (RUT):	0.24*POWER(RUT,0.8026)+0.001

Thermal Fracture

Level 3: NCHRP 1-37A coefficients (nationally calibrated values)

k1	1.5

Std. Dev. (THERMAL):	0.1468 * THERMAL + 65.027

CSM Fatigue

Level 3: NCHRP 1-37A coefficients (nationally calibrated values)

k1	1
k2	1

Subgrade Rutting

Level 3: NCHRP 1-37A coefficients (nationally calibrated values)

Granular:

k1	2.03

Fine-grain:

k1	1.35

AC Cracking

AC Top Down Cracking

C1 (top)	7
C2 (top)	3.5
C3 (top)	0
C4 (top)	1000
Standard Deviation (TOP)	200 + 2300/(1+exp(1.072-2.1654*log(TOP+0.0001)))

AC Bottom Up Cracking

C1 (bottom)	1
C2 (bottom)	1
C3 (bottom)	0
C4 (bottom)	6000
Standard Deviation (TOP)	1.13+13/(1+exp(7.57-15.5*log(BOTTOM+0.0001)))

CSM Cracking

C1 (CSM)	1

C2 (CSM)	1
C3 (CSM)	0
C4 (CSM)	1000
Standard Deviation (CSM)	CTB*1

IRI

IRI HMA Pavements New

C1(HMA)	40
C2(HMA)	0.4
C3(HMA)	0.008
C4(HMA)	0.015

IRI HMA/PCC Pavements

C1(HMA/PCC)	40.8
C2(HMA/PCC)	0.575
C3(HMA/PCC)	0.0014
C4(HMA/PCC)	0.00825

A.1.6 List of Pavement Performances for All 206 Canadian Weather Stations Prepared by TAC for the MEPDG Application

Provinces of Canada	Weather Stations	Latitude	Longitude	Predicted Distresses					
				IRI	Asphalt layer Rutting	Tot. Perm. Deform.	Transverse Cracking	Alligator Cracking	Longitudinal Cracking
				m/km	mm	mm	m/km	(%)	m/km
Alberta	Calgary Int. Airport	51.114	-114.02	1.91	6.6	15.5	0.19	1.9	3.56
	Cold Lake Airport	54.417	-110.283	1.92	6.4	15.2	0.19	1.9	3.43
	Coronation Airport	52.067	-111.45	1.92	6.4	15.2	0.19	1.9	3.31
	Cowley Airport	49.633	-114.083	1.91	6.1	15	0.19	1.9	3.5
	Namao Airport	53.667	-113.467	1.92	6.1	15	0.19	1.9	3.24
	City Centre Airport	53.573	-113.518	1.94	6.9	16	0.19	2.1	4.43
	Edmonton Int. Airport	53.317	-113.583	1.93	6.4	15.5	0.19	2	3.56
	Edson Airport	53.583	-116.467	1.91	5.6	14.5	0.19	1.9	3.18
	Edson	53.583	-116.417	1.91	5.6	14.5	0.19	1.9	3.18
	Embarras Airport	58.2	-111.383	1.95	6.9	16	0.19	2.2	6.25
	Fort Chipewyan	58.717	-111.15	1.94	6.1	15.5	0.19	2.2	7.25

Provinces of Canada	Weather Stations	Latitude	Longitude	Predicted Distresses					
				IRI	Asphalt layer Rutting	Tot. Perm. Deform.	Transverse Cracking	Alligator Cracking	Longitudinal Cracking
				m/km	mm	mm	m/km	(%)	m/km
	Fort Mcmurray Airport	56.65	-111.217	1.95	6.6	16	0.19	2.2	5.62
	Grande Prairie Airport	55.18	-118.885	1.92	6.1	15	0.19	1.9	3.14
	High Level Airport	58.621	-117.165	1.95	6.9	16	0.19	2.1	5.21
	Lac La Biche	54.767	-111.967	1.93	6.6	15.7	0.19	2	3.96
	Lac La Biche 1	54.767	-112.017	1.94	6.6	15.7	0.19	2.1	4.75
	Lethbridge Airport	49.63	-112.8	1.95	8.4	17	0.19	2.1	6
	Lloydminster Airport	53.309	-110.073	1.92	6.1	15	0.19	1.9	3.09
	Medicine Hat Airport	50.019	-110.721	1.98	9.7	18.3	0.19	2.1	7.59
	Peace River Airport	56.227	-117.447	1.9	5.6	14.7	0.19	1.8	2.59
	Pincher Creek	49.5	-113.95	1.96	7.9	16.8	0.19	2.1	6.44
	Rocky Mtn House	52.383	-114.917	1.93	6.4	15.5	0.19	2	4.13
	Slave Lake Airport	55.3	-114.783	1.91	5.3	14.2	0.19	1.8	2.4

Provinces of Canada	Weather Stations	Latitude	Longitude	Predicted Distresses					
				IRI	Asphalt layer Rutting	Tot. Perm. Deform.	Transverse Cracking	Alligator Cracking	Longitudinal Cracking
				m/km	mm	mm	m/km	(%)	m/km
	Springbank Airport	51.103	-114.374	1.9	5.6	14.2	0.19	1.8	2.76
	Vermilion Airport	53.35	-110.833	1.92	6.1	15.2	0.19	2	3.5
	Whitecourt	54.133	-115.667	1.93	6.1	15.2	0.19	2	4.01
	Whitecourt Airport	54.144	-115.787	1.95	6.6	15.7	0.19	2.1	4.9
British ColumbiaC	Abbotsford Airport	49.025	-122.363	1.95	8.4	17	0.19	2.7	15.69
	Beatton River Airport	57.383	-121.383	1.88	4.3	13.2	0.19	1.7	2.2
	Cape St. James	51.933	-131.017	1.74	2	9.7	0.19	1.2	0.09
	Castlegar Airport	49.296	-117.633	2.05	12.2	20.8	0.19	2.5	15.85
	Comox Airport	49.717	-124.9	1.85	6.1	14.2	0.19	2.1	5.17
	Cranbrook Airport	49.612	-115.782	2	10.7	19.1	0.19	2.1	9.01
	Fort Nelson Airport	58.836	-122.597	1.97	7.4	16.8	0.19	2.2	6.32
	Fort St John Airport	56.238	-120.74	1.9	5.6	14.5	0.19	1.8	2.57
	Kamloops Airport	50.702	-120.442	2.02	12.7	21.1	0.19	2.2	11.79

Provinces of Canada	Weather Stations	Latitude	Longitude	Predicted Distresses					
				IRI	Asphalt layer Rutting	Tot. Perm. Deform.	Transverse Cracking	Alligator Cracking	Longitudinal Cracking
				m/km	mm	mm	m/km	(%)	m/km
	Kelowna Airport	49.956	-119.378	2.01	11.9	20.3	0.19	2.1	9.98
	Kimberley Airport	49.733	-115.783	1.98	9.7	18.3	0.19	2	7.06
	Lytton1	50.233	-121.567	2.12	15.5	24.1	0.19	2.5	16.49
	Lytton2	50.233	-121.583	1.96	10.4	18.5	0.19	1.9	6.63
	Nanaimo Airport	49.052	-123.87	1.94	8.6	17	0.19	2.4	11.89
	Penticton Airport	49.463	-119.602	1.98	11.7	19.6	0.19	2.1	9.66
	Port Hardy Airport	50.68	-127.366	1.8	3.3	11.4	0.19	1.7	1.15
	Prince Geoge Airport	53.891	-122.679	1.93	6.9	15.7	0.19	2	4.43
	Prince Rupert Airport	54.293	-130.445	1.84	3	11.2	0.19	1.7	0.91
	Princeton Airport	49.468	-120.512	2.04	12.2	20.8	0.19	2.3	11.17
	Quesnel Airport	53.026	-122.51	2.02	10.2	19.1	0.19	2.3	9.18
	Sandspit Airport	53.254	-131.813	1.77	2.8	10.7	0.19	1.5	0.49
	Smith River Airport	59.9	-126.433	1.9	4.6	13.7	0.19	1.9	4.41
	Smithers Airport	54.825	-127.183	1.96	8.1	17	0.19	2.1	6.4

Provinces of Canada	Weather Stations	Latitude	Longitude	Predicted Distresses					
				IRI	Asphalt layer Rutting	Tot. Perm. Deform.	Transverse Cracking	Alligator Cracking	Longitudinal Cracking
				m/km	mm	mm	m/km	(%)	m/km
	Terrace Airport	54.466	-128.578	1.94	6.6	15.2	0.19	2.4	10.03
	Tofino Airport	49.081	-125.778	1.82	3.6	11.7	0.19	1.7	1.48
	Vancouver Int. Airport	49.195	-123.182	1.85	5.8	14	0.19	2.1	4.81
	Gonzales Heights	48.417	-123.317	1.78	4.8	12.4	0.19	1.5	1.57
	Williams Lake Airport	52.183	-122.054	1.93	7.4	16	0.19	1.9	4.22
Manitoba	Bird	56.5	-94.2	1.91	4.6	13.7	0.19	2.2	12.4
	Brandon Airport	49.917	-99.95	1.97	7.6	17	0.19	2.2	5.72
	Dauphin Airport	51.1	-100.05	1.99	7.9	17.3	0.19	2.4	7.97
	Gimli	50.633	-97.017	1.99	7.9	17.3	0.19	2.3	7.42
	Gimli Airport	50.633	-97.05	1.97	7.1	16.3	0.19	2.2	5.57
	Lynn Lake Airport	56.864	-101.076	1.94	5.8	15	0.19	2.2	9.62
	Rivers Airport	50.017	-100.317	1.96	6.9	16.3	0.19	2.1	5.3
	The Pas Airport	53.967	-101.1	1.96	6.9	16.3	0.19	2.2	5.98
	Thompson Airport	55.803	-97.863	1.96	6.4	15.7	0.19	2.3	10.41

Provinces of Canada	Weather Stations	Latitude	Longitude	Predicted Distresses					
				IRI	Asphalt layer Rutting	Tot. Perm. Deform.	Transverse Cracking	Alligator Cracking	Longitudinal Cracking
				m/km	mm	mm	m/km	(%)	m/km
	Richardson Int. Airport	49.917	-97.233	2	8.4	17.8	0.19	2.4	7.4
New Brunswick	Campbellton Airport	48	-66.667	1.96	6.4	15.7	0.19	2.5	7.36
	Charlo Airport	47.983	-66.333	1.96	6.1	15.5	0.19	2.5	7.1
	Fredericton Airport	45.872	-66.528	2.01	7.9	17.3	0.19	2.9	15.3
	Moncton Airport	46.104	-64.688	1.96	6.4	15.5	0.19	2.6	9.09
	Saint John Airport	45.318	-65.886	1.94	5.3	14.2	0.19	2.4	5.87
	St. Leonard Airport	47.158	-67.832	1.97	6.1	15.7	0.19	2.6	7.86
Newfoundland & Labrador	Argentia Airport	47.3	-54	1.8	2.8	10.7	0.19	1.5	0.55
	Battle Harbourlor	52.25	-55.6	1.81	1.5	9.9	0.19	1	0.19
	Bonavista Airport	48.667	-53.114	1.84	3	11.4	0.19	1.5	0.78
	Buchans Airport	48.85	-56.833	1.88	3.6	12.4	0.19	1.8	1.86
	Burgeo	47.617	-57.617	1.86	3	11.4	0.19	1.6	0.8
	Cape Harrison	54.767	-58.45	1.86	3	11.9	0.19	1.4	1.25
	Cartwright Airport	53.708	-57.035	1.88	3	12.2	0.19	1.6	1.42

Provinces of Canada	Weather Stations	Latitude	Longitude	Predicted Distresses					
				IRI	Asphalt layer Rutting	Tot. Perm. Deform.	Transverse Cracking	Alligator Cracking	Longitudinal Cracking
				m/km	mm	mm	m/km	(%)	m/km
	Churchill Falls Airport	53.55	-64.1	1.91	3.8	12.7	0.19	1.9	5.76
	Gander Int. Airport	48.946	-54.577	1.9	4.3	13.2	0.19	2	3.48
	Goose Bay Airport	53.317	-60.417	1.92	4.6	13.7	0.19	2	3.99
	Hopedale Airport	55.45	-60.217	1.83	2	10.4	0.19	1.1	0.57
	Mary's Harbour Airport	52.304	-55.834	1.86	3	11.9	0.19	1.5	1.29
	Port Aux Basques Airport	47.574	-59.155	1.85	2.8	11.2	0.19	1.5	0.68
	St. Andrews	47.767	-59.333	1.87	4.1	12.7	0.19	1.9	3.18
	St.Anthony	51.367	-55.583	1.84	2.8	11.4	0.19	1.4	0.7
	St.Anthony Airport	51.4	-56.083	1.83	2.5	11.2	0.19	1.3	0.51
	St.Anthony1	51.367	-55.6	1.86	2.5	11.2	0.19	1.4	0.76
	St. John's Airport	47.622	-52.743	1.88	4.1	12.4	0.19	1.8	2.65
	St. Lawrence	46.917	-55.383	1.81	2.3	10.2	0.19	1.3	0.23
	Stephenville Airport	48.533	-58.55	1.9	4.3	13.2	0.19	2.1	3.2

Provinces of Canada	Weather Stations	Latitude	Longitude	Predicted Distresses					
				IRI	Asphalt layer Rutting	Tot. Perm. Deform.	Transverse Cracking	Alligator Cracking	Longitudinal Cracking
				m/km	mm	mm	m/km	(%)	m/km
Nova Scotia	Copper Lake	45.383	-61.967	1.94	5.8	14.7	0.19	2.5	9.56
	Debert Airport	45.417	-63.45	1.92	5.3	14	0.19	2.3	6.83
	Eddy Point	45.517	-61.25	1.92	5.3	14	0.19	2.3	6.65
	Greenwood Airport	44.983	-64.917	1.97	7.6	16.3	0.19	2.8	14.73
	Halifax	44.65	-63.567	1.91	5.3	14	0.19	2.3	6.27
	Stanfield Int. Airport	44.883	-63.517	1.94	6.1	14.7	0.19	2.4	8.75
	Sable Island Airport	43.932	-60.009	1.84	3.8	11.9	0.19	1.9	2.08
	Shearwater Airport	44.633	-63.5	1.92	5.6	14.2	0.19	2.3	6.97
	Shelburne	43.717	-65.25	1.91	5.3	14	0.19	2.3	6.95
	Sydney Airport	46.167	-60.048	1.93	5.6	14.2	0.19	2.3	6.85
	Truro	45.367	-63.267	1.92	5.6	14.2	0.19	2.3	6.4
	Yarmouth Airport	43.831	-66.089	1.88	4.6	13	0.19	2.1	4.07
Northwest Territory	Cape Parry Airport	70.167	-124.717	1.69	1.5	6.9	0.19	0.9	24.99
	Fort Reliance	62.717	-109.167	1.88	4.6	13.5	0.19	1.9	11.66

Provinces of Canada	Weather Stations	Latitude	Longitude	Predicted Distresses					
				IRI	Asphalt layer Rutting	Tot. Perm. Deform.	Transverse Cracking	Alligator Cracking	Longitudinal Cracking
				m/km	mm	mm	m/km	(%)	m/km
	Fort Resolution Airport	61.181	-113.69	1.9	5.1	14.2	0.19	2	7.4
	Fort Simpson	61.867	-121.35	1.9	5.1	14.2	0.19	2	7.4
	Fort Simpson Airport	61.76	-121.237	1.99	7.9	17.3	0.19	2.4	12.67
	Hay River Airport	60.84	-115.783	1.91	5.6	14.7	0.19	1.9	5.28
	Inuvik Airport	68.304	-133.483	1.87	4.6	13.2	0.19	1.8	17.89
	Mould Bay Airport	76.233	-119.333	1.48	1	6.4	0.19	0.7	2006.76
	Norman Wells Airport	65.283	-126.8	1.92	5.8	15	0.19	2	10.81
	Sachs Harbour Airport	72	-125.267	1.69	1.3	6.9	0.19	0.9	173.41
	Yellowknife Airport	62.463	-114.44	1.9	5.3	14.2	0.19	2	7.35
Nunavut	Baker Lake Airport	64.299	-96.078	1.75	2.3	8.4	0.19	1.4	113.02
	Cambridge Bay Airport	69.108	-105.138	1.51	1.5	7.1	0.19	1.1	912.51
	Cape Dyer Airport	66.583	-61.617	1.78	2	8.1	0.19	1.3	39

Provinces of Canada	Weather Stations	Latitude	Longitude	Predicted Distresses					
				IRI	Asphalt layer Rutting	Tot. Perm. Deform.	Transverse Cracking	Alligator Cracking	Longitudinal Cracking
				m/km	mm	mm	m/km	(%)	m/km
	Chesterfield	63.333	-90.717	1.73	2	7.6	0.19	1.2	46.19
	Clyde River Airport	70.486	-68.517	1.71	1.3	6.9	0.19	0.9	38.81
	Contwoyto Lake	65.483	-110.367	1.77	2.5	8.9	0.19	1.6	146.91
	Coppermine	67.833	-115.117	1.75	2.3	8.1	0.19	1.4	52.63
	Ennadai Lake	61.133	-100.9	1.77	2.8	8.9	0.19	1.5	51.49
	Hall Beach Airport	68.776	-81.244	1.51	1.3	6.9	0.19	0.9	210.14
	IqaluitAirport	63.75	-68.55	1.74	1.8	7.4	0.19	1	21.77
	Rankin Inlet Airport	62.817	-92.117	1.75	2	8.1	0.19	1.3	40.51
	Rea Point Airport	75.367	-105.717	1.45	0.8	6.1	0.19	0.7	2006.76
	Resolute Airport	74.717	-94.986	1.49	1	6.4	0.19	0.7	1968.89
Ontario	Armstrong Airport	50.294	-88.905	1.96	6.1	15.5	0.19	2.4	7.67
	Atikokan	48.75	-91.617	2.01	7.9	17.3	0.19	2.7	11.15
	Big Trout Lake	53.833	-89.867	1.94	5.3	14.7	0.19	2.2	9.24
	Chapleau	47.833	-83.433	1.96	6.1	15.5	0.19	2.4	7.18
	Earlton Airport	47.7	-79.85	1.98	6.6	16.3	0.19	2.5	8.27

Provinces of Canada	Weather Stations	Latitude	Longitude	Predicted Distresses					
				IRI	Asphalt layer Rutting	Tot. Perm. Deform.	Transverse Cracking	Alligator Cracking	Longitudinal Cracking
				m/km	mm	mm	m/km	(%)	m/km
	Geraldton	49.7	-86.95	1.95	5.8	15.2	0.19	2.3	6.29
	Geraldton Airport	49.783	-86.931	1.95	5.8	15.2	0.19	2.3	6.29
	Gore Bay Airport	45.883	-82.567	1.97	7.4	16.5	0.19	2.5	7.91
	Graham Airport	49.267	-90.583	1.95	5.6	15	0.19	2.3	6.59
	Hamilton Airport	43.172	-79.934	2.01	9.1	18	0.19	2.7	13.97
	Kapuskasing Airport	49.414	-82.468	1.98	6.4	16	0.19	2.5	8.99
	Kenora Airport	49.79	-94.365	2	7.9	17.3	0.19	2.5	8.5
	Killaloe	45.567	-77.417	2.01	8.6	18	0.19	2.6	8.99
	London Airport	43.033	-81.151	2.02	9.1	18.3	0.19	2.9	21.96
	Mount Forest	43.983	-80.75	1.98	7.6	16.8	0.19	2.6	12.4
	Nakina Airport	50.183	-86.7	1.96	6.1	15.5	0.19	2.4	8.05
	North Bay Airport	46.364	-79.423	2	7.1	16.8	0.19	2.9	11.79
	Ottawa Rockcliffe Airport	45.45	-75.633	2.03	9.1	18.5	0.19	2.8	11.85
	Macdonald-Cartier Int. Airport	45.323	-75.669	2.05	9.9	19.3	0.19	3	18.12

Provinces of Canada	Weather Stations	Latitude	Longitude	Predicted Distresses					
				IRI	Asphalt layer Rutting	Tot. Perm. Deform.	Transverse Cracking	Alligator Cracking	Longitudinal Cracking
				m/km	mm	mm	m/km	(%)	m/km
	Petawawa Airport	45.95	-77.317	2.02	8.4	18	0.19	2.8	11.15
	Saulte Marie Airport	46.483	-84.509	1.99	7.6	16.8	0.19	2.6	10.79
	Simcoe	42.85	-80.267	1.99	8.6	17.5	0.19	2.6	14.9
	Sioux Lookout Airport	50.117	-91.9	1.99	7.1	16.5	0.19	2.5	9.13
	Stirling	44.317	-77.633	2.02	9.7	18.5	0.19	2.7	13.42
	Sudbury Airport	46.625	-80.799	2.01	7.9	17.5	0.19	2.8	11.91
	Thunder Bay Airport	48.369	-89.327	1.97	6.9	16.3	0.19	2.4	6.44
	Victor Power Airport	48.57	-81.377	1.98	6.6	16.3	0.19	2.6	10.62
	Buttonville Airport	43.862	-79.37	2.02	9.9	18.5	0.19	2.6	15.94
	Lester B. Pearson Int. Airport	43.677	-79.631	2.01	9.9	18.5	0.19	2.6	15.39
	Trenton Airport	44.117	-77.533	1.99	8.4	17.3	0.19	2.6	13.54
	White River	48.6	-85.283	1.98	6.6	16.3	0.19	2.7	10.34
	Wiarton Airport	44.746	-81.107	2.01	8.4	17.5	0.19	2.9	18.02

Provinces of Canada	Weather Stations	Latitude	Longitude	Predicted Distresses					
				IRI	Asphalt layer Rutting	Tot. Perm. Deform.	Transverse Cracking	Alligator Cracking	Longitudinal Cracking
				m/km	mm	mm	m/km	(%)	m/km
	Windsor Airport	42.276	-82.956	2.04	10.7	19.3	0.19	2.9	20.26
	Winisk Airport	55.233	-85.117	1.86	3.3	11.9	0.19	1.6	4.83
PEI (Prince Edward Island)	Charlottetown Airport	46.289	-63.129	1.94	5.8	14.7	0.19	2.4	7.14
	Summerside Airport	46.439	-63.832	1.93	5.6	14.5	0.19	2.4	5.83
Quebec	Bagotville Airport	48.333	-71	1.99	7.1	16.5	0.19	2.6	9.67
	Baie-Comeau Airport	49.133	-68.2	1.9	4.1	13.2	0.19	2	2.22
	Gaspe Airport	48.777	-64.478	2.14	6.1	15.5	256.28	2.5	7.65
	Gatineau Airport	45.517	-75.567	2.09	10.7	19.3	298.27	2	8.67
	Grindstone Island	47.383	-61.867	1.86	3.6	12.2	0.19	1.8	1.34
	Inukjuas Airport	58.467	-78.083	2.07	2	9.9	399.84	1	4.43
	Kuujjuaq Airport	58.1	-68.417	1.86	3.3	11.9	0.19	1.5	4.3
	La Grande Riviere Airport	53.633	-77.7	1.93	4.8	14.2	0.19	2.2	9.18
	Maniwaki U Airport	46.302	-76.006	2.04	8.1	18.3	0.19	3.4	18.53

Provinces of Canada	Weather Stations	Latitude	Longitude	Predicted Distresses					
				IRI	Asphalt layer Rutting	Tot. Perm. Deform.	Transverse Cracking	Alligator Cracking	Longitudinal Cracking
				m/km	mm	mm	m/km	(%)	m/km
	Mont-Joli Airport	48.6	-68.217	1.95	6.1	15.2	0.19	2.3	5.19
	St-Hubert Airport	45.517	-73.417	2.03	8.9	18.3	0.19	3	16.13
	Mirabel Int. Airport	45.667	-74.033	2.06	9.9	19.3	0.19	3.3	21.77
	Pierre Elliottrudeau Int. Airport	45.467	-73.75	2.03	9.1	18.5	0.19	3	17.17
	Nitchequon	53.2	-70.9	2.16	3.6	12.7	399.84	2	5.58
	Jean Lesage Int. Airport	46.8	-71.383	1.97	8.1	17	0.19	2.2	8.27
	Roberval Airport	48.517	-72.267	1.99	7.4	16.8	0.19	2.6	9.16
	Rouyn Airport	48.217	-78.833	2.09	7.4	16	399.84	1.8	5.53
	Sept-Iles Airport	50.217	-66.267	1.89	4.1	13	0.19	1.8	1.95
	Ste Agathe DesS Monts	46.05	-74.283	2.02	7.6	17.3	0.19	3.1	16.51
	Val-D'or Airport	48.056	-77.787	2.25	6.4	16	399.84	2.6	10.56
Saskatchewan	Broadviewi Airport	50.368	-102.571	1.95	6.9	16.3	0.19	2.1	4.81

Provinces of Canada	Weather Stations	Latitude	Longitude	Predicted Distresses					
				IRI	Asphalt layer Rutting	Tot. Perm. Deform.	Transverse Cracking	Alligator Cracking	Longitudinal Cracking
				m/km	mm	mm	m/km	(%)	m/km
	Broadview Airport	50.25	-102.533	1.94	6.6	16	0.19	2	4.79
	Estevan Airport	49.217	-102.967	1.98	8.4	17.5	0.19	2.2	6.06
	Hudson Bay	52.867	-102.4	2.22	6.6	16	399.84	2.2	5.98
	Kindersley Airport	51.517	-109.183	1.95	7.9	16.8	0.19	2	4.58
	La Ronge Airport	55.15	-105.267	1.94	6.1	15.5	0.19	2.1	4.43
	Moose Jaw Airport	50.333	-105.55	1.97	8.6	17.5	0.19	2.2	6.51
	North Battleford Airport	52.772	-108.256	1.94	6.9	16	0.19	2	4.51
	Prince Albert Airport	53.217	-105.667	1.95	7.1	16.3	0.19	2.1	5.05
	Regina Airport	50.433	-104.667	1.96	7.9	17	0.19	2.1	5.11
	Diefenbaker Int. Airport	52.167	-106.717	1.95	7.4	16.5	0.19	2	4.51
	Stony Rapids Airport	59.25	-105.833	1.97	7.1	16.3	0.19	2.4	12.12
	Uranium City Airport	59.567	-108.483	1.93	6.4	15.2	0.19	2.1	9.22

Provinces of Canada	Weather Stations	Latitude	Longitude	Predicted Distresses					
				IRI	Asphalt layer Rutting	Tot. Perm. Deform.	Transverse Cracking	Alligator Cracking	Longitudinal Cracking
				m/km	mm	mm	m/km	(%)	m/km
	Wynyard Airport	51.767	-104.2	1.94	6.9	16	0.19	2	4.37
	Yorkton Airport	51.267	-102.467	1.95	7.1	16.3	0.19	2.1	5.36
Yukon	Aishihik Airport	61.65	-137.483	1.83	3.6	11.9	0.19	1.4	3.24
	Dawson	64.05	-139.433	2.2	6.1	15.2	399.84	2.3	13.14
	Dawson Airport	64.043	-139.128	2.25	7.9	17	399.84	2.5	14.52
	Mayo Airport	63.617	-135.867	2.25	8.4	17.8	399.84	2.3	10.11
	Snag Airport	62.367	-140.4	2.18	5.3	14.5	399.84	2.2	11.55
	Teslin Airport	60.174	-132.736	2.14	4.8	13.5	399.84	1.6	2.57
	Watson Lake Airport	60.118	-128.822	1.93	6.1	15.2	0.19	2	5.36
	Whitehorse Airport	60.71	-135.068	1.86	5.1	13.7	0.19	1.5	1.82

Note: Tot. = Total, Perm. = Permanent, Deform. = Deformation

Appendix 2

A.2.1 Predicted Pavement Distresses by the MEPDG at 85% Reliability and at the End of 20-year Analysis Period for Six Different Pavement Structure Cases

AC layer rutting is not found directly from the output results with design reliability (85%). This has been merged within total rutting. The other pavement distresses are summarized for different cases as below.

CASE 1: Traffic-0.3 million ESAL / 40 - AADTT, AC layer thickness- 140 mm, GB layer thickness- 220 mm, Poor Subgrade having modulus 25 MPa

Weather stations of Alberta	IRI	Total rutting	Longitudinal Cracking	Alligator Cracking	Transverse Cracking
	(m/km)	(mm)	(m/km)	(%)	(m/km)
Pincher Creek	2.49	19.30	43.49	1.52	12.95
Lethbridge Airport	2.48	19.45	42.70	1.52	12.95
Cowley Airport	2.49	19.49	42.68	1.53	12.95
Medicine Hat Airport	2.45	18.80	42.13	1.48	12.95
Springbank Airport	2.49	19.26	43.42	1.5	12.95
Calgary Int. Airport	2.47	19.09	42.05	1.49	12.95
Coronation Airport	2.50	20.06	44.36	1.49	12.95
Rocky Mtn House	2.52	20.11	45.35	1.54	12.95
Lloydminster Airport	2.51	20.05	45.45	1.5	12.95
Edmonton Int. Airport	2.51	20.01	45.00	1.51	12.95
Vermilion Airport	2.52	20.26	46.31	1.52	12.95
City Centre Airport	2.50	19.90	42.77	1.52	12.95
Edson	2.52	19.92	46.93	1.52	12.95
Edson Airport	2.53	20.29	46.50	1.55	12.95
Namao Airport	2.50	19.68	44.12	1.5	12.95
Whitecourt	2.53	20.26	47.49	1.54	12.95
Whitecourt Airport	2.53	20.26	45.43	1.55	12.95
Cold Lake Airport	2.52	20.28	45.54	1.51	12.95
Lac La Biche 1	2.51	20.33	48.56	1.54	12.95
Lac La Biche 2	2.53	20.58	46.53	1.54	12.95
Grande Prairie Airport	2.51	20.07	45.12	1.51	12.95
Slave Lake Airport	2.52	19.92	45.07	1.5	12.95
Peace River Airport	2.51	20.03	44.84	1.49	12.95
Fort Mcmurray Airport	2.53	20.46	48.50	1.56	12.95

Weather stations of Alberta	IRI	Total rutting	Longitudinal Cracking	Alligator Cracking	Transverse Cracking
	(m/km)	(mm)	(m/km)	(%)	(m/km)
Embarras Airport	2.53	20.51	48.06	1.55	12.95
High Level Airport	2.53	20.48	47.59	1.54	12.95
Fort Chipewyan	2.53	20.23	53.01	1.55	12.95

CASE 2: Traffic-4 million ESAL / 535-AADTT, AC layer thickness- 180 mm, GB layer thickness-450 mm, Poor Subgrade having modulus 25 MPa

Weather stations of Alberta	IRI	Total rutting	Longitudinal Cracking	Alligator Cracking	Transverse Cracking
	(m/km)	(mm)	(m/km)	(%)	(m/km)
Pincher Creek	2.61	23.49	43.13	2.6	12.95
Lethbridge Airport	2.59	23.41	43.10	2.51	12.95
Cowley Airport	2.59	22.67	44.59	2.51	12.95
Medicine Hat Airport	2.61	24.30	41.05	2.55	12.95
Springbank Airport	2.58	22.45	47.11	2.37	12.95
Calgary Int. Airport	2.58	22.62	44.45	2.36	12.95
Coronation Airport	2.59	22.93	42.92	2.34	12.95
Rocky Mtn House	2.61	23.27	44.94	2.6	12.95
Lloydminster Airport	2.59	22.85	46.67	2.35	12.95
Edmonton Int. Airport	2.60	23.11	47.06	2.43	12.95
Vermilion Airport	2.59	22.73	43.06	2.39	12.95
City Centre Airport	2.60	23.22	44.10	2.49	12.95
Edson	2.60	22.57	43.87	2.43	12.95
Edson Airport	2.62	23.26	44.72	2.67	12.95
Namao Airport	2.59	22.67	48.76	2.37	12.95
Whitecourt	2.61	22.88	46.76	2.54	12.95
Whitecourt Airport	2.62	23.55	47.84	2.72	12.95
Cold Lake Airport	2.60	23.02	45.17	2.41	12.95
Lac La Biche 1	2.60	23.21	49.54	2.6	12.95
Lac La Biche 2	2.61	23.06	44.51	2.51	12.95
Grande Prairie Airport	2.60	22.94	45.95	2.4	12.95
Slave Lake Airport	2.59	22.39	44.91	2.32	12.95
Peace River Airport	2.58	22.57	43.40	2.3	12.95
Fort Mcmurray Airport	2.62	23.47	46.53	2.72	12.95

Weather stations of Alberta	IRI	Total rutting	Longitudinal Cracking	Alligator Cracking	Transverse Cracking
	(m/km)	(mm)	(m/km)	(%)	(m/km)
Embarras Airport	2.61	23.10	44.84	2.49	12.95
High Level Airport	2.60	23.11	43.90	2.43	12.95
Fort Chipewyan	2.60	22.54	45.08	2.5	12.95

CASE 3: Traffic-20 million ESAL /2635 - AADTT, AC layer thickness- 250 mm, GB layer thickness-500 mm, Poor Subgrade having modulus 25 MPa

Weather stations of Alberta	IRI	Total rutting	Longitudinal Cracking	Alligator Cracking	Transverse Cracking
	(m/km)	(mm)	(m/km)	(%)	(m/km)
Pincher Creek	2.66	25.56	41.64	2.18	12.95
Lethbridge Airport	2.65	25.65	41.34	2.14	12.95
Cowley Airport	2.59	23.11	43.78	1.93	12.95
Medicine Hat Airport	2.67	26.99	42.75	2.16	12.95
Springbank Airport	2.61	23.51	45.57	2.03	12.95
Calgary Int. Airport	2.59	23.54	41.05	1.92	12.95
Coronation Airport	2.60	23.62	52.07	1.89	12.95
Rocky Mtn House	2.64	24.61	48.16	2.11	12.95
Lloydminster Airport	2.62	24.25	52.93	2.02	12.95
Edmonton Int. Airport	2.65	25.21	48.75	2.01	12.95
Vermilion Airport	2.63	24.46	55.48	2.08	12.95
City Centre Airport	2.62	24.57	41.07	1.98	12.95
Edson	2.66	25.01	51.71	2.16	12.95
Edson Airport	2.69	26.11	51.57	2.3	12.95
Namao Airport	2.60	23.17	47.72	1.9	12.95
Whitecourt	2.67	25.47	54.49	2.24	12.95
Whitecourt Airport	2.70	26.68	50.56	2.33	12.95
Cold Lake Airport	2.63	24.47	52.68	2.05	12.95
Lac La Biche 1	2.67	26.15	54.91	2.29	12.95
Lac La Biche 2	2.68	26.01	54.55	2.26	12.95
Grande Prairie Airport	2.67	25.79	50.74	2.16	12.95
Slave Lake Airport	2.65	24.86	54.36	2.12	12.95
Peace River Airport	2.65	25.27	52.40	2.1	12.95
Fort Mcmurray Airport	2.70	26.69	53.00	2.35	12.95

Weather stations of Alberta	IRI	Total rutting	Longitudinal Cracking	Alligator Cracking	Transverse Cracking
	(m/km)	(mm)	(m/km)	(%)	(m/km)
Embarras Airport	2.69	26.18	58.82	2.23	12.95
High Level Airport	2.90	32.11	43.64	1.35	12.95
Fort Chipewyan	2.65	24.35	61.38	2.18	12.95

CASE 4: Traffic-0.3 million ESAL /40- AADTT, AC layer thickness- 105 mm, GB layer thickness -160 mm, Poor Subgrade having modulus 50 MPa

Weather stations of Alberta	IRI	Total rutting	Longitudinal Cracking	Alligator Cracking	Transverse Cracking
	(m/km)	(mm)	(m/km)	(%)	(m/km)
Pincher Creek	2.43	16.42	314.44	7.16	12.95
Lethbridge Airport	2.41	16.40	302.29	6.09	12.95
Cowley Airport	2.43	16.69	313.26	6.62	12.95
Medicine Hat Airport	2.40	16.24	293.22	4.74	12.95
Springbank Airport	2.43	16.56	303.22	5.06	12.95
Calgary Int. Airport	2.40	16.14	293.58	5.12	12.95
Coronation Airport	2.45	17.45	302.29	4.51	12.95
Rocky Mtn House	2.46	17.52	320.67	6.62	12.95
Lloydminster Airport	2.45	17.43	302.92	4.57	12.95
Edmonton Int. Airport	2.45	17.35	307.36	5.25	12.95
Vermilion Airport	2.46	17.53	313.22	5.12	12.95
City Centre Airport	2.44	17.16	303.24	5.59	12.95
Edson	2.46	17.41	317.11	5.67	12.95
Edson Airport	2.48	17.73	328.01	7	12.95
Namao Airport	2.44	17.09	303.53	5.06	12.95
Whitecourt	2.48	17.64	330.70	6.69	12.95
Whitecourt Airport	2.47	17.58	326.55	6.78	12.95
Cold Lake Airport	2.46	17.51	309.88	5.12	12.95
Lac La Biche 1	2.45	17.56	318.28	5.53	473.42
Lac La Biche 2	2.48	17.88	325.47	6.46	473.42
Grande Prairie Airport	2.46	17.47	307.73	5.25	12.95
Slave Lake Airport	2.46	17.44	305.16	4.69	12.95
Peace River Airport	2.45	17.50	305.48	4.56	12.95
Fort Mcmurray Airport	2.47	17.66	336.52	7.56	12.95

Weather stations of Alberta	IRI	Total rutting	Longitudinal Cracking	Alligator Cracking	Transverse Cracking
	(m/km)	(mm)	(m/km)	(%)	(m/km)
Embarras Airport	2.48	17.95	332.33	6.78	12.95
High Level Airport	2.47	17.81	330.28	6.16	12.95
Fort Chipewyan	2.80	17.54	341.73	6.39	473.42

CASE 5: Traffic-4.0 million ESAL /535- AADTT, AC layer thickness- 160 mm, GB layer thickness-320 mm, Poor Subgrade having modulus 50 MPa

Weather stations of Alberta	IRI	Total rutting	Longitudinal Cracking	Alligator Cracking	Transverse Cracking
	(m/km)	(mm)	(m/km)	(%)	(m/km)
Pincher Creek	2.53	19.80	172.80	15.38	12.95
Lethbridge Airport	2.52	19.86	165.89	15.12	12.95
Cowley Airport	2.51	19.05	171.30	15.16	12.95
Medicine Hat Airport	2.53	20.62	168.98	15.19	12.95
Springbank Airport	2.50	18.67	162.70	13.79	12.95
Calgary Int. Airport	2.50	19.04	150.65	13.74	12.95
Coronation Airport	2.50	19.16	157.83	13.11	12.95
Rocky Mtn House	2.53	19.49	183.01	15.3	12.95
Lloydminster Airport	2.51	19.11	165.09	13.4	12.95
Edmonton Int. Airport	2.52	19.47	169.00	14.44	12.95
Vermilion Airport	2.52	19.20	175.04	13.95	12.95
City Centre Airport	2.52	19.64	165.89	14.67	12.95
Edson	2.52	18.88	177.28	14	12.95
Edson Airport	2.54	19.45	190.62	15.34	12.95
Namao Airport	2.51	19.11	161.89	13.79	12.95
Whitecourt	2.53	19.25	189.26	15.08	12.95
Whitecourt Airport	2.54	19.74	187.88	15.58	12.95
Cold Lake Airport	2.52	19.32	168.98	14.01	12.95
Lac La Biche 1	2.51	19.24	191.30	14.8	12.95
Lac La Biche 2	2.54	19.56	184.43	14.95	12.95
Grande Prairie Airport	2.52	19.25	165.09	14.1	12.95
Slave Lake Airport	2.51	18.70	160.27	12.87	12.95

Weather stations of Alberta	IRI	Total rutting	Longitudinal Cracking	Alligator Cracking	Transverse Cracking
	(m/km)	(mm)	(m/km)	(%)	(m/km)
Peace River Airport	2.50	18.88	158.63	12.8	12.95
Fort Mcmurray Airport	2.54	19.71	210.84	15.71	12.95
Embarras Airport	2.54	19.67	202.32	15.34	12.95
High Level Airport	2.53	19.66	194.61	14.83	12.95
Fort Chipewyan	2.54	19.30	228.25	15.55	12.95

CASE 6: Traffic-20 million ESAL /2673 AADTT, AC layer thickness- 240 mm, GB layer thickness- 370 mm, Poor Subgrade having modulus 50 MPa

Weather stations of Alberta	IRI	Total rutting	Longitudinal Cracking	Alligator Cracking	Transverse Cracking
	(m/km)	(mm)	(m/km)	(%)	(m/km)
Pincher Creek	2.53	20.72	51.06	3.59	12.95
Lethbridge Airport	2.53	21.20	50.33	3.59	12.95
Cowley Airport	2.50	19.33	49.94	3.15	12.95
Medicine Hat Airport	2.56	22.52	51.27	3.85	12.95
Springbank Airport	2.49	19.05	49.75	2.95	12.95
Calgary Int. Airport	2.49	19.66	47.11	3.11	12.95
Coronation Airport	2.51	19.97	53.75	3.04	12.95
Rocky Mtn House	2.52	20.15	52.31	3.43	12.95
Lloydminster Airport	2.50	19.75	53.25	3.04	12.95
Edmonton Int. Airport	2.55	21.41	54.52	3.97	12.95
Vermilion Airport	2.52	19.93	54.54	3.26	12.95
City Centre Airport	2.56	21.67	53.62	4.37	12.95
Edson	2.53	20.09	55.01	3.56	12.95
Edson Airport	2.56	21.10	57.44	4.47	12.95
Namao Airport	2.50	19.34	50.36	3.03	12.95
Whitecourt	2.55	20.76	58.36	4.14	12.95
Whitecourt Airport	2.57	21.71	58.06	4.94	12.95
Cold Lake Airport	2.55	21.13	55.18	3.84	12.95
Lac La Biche 1	2.54	21.08	58.21	4.51	12.95
Lac La Biche 2	2.56	21.33	59.73	4.33	12.95

Weather stations of Alberta	IRI	Total rutting	Longitudinal Cracking	Alligator Cracking	Transverse Cracking
	(m/km)	(mm)	(m/km)	(%)	(m/km)
Grande Prairie Airport	2.54	21.00	53.54	3.77	12.95
Slave Lake Airport	2.52	19.94	54.01	3.37	12.95
Peace River Airport	2.52	20.37	52.97	3.31	12.95
Fort Mcmurray Airport	2.57	21.63	59.73	4.83	12.95
Embarras Airport	2.57	21.56	64.92	4.28	12.95
High Level Airport	2.54	20.69	58.36	3.56	12.95
Fort Chipewyan	2.55	20.78	67.80	4.47	12.95

A.2.2 Measured IRI Data from Pavement Management System (PMS) of Alberta

					PAVEMENT						TRAFFIC		CONDITION	
Highway					Base		Last Activity							
			From	To					Surf	Seal		ESAL		
Type	No.	Dir	km	km	Type	Year	Type	Year	mm	Coat	AADT	/Day	IRI	Age
PH	2:40	C	42.583	43.072	GBC	1991	ACP	1991	163	0	5200	209	2.4	19
PH	29:02:00	C	20.004	24.1	GBC	1991	ACP	1991	100	0	1000	112	1.5	19
PH	29:02:00	C	24.1	24.6	GBC	1991	ACP	1991	100	0	1000	112	2.4	19
PH	29:02:00	C	24.6	24.96	GBC	1991	ACP	1991	100	0	1000	112	1.9	19
PH	29:02:00	C	24.96	25.46	GBC	1991	ACP	1991	100	0	1000	112	1.5	19
PH	29:02:00	C	25.46	25.6	GBC	1991	ACP	1991	100	0	1000	112	2.4	19
PH	29:02:00	C	25.6	26.1	GBC	1991	ACP	1991	100	0	1000	112	1.7	19
PH	29:02:00	C	26.1	26.5	GBC	1991	ACP	1991	100	0	1000	112	2.5	19
PH	29:02:00	C	26.5	27	GBC	1991	ACP	1991	100	0	1000	112	3	19
PH	29:02:00	C	27	27.38	GBC	1991	ACP	1991	100	0	1000	112	1.7	19
PH	29:02:00	C	27.38	27.88	GBC	1991	ACP	1991	100	0	1000	112	2.8	19
PH	29:02:00	C	27.88	28.26	GBC	1991	ACP	1991	100	0	1000	112	1.4	19
PH	29:02:00	C	29.4	30.5	GBC	1991	ACP	1991	100	0	1000	112	1.5	19
PH	29:02:00	C	30.5	31	GBC	1991	ACP	1991	100	0	1000	112	1.6	19
PH	29:02:00	C	31	32.576	GBC	1991	ACP	1991	100	0	1000	112	1.9	19
PH	49:08:00	C	14.52	16.36	GBC	1991	ACP	1991	120	0	860	180	2.8	19
PH	525:02:00	C	0	0.53	GBC	1991	ACP	1991	100	0	210	30	1.7	19
PH	620:04:00	C	26.94	27.292	GBC	1991	ACP	1991	110	0	1630	399	1.7	19
PH	740:02:00	C	49.714	49.86	GBC	1991	ACP	1991	100	0	320	30	3.1	19
PH	791:06:0	C	0	1.2	GBC	1991	ACP	1991	100	0	440	37	2	19

					PAVEMENT						TRAFFIC		CONDITION	
Highway					Base		Last Activity							
			From	To					Surf	Seal		ESAL		
	0													
PH	845:04:00	C	1.95	2.18	GBC	1991	ACP	1991	100	0	2320	326	2.2	19
PH	845:04:00	C	2.74	3.7	GBC	1991	ACP	1991	100	0	2320	326	2.3	19
PH	845:04:00	C	5.36	5.52	GBC	1991	ACP	1991	100	0	2320	326	2.4	19
PH	845:04:00	C	5.84	6	GBC	1991	ACP	1991	100	0	2320	326	2.6	19
PH	845:04:00	C	7.49	7.63	GBC	1991	ACP	1991	100	0	2320	326	1.9	19
PH	845:04:00	C	8.28	8.56	GBC	1991	ACP	1991	100	0	2320	326	2.7	19
PH	845:04:00	C	9.66	9.84	GBC	1991	ACP	1991	100	0	2320	326	1.6	19
PH	845:04:00	C	10.12	11.15	GBC	1991	ACP	1991	100	0	2320	326	1.6	19
PH	845:04:00	C	12.23	12.42	GBC	1991	ACP	1991	100	0	2320	326	1.5	19
PH	855:16:00	C	20.48	20.585	GBC	1991	ACP	1991	100	0	1061	100	3.4	19
PH	881:24:00	C	42.59	42.8	GBC	1991	ACP	1991	170	0	2890	347	1.8	19
PH	897:02:00	C	2.4	3.4	CSB	1991	ACP	1991	100	0	410	60	2.3	19